Slow Active Suspension Control for Rollover Prevention

by

Sarel Francois van der Westhuizen

Submitted in partial fulfilment of the requirements for the degree

Master of Engineering

In the Faculty of

Engineering, Built Environment and Information Technology

University of Pretoria

August 2012

Slow active suspension control for rollover prevention

Author: Sarel Francois van der Westhuizen

Supervisor: Prof. Pieter Schalk Els

Department: Mechanical and Aeronautical Engineering

Degree: Master of Engineering

Keywords: *Suspension control, Hydropneumatic suspension, Roll stability, Sports Utility Vehicle, Rollover prevention*

Abstract

Rollover prevention in Sports Utility Vehicles (SUV's) offers a great challenge in vehicle safety. By reducing the body roll angle of the vehicle the load transfer will increase and thus decrease the lateral force that can be generated by the tires. This decrease in the lateral force can cause the vehicle to slide rather than to roll over. This study presents the possibility of using slow active suspension control to reduce the body roll and thus reduce the rollover propensity of a vehicle fitted with a hydro-pneumatic suspension system. The slow active control is obtained by pumping oil into and draining oil out of each hydro-pneumatic suspension unit individually.

A real gas model for the suspension units as well as for the accumulator that supplies the oil is incorporated in a validated full vehicle Adams model. This model is then used to simulate a double lane change manoeuvre performed by a SUV at 60 km/h and it is shown that a significant improvement in body roll can be obtained with relatively low energy requirements.

The proposed control is successfully implemented on a Land Rover Defender test vehicle. A Proportional-Derivative (PD) controller is used to control on-off solenoid operated valves and the flow is adjusted using the lateral acceleration as a parameter. Experimental results confirm that a significant improvement in body roll is possible.

.

Stadige aktiewe suspensiebeheer om omrol te voorkom

Outeur: Sarel Francois van der Westhuizen

Studieleier: Prof. Pieter Schalk Els

Departement: Meganiese en Lugvaartkundige Ingenieurswese

Graad: Magister in Ingenieurswese

Sleutelwoorde: *Suspensiebeheer, hidropneumatiese suspensie, Rolstabiliteit, Sportnutsvoertuig, Omrolvoorkoming*

Opsomming

Omrolvoorkoming in Sportnutsvoertuie bied geweldige uitdagings in terme van voertuigveiligheid. Deur die rolhoek van die voertuig te verminder word die laterale lasoordrag verhoog en word die laterale krag wat die bande kan genereer minder. As die laterale krag genoeg verminder sal die voertuig eerder gly as omrol. Die studie ondersoek die moontlikheid om stadig-aktiewe suspensiebeheer op ‘n voertuig met ‘n hidropneumatiese suspensie te gebruik om bakrol te verminder en dus die omrolgeneigdheid van die voertuig te verlaag. Die beheer word toegepas deur olie in elke hidropneumaties suspensie-eenheid individueel in te pomp of te dreineer.

‘n Werklike gas model word gebruik om die supensie-eenhede asook die akkumulator, wat die olie aan die suspensie voorsien, te modeleer. Hierdie modelle word in ‘n gevalideerde volvoertuig ADAMS model geïnkorporeer en ‘n dubbel laanverwisseling word gesimuleer teen 60 km/h. Die resultate toon dat ‘n beduidende verbetering in die rolhoek moontlik is met relatiewe lae energievereistes.

Die voorgestelde beheer is suksesvol op ‘n Land Rover Defender geïmplimenteer en ‘n Proportioneele-Differensiaal (PD) beheerder word gebruik om die aan-af solenoïde kleppe te beheer terwyl die vloei aangepas word na gelang van die laterale versnelling. Eksperimentele resultate bevestig dat ‘n beduidende verbetering in bakrol moontlik is.

Acknowledgements

My thanks and appreciation to the following:

- My Heavenly Father only through You this work was possible. As it says in Your Word: "Our help is in the name of the LORD, who made heaven and earth." (Psalm 124:8)
- My wife Jenni for all her special love and support
- Professor Els for giving me an opportunity, for his many hours of help and for sharing his seemingly infinite knowledge, I hope that this relationship will still continue for many years
- My parents and grandparents for their love and support (including financial support)
- Theunis, Herman, Joachim, Carl, Cor-Jacques, Anria, Donna-Lee and Johan for everything from helping with problems to making jokes and enjoying a good laugh
- Eugene at Axiom Hydraulics for his willingness to help
- Gerotek for the use of their facilities

Table of Contents

Abbreviations i

List of Symbols ii

List of Tables iv

List of figures v

1. Introduction 1

2. Literature Overview 4

2.1 Rollover 4

2.2 Handling 8

2.3 Methods to improve rollover and handling characteristics 12

2.3.1 Four wheel steering 13

2.3.2 Passive interconnected suspensions 13

2.3.3 Semi-Active and Active Suspension Systems 15

2.3.3.1 Four State Semi-Active Suspension ($4S_4$) 15

2.3.3.2 Other Semi-Active Systems 19

2.3.4 Active Systems 19

2.3.4.1 Active Anti Roll Bar on the $4S_4$ 19

2.3.4.2 Other Active Anti Roll Bars 21

2.3.5 Stability Control 21

2.3.6 Tilting Vehicle 22

2.4 Effect of height control on suspension characteristics 22

2.5 Conclusion 24

3. Simulation Results 25

3.1 Full Vehicle Model 25

3.2 System Requirements 29

3.3 Hydraulic Circuit 30

3.4 Suspension Model 34

3.4.1 Ideal Gas Spring Model 35

3.4.2 BWR Spring Model 36

3.5 Control Strategies 36

3.5.1 Control Strategy 1 37

3.5.2 Control Strategy 2 39

3.5.3 PID Controller 42
3.5.4 On-off valve control 44
3.5.4.1 60 Millisecond sampling increments 44
3.5.4.2 90 Millisecond sampling increments 47
3.6 Conclusion 50
4. Experimental Work and Results 51
4.1 Initial Verification Tests 51
4.2 Voltage Controlled Current Source 56
4.3 Proportional Valve Characterisation 59
4.4 PID Control Algorithm 61
4.5 Volume Estimation 62
4.6 Vehicle Implementation and Experimental Results 65
4.6.1 Initial problems and modifications 65
4.6.1.1 Battery Power 65
4.6.1.2 Volume Limit 66
4.6.1.3 Valve Response 67
4.6.2 Experimental Results 68
4.7 Simulation Verification 73
4.8 Conclusion 77
5. Conclusion 78
6. Recommendations for future work 79
7. Bibliography / References 80
Appendix A Derivation of the differential equation used to calculate the gas temperature in the suspension 86
Appendix B BWR and Nitrogen Constants 90
Appendix C Equation for volume estimation 91

Abbreviations

AARB	Active Anti-Roll Bar
ARB	Anti-Roll Bar
BWR	Benedict Webb Rubin
DC	Direct Current
CG	Centre of Gravity
DLC	Double Lane Change
ER	Electro-Rheological
FTF	Fixed Timing Fishhook
GPS	Global Positioning System
HIS	Hydraulic Interconnected Suspensions
ISO	International Organisation for Standardisation
MR	Magneto-Rheological
NHTSA	National Highway Traffic Safety Administration
PD	Proportional Derivative
PID	Proportional Integral Derivative
RRFF	Roll Rate Feedback Fishhook
SSF	Static Stability Factor
STC	Steering Tilt Control
SUV	Sports Utility Vehicle
USA	United States of America
VSC	Vehicle Stability Control
2WS	2 Wheel Steer
$4S_4$	4 State Semi-active Suspension System
4WS	4 Wheel Steer

List of Symbols

A	Piston area
a	BWR constant
A_o	BWR constant
b	Distance from CG to front axle or BWR constant (Context dependant)
B_o	BWR constant
c	Distance from CG to rear axle or BWR constant (Context dependant)
C_o	BWR constant
$C_{\alpha f}$	Cornering stiffness of the front tires
$C_{\alpha r}$	Cornering stiffness of the rear tires
c_v	Specific heat
c_v^0	Ideal gas specific heat
d	Displacement of the gas accumulator's piston
F	Upwards force exerted by pressurised gas
F_{zo}	Vertical force on the outside wheel
F_{zi}	Vertical force on the inside wheel
F_y	Lateral force
g	Acceleration due to gravity
h_{CG}	Height of CG
h_r	Roll centre height
I	Current
k	Constant
k_1, k_2, k_3	PID controller gains
K	Understeer gradient
$K_\emptyset$	Roll stiffness of the suspension
L	Wheelbase
M	Sprung mass
m	Mass of the gas
n	Amount of substance
N_1 to N_9	Constants for ideal gas specific heat
P	Pressure *
P_{max}	Maximum suspension pressure
ΔP	Pressure difference
Q_{max}	Maximum suspension oil flow
R	Radius of turn, Resistance or Specific Gas constant (Context dependant)
t	Track width
T	Temperature*
T_s	Atmospheric temperature
V	Forward speed, Voltage or Volume* (Context dependant)
V_{max}	Maximum suspension velocity
$\dot{V}$	Change of volume

v	Specific volume
W_f	Load (Vertical Force) on the front axle
W_r	Load (Vertical Force) on the rear axle
W_b	Weighting function
$\dot{W}$	Rate of piston work
x	Suspension displacement
x_o	Suspension displacement at the static position

Greek Symbols

α_f	Tire slip angle front
α_r	Tire slip angle rear
α	BWR constant
β	Bulk modulus
δ	Steer angle of the front wheels
γ	BWR constant
γ_{IG}	Heat capacity ratio
τ	Thermal time constant
$\emptyset$	Roll angle of the body
ω_n	Natural frequency

* Subscripts o = oil and g = gas

List of Tables

Table 1 Lane change track dimensions (International Organisation for Standardisation, 1975) 12
Table 2 Weighted RMS of vertical acceleration for test runs on a Belgian paving (Cronje, 2008)..... 20
Table 3 Valve opening commands for different lateral accelerations..... 69
Table 4 RMS of the displacement for run 1..... 71
Table 5 RMS of the roll angle for two different runs..... 72

List of figures

Figure 1 Pie chart of the fatal car crashes in South Africa during 2009 2
Figure 2 Pie chart of the fatalities in car crashes in South Africa during 2009 3
Figure 3 Roll over of a vehicle with a high CG (New Zealand Crash Investigators, 2010) 4
Figure 4 Force analysis of a vehicle (seen from the rear) during cornering (Gillespie, 1992) 6
Figure 5 Lateral forces generated by different vertical forces 6
Figure 6 NHTSA RRFF manoeuvre description (National Highway Traffic Safety Administration, (2002) 8
Figure 7 Constant Radius Test (Gillespie, 1992) 9
Figure 8 Cornering of a bicycle model (Gillespie, 1992) 10
Figure 9 Lane change track and cone placement 11
Figure 10 Nominal fluid flow distribution in an idealised suspension modes (a) bounce, (b) roll, (c) pitch, and (d) articulation (Smith and Zhang, 2009) 14
Figure 11 (a) Conventional passive suspension system. (b) Electromagnetic suspension system. Geysen et al (2010) 15
Figure 12 Suspension Design (Holdmann and Holle, 1999) 16
Figure 13 Schematic diagram of the $4S_4$ (Els, 2006) 17
Figure 14 Soft and Stiff spring characteristics of the $4S_4$ (Els, 2006) 18
Figure 15 Damper characteristics of the $4S_4$ (Els,2006) 18
Figure 16 Average body roll angles for different ARB settings on the stiff suspension during a 20
Figure 17 Average body roll angle vs. lateral acceleration during a constant radius test (Cronje, 2008) 21
Figure 18 Tilting Vehicles (Rotpod, 2012) 22
Figure 19 Natural frequency as a function of spring load for for a mechanical, pneumatic and 23
Figure 20 Spring rate as a function of spring load for a mechanical, pneumatic and a 23
Figure 21 Simulation model interaction (Cronje, 2008). 26
Figure 22 Schematic of the front suspension (Thoresson, 2007). 27
Figure 23 Front suspension in ADAMS model (Thoresson, 2007). 27
Figure 24 Schematic of the rear suspension (Thoresson, 2007). 28
Figure 25 Front suspension in ADAMS model (Thoresson, 2007). 28
Figure 26 Validation of the ADAMS model's handling dynamics for a DLC at 65km/h 29
Figure 27 Hydraulic circuit for a single suspension unit 30
Figure 28 Performance graphs for SV10-24 valve (Hydraforce, 2012) 31
Figure 29 Flow vs Pressure Drop for SV10-24 valve 31
Figure 30 Flow vs Pressure graphs for the SV12-33 (Hydraforce, 2011) directional valve (left) and the FPCC (Sun Hydraulics, 2011) proportional valve (right) 32
Figure 31 Flow diagram of the hydraulic setup in the test vehicle 33
Figure 32 Suspension model interaction 34
Figure 33 Main principle of the suspension model 36
Figure 34 Body roll angle for a DLC manoeuvre at 60 km/h 37
Figure 35 Suspension responses for a DLC manoeuvre at 60 km/h 38
Figure 36 Body roll angle for a DLC manoeuvre at 60 km/h 39

Figure 37 Suspension responses for a DLC manoeuvre at 60 km/h 40
Figure 38 Suspension responses for a DLC manoeuvre at 60 km/h for unconstrained outflow 41
Figure 39 Suspension responses for a DLC manoeuvre at 60 km/h for constrained outflow 41
Figure 40 Body roll angle for a DLC manoeuvre at 60 km/h using a PID controlled proportional valve 42
Figure 41 Suspension responses for a DLC manoeuvre at 60 km/h for PID controlled proportional 43
Figure 42 Body roll angle for a DLC manoeuvre at 60 km/h using a PID controlled on-off valve 45
Figure 43 Suspension responses for a DLC manoeuvre at 60 km/h for on-off valves 45
Figure 44 Flow rates for each suspension unit 46
Figure 45 Total volume of oil pumped into the suspension 46
Figure 46 Total flow rate required 47
Figure 47 Body roll angle for a DLC manoeuvre at 60 km/h using a PID controlled on-off valve 48
Figure 48 Suspension responses for a DLC manoeuvre at 60 km/h for on-off valves 48
Figure 49 Flow rates for each suspension unit 49
Figure 50 Total volume of oil pumped into the suspension 49
Figure 51 Total flow rate required 50
Figure 52 Comparison between the measured results and the simulation results with and without 51
Figure 53 Comparison between simulation results of the ideal gas model with flow 12.8l/m and 53
Figure 54 Simulation results of BWR equation model with flow 12.8l/m 53
Figure 55 Specific volume during the simulation 53
Figure 56 Measured and simulated results for Ideal gas and BWR model 54
Figure 57 Simulation results of BWR equation model with flow 12.8l/m (no friction & 50% damping) 54
Figure 58 Roll angles for a baseline and controlled DLC at 60km/h 56
Figure 59 Voltage controlled current source with a voltage divider in the reference voltage signal 56
Figure 60 Comparative test between a 1Ω-10W coil resistor at R3 and two 1.5Ω-2W axial resistors in parallel 57
Figure 61 Test setup with MR damper as load 58
Figure 62 Output signal for an input signal of 2-5V in 0.5V increments 58
Figure 63 Input and output signal for an input signal of 5V 59
Figure 64 Valve test with a 50% command input. 60
Figure 65 Valve test with a 60% command input. 60
Figure 66 Valve test with a 70% command input. 60
Figure 67 Valve test with a 80% command input. 61
Figure 68 Flow vs Pressure curve obtained for different valve openings. 61
Figure 69 Noise on the displacement Signals 62
Figure 70 PID signals for the averaged PID (left) and for the averaged displacement (right) 62
Figure 71 Suspension displacements 63
Figure 72 Estimated volume of oil in suspension 64
Figure 73 Suspension displacements during fall test 64
Figure 74 Estimated volume of oil in suspension during fall test 65
Figure 75 10 ℓ bladder type accumulator being charged to 7 MPa 66
Figure 76 Estimated Volume during a DLC at 60 km/h 67
Figure 77 Valves for the rear suspension unit during characterisation 68

Figure 78 Land Rover Defender test vehicle being prepared for testing 70
Figure 79 Laser displacement sensor on the side of the vehicle 70
Figure 80 Suspension displacements for Run 1 during a DLC at 60km/h 71
Figure 81 Body roll angle for DLC's at 60km/h 72
Figure 82 Vehicle path and speed for the baseline run and controlled run1 72
Figure 83 Simulated and experimental roll angle for a controlled DLC at 60 km/h 74
Figure 84 Simulated and Experimental controlled suspension displacement for a DLC at 60km/h 74
Figure 85 Suspension displacement for average total inflow of 0.54 l/m during a DLC at 60km/h 75
Figure 86 Suspension displacement for average total inflow of 1.35 l/m during a DLC at 60km/h 75
Figure 87 Suspension displacement for average total inflow of 3.37 l/m during a DLC at 60km/h 76
Figure 88 Suspension displacement for average total inflow of 6.75 l/m during a DLC at 60km/h 76
Figure 89 Roll angle for different total flow magnitudes during a DLC at 60km/h 77

1. Introduction

SUV's are becoming increasingly popular as family vehicles and are able to drive at reasonably high speeds. These vehicles can give the driver a sense of safety because of their size and robustness and can thus encourage reckless driving behaviour. In reality these vehicles generally have a high centre of gravity (CG) and soft suspensions with large wheel travel to provide good off-road abilities and comfort, which result in a vehicle that is prone to untripped rollover. These problems also occur in many other vehicles used in construction, mining, military and agricultural applications.

Road accident statistics also show that SUV's are prone to rollover and that rollover is a very dangerous type of accident:

According to the **Governor's Office of Consumer Affairs (2010)** in Georgia, more than 40% of Americans think that they are safer in a SUV than in a regular car and nearly 50% do not take into account that loading increases the risk of rollover. This is shocking in the light that 37% of fatal crashes reported in the study were due to SUV rollovers where only 15% of fatal accidents in passenger cars were due to rollover. In 2006 SUVs also had the highest occupant fatality rate in rollover crashes namely 7.77 per 100,000 registered vehicles and single-vehicle rollover crashes made up 47% of driver deaths in SUVs. In 2006, 65% of single vehicle crashes involved SUVs.

The rollover statistics for Pennsylvania shows similar trends. In 2008, 8.5% of light truck, van and SUV accidents were due to rollover where 5% of passenger cars rolled over. Of these rollover cases the occupant deaths were nearly 70% higher in SUVs than in passenger cars. **(Edgar Snyder and Associates, 2010)**

In South Africa, rollover accidents made up 24% of the fatal crashes for 2009 and it made up 25% of the fatalities for 2009 (see Figure 1 and Figure 2). This again shows the severity of a rollover accident. **(Road Traffic Management Corporation, 2009)**

According to **Takubo and Mizuno (2000)** the particular use of SUV's in Japan make them more prone to accidents.

SUV's are used to:

- Travel long distances for leisure
- Travel on crowded roads
- Travel unfamiliar roads to a holiday destination where the scenery can distract the driver
- Drive winding roads in recreational areas
- Drive children around
- Drive in places of heavy pedestrian traffic

This, combined with the fact that these vehicles are popular amongst younger people that often drive more recklessly, and that the dynamics of these vehicles are worse than those of normal passenger cars, results therein that these vehicles can be very dangerous to drive. The large side area of the vehicle combined with general softer suspension makes it vulnerable to side winds while the high CG magnifies the rolling motions during cornering. The high viewpoint of the driver also inspires confidence, because the driver can see further, and the driver may become over confident.

These are just a few examples of the very urgent need for better rollover stability or control in Sports Utility and other high CG vehicles. From these statistics it becomes clear that rollover is a very dangerous type of accident with a high fatality rate. This is because there is very little structural occupant protection in vehicles in the case of a rollover accident compared to front and rear impacts.

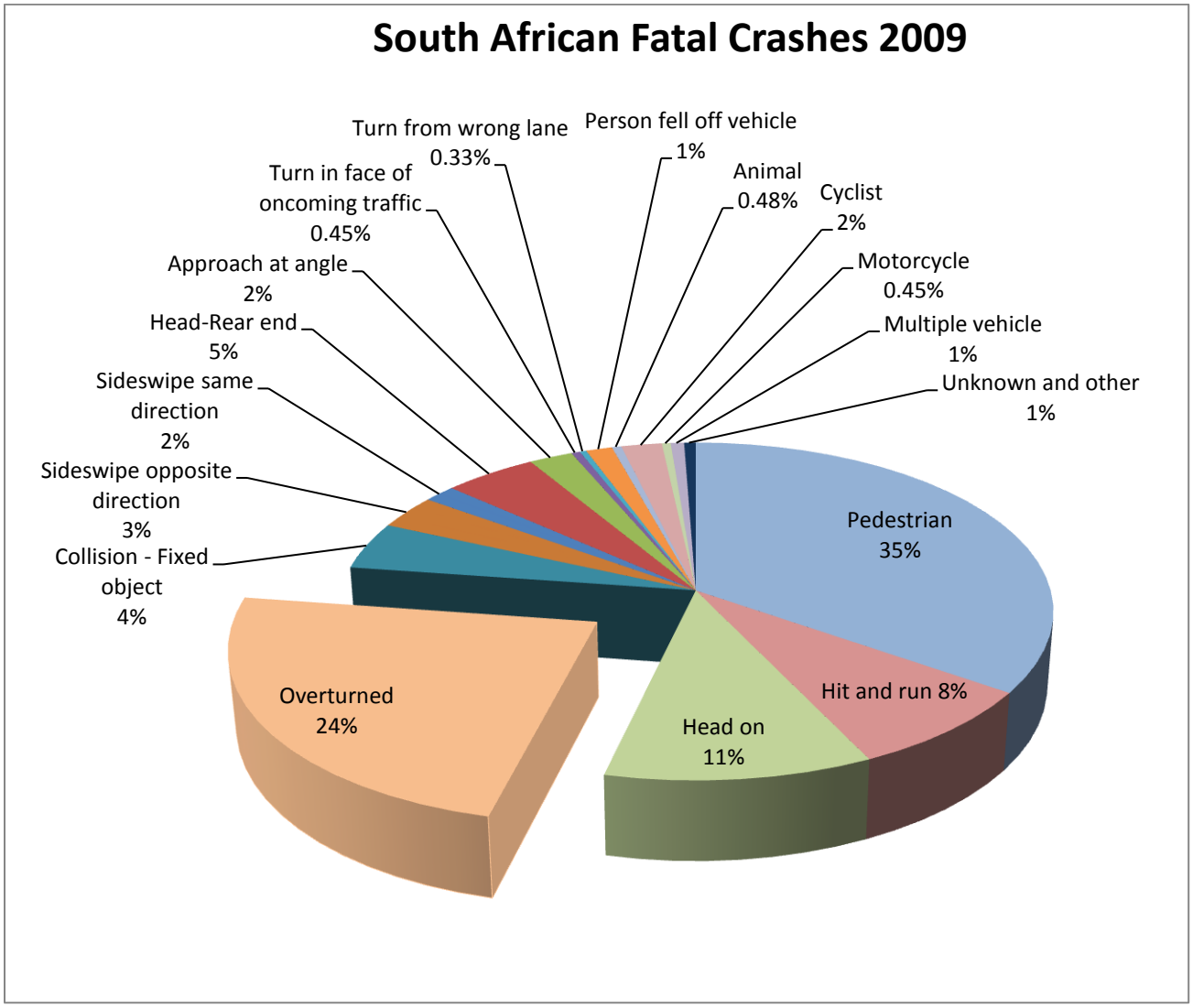

Figure 1 **Pie chart of the fatal car crashes in South Africa during 2009 (Road Traffic Management Corporation, 2009)**

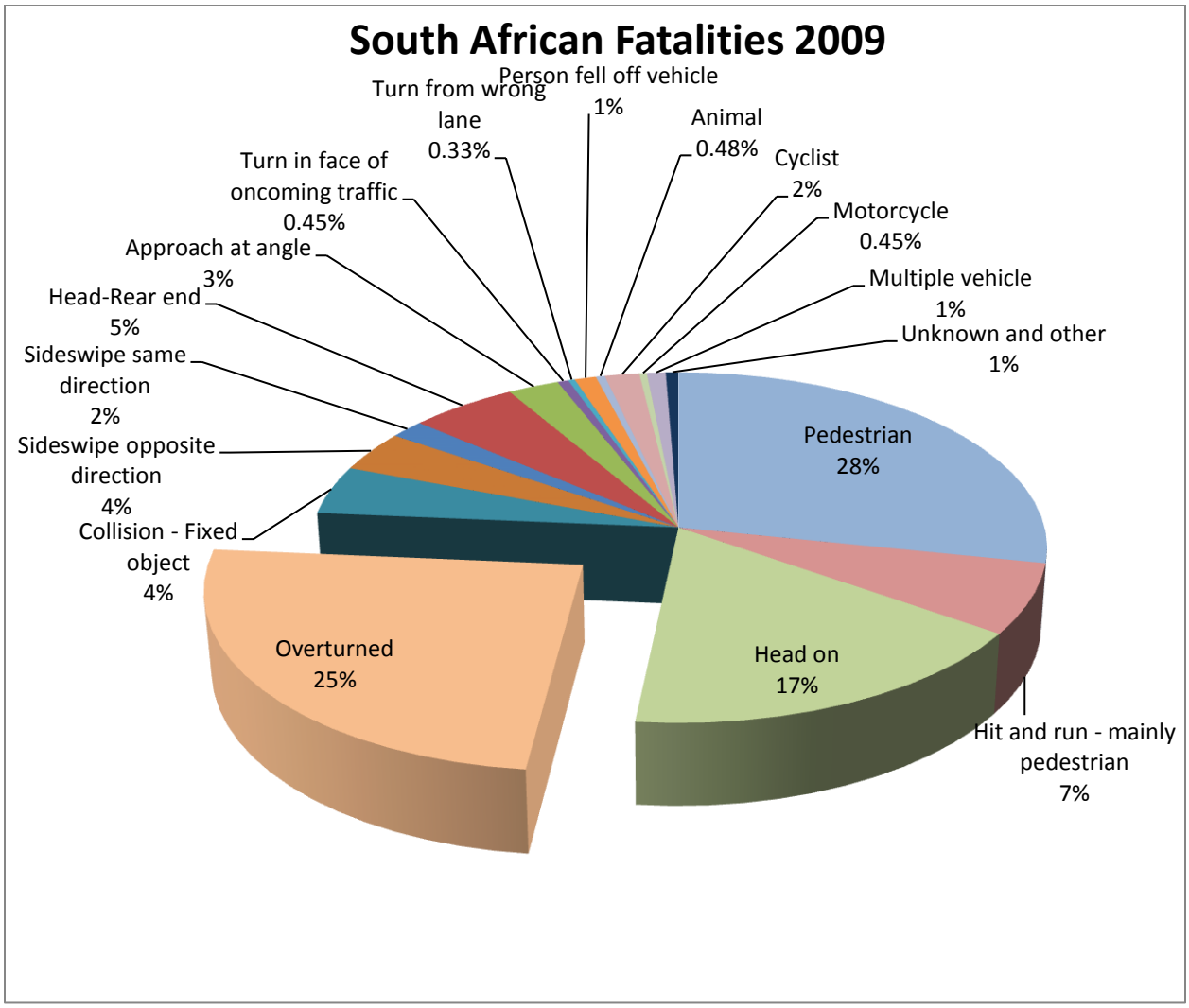

Figure 2 **Pie chart of the fatalities in car crashes in South Africa during 2009 (Road Traffic Management Corporation, 2009)**

This study will investigate the feasibility of using slow active suspension control, on a four state semi active hydropneumatic suspension installed on a Land Rover Defender test vehicle, to improve the body roll of the vehicle and thus decrease the vehicle's tendency to roll over. Oil is pumped into and drained out of each suspension unit individually to counter compression and extension. Simulations are performed using a validated ADAMS **(MSC.Software, 2011)** model. The suspension control is implemented on a test vehicle and experimental tests are performed. The simulated an experimental data obtained is then compared.

An overview of the relevant literature is given in Chapter 2. The simulation model, theoretical development and simulation results used to determine the feasibility of slow active suspension control are given in Chapter 3, while the experimental results and a comparison between the experimental and simulation results are given in Chapter 4. A conclusion is given in Chapter 5 and recommendations for future work in Chapter 6.

2. Literature Overview

This chapter summarises the relevant literature on rollover and handling, methods to measure rollover and handling, methods to improve rollover and handling, characteristics of different suspensions and some background on the simulation model used in this study. The semi-active suspension used in this study is also described in this chapter.

2.1 Rollover

Roll over is defined as a vehicle rotation of 90˚ around the longitudinal or lateral axis but during dynamic testing rollover is generally defined as two or more wheels lifting more than 51mm off the ground for more than 0.5s **(Ponticel, 2003)**. There are two types of rollover namely tripped rollover and untripped rollover. In many cases the moment around the roll axis (due to the centrifugal force on the CG and the lateral force generated by the tire) in vehicles with a high CG like SUV's can become large enough to cause untripped rollover. The magnitude of this moment can be reduced by lowering the CG, reducing the centrifugal force on the CG or reducing the lateral force generated by the tyre. The centrifugal force can be reduced by reducing the speed of the vehicle when cornering and the lateral force by changing the load transfer (described later on). If the lateral force that the tires can generate is reduced sufficiently the vehicle will slide rather than to roll over untripped. Sliding is not desirable because the vehicle will not follow the desired path but it is preferable to rolling over. Although sliding can cause tripped rollover it dissipates energy and thus reduces the vehicle speed which in turn reduces the probability of rollover.

Therefore this study will focus on reducing the risk of untripped rollover which occurs when the vehicle rolls over without hitting an obstacle. Figure 3 shows a vehicle where static rollover starts to occur when the CG passes the point of contact with the ground (Point A). From this it becomes clear that the higher the CG, the smaller the angle necessary for roll over.

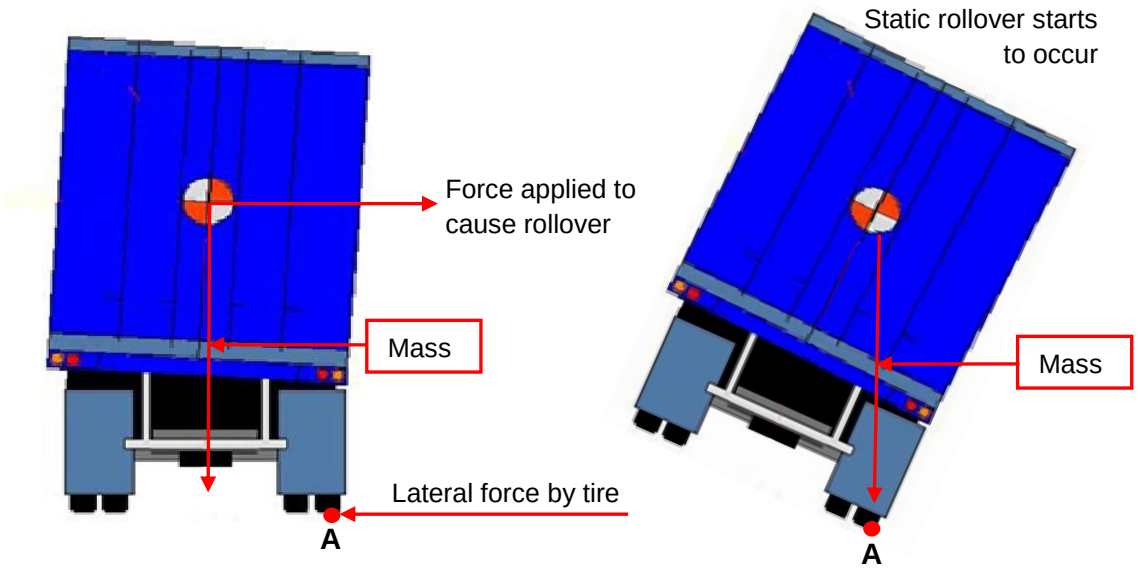

Figure 3 Roll over of a vehicle with a high CG (New Zealand Crash Investigators, 2010)

When cornering at high speeds, lateral acceleration is generated which causes a centrifugal force to act on the CG (F_y in Figure 4), one can see here that the magnitude of the moment around A will increase as the height of the CG increases. The roll centre of the vehicle is the point where the lateral forces are transferred from the axle to the body of the vehicle. The difference between the vertical force on the inside and the outside wheels can be determined using the following equation given by **Gillespie (1992):**

$$F_{zo} - F_{zi} = 2F_y \frac{h_r}{t} + 2K_\emptyset \frac{\emptyset}{t} \quad (1)$$

Where:

F_{zo} = Vertical force on the outside wheel

F_{zi} = Vertical force on the inside wheel

F_y = Lateral Force

h_r = Roll centre height

$K_\emptyset$ = Roll stiffness of the suspension

t = Track width

$\emptyset$ = Roll angle of the body (+ is clockwise, when looking at the rear of the vehicle)

The first part of the equation $2F_y \frac{h_r}{t}$ is a transfer of the lateral load due to the cornering forces and can only be improved by widening the track of the vehicle or by lowering the CG. Although ride height control is not the focus of this study, slow active ride height control can be easily implemented using the same hydraulic and control hardware developed in this study, but with changes to the algorithms.

The second part $2K_\emptyset \frac{\emptyset}{t}$ is a transfer of the lateral load due to body roll. It can be seen here that if the roll angle is reduced the load transfer will be smaller and the vehicles tendency to roll over will be less due to the moment of the mass around point A in Figure 4. However to reduce the roll angle, $K_\emptyset$ needs to increase which increases the load transfer and this, due to the non-linearity between the vertical force and the lateral force, reduces the lateral force that the tyres can generate. If the lateral force is reduced enough the vehicle will slide rather than roll over. Figure 5 indicates a typical lateral tyre force vs. vertical tyre force graph for a constant slip angle. It shows two cases; one where both wheels experience a vertical force of 4 kN and the other where one wheel experiences a vertical force of 3 kN and the other 5 kN. One can see that the total lateral force generated for the first case is about 5 kN and for the second case 4.9 kN, thus there is a decrease in the lateral force due to the load transfer between the wheels. **(Gillespie, 1992)**

A popular method to characterise rollover resistance is the Static Stability Factor (SSF). The SSF is defined as the half of the track width divided by the height of the CG if the nomenclature of Figure 4 is used the SSF will be:

$$SSF = \frac{0.5t}{h_{CG}} \quad (2)$$

(**National Highway Traffic Safety Administration, 2012)**

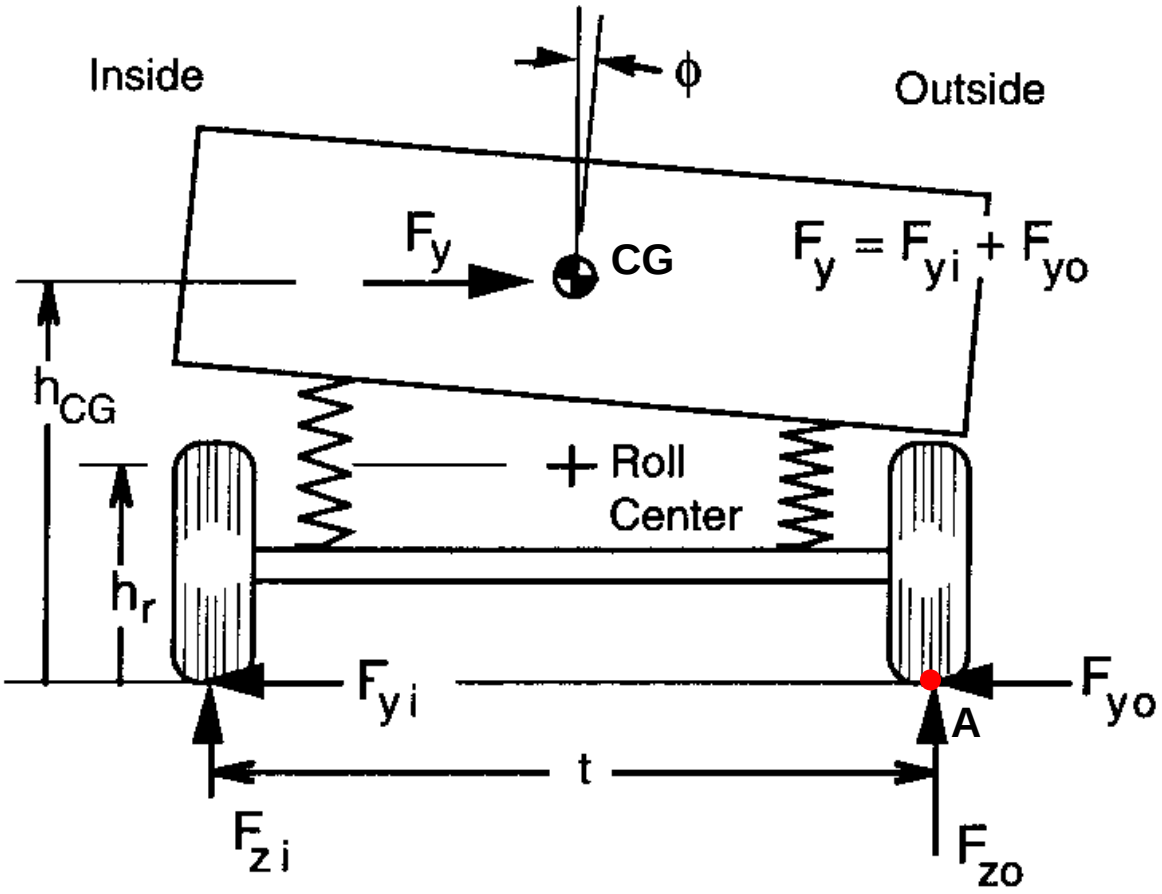

Figure 4 **Force analysis of a vehicle (seen from the rear) during cornering (Gillespie, 1992)**

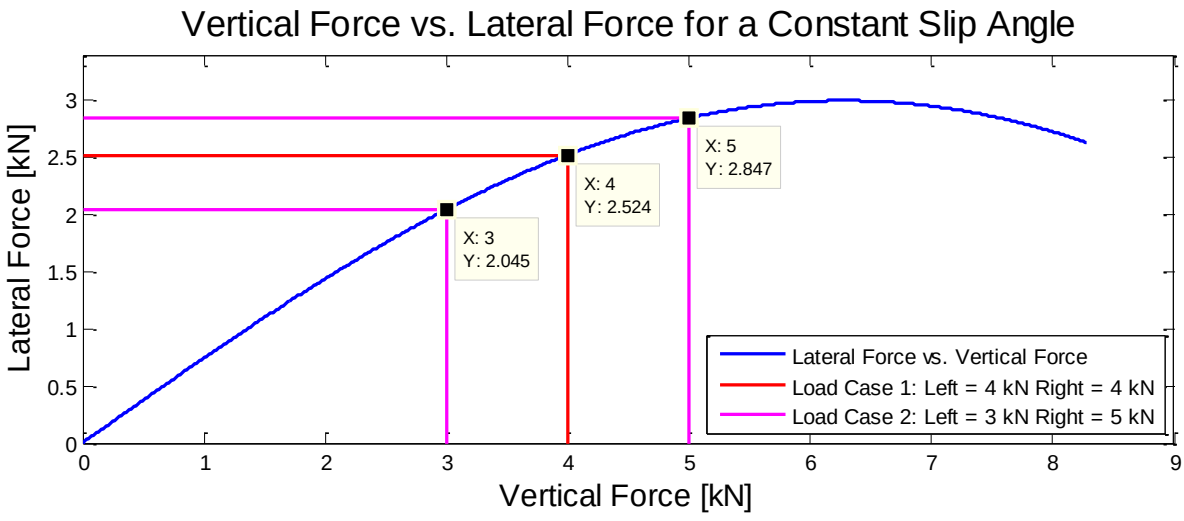

Figure 5 **Lateral forces generated by different vertical forces**

Ungoren et.al. (2001) evaluates the effect of a Vehicle Stability Control (VSC) system on the rollover propensity of a SUV using CarSim **(Mechanical Simulation, 2012a)** and TruckSim **(Mechanical Simulation, 2012b)**. According to the National Highway Traffic Safety Administration (NHTSA) of the United States of America the SSF is the most reliable measure of the vehicle's tendency towards untripped rollover. The authors use an evaluation method where the disturbances are modelled as a worst case while the control input is optimised for the disturbance inputs. The authors come to the conclusion that the vehicle's tendency to roll over can be reduced by a VSC system. This shows that the dynamics of a vehicle with undesirable geometry like an SUV can be improved by other means than to change the geometry.

When cornering in a passively suspended vehicle, the sprung mass shifts to the outside of the vehicle's centreline. This has a negative effect on the roll stability of the vehicle. In terms of mass distribution it would be preferable to have the vehicle lean into the corner to move the CG to the inside of the vehicles centreline. This will create a moment that will act against the centrifugal force that can cause rollover **(Sampson and Cebon, 2003)**. The effect of this is very small but if the inside of the vehicle body is lowered this will also lower the CG which might have a bigger effect on the rollover propensity. This will have a desirable effect if cornering is only done in one direction, but if the weight suddenly shifts to the lowered suspension units as will be the case in a dynamic handling manoeuvre it can cause rollover. Thus it is not desirable to lower the units under normal or even hard driving conditions but it might be useful in an extreme case where rollover is about to occur. In order to do this a robust algorithm is needed that can predict rollover accurately. **Ozaki (2002)** concluded that the basic driving stability is equal for inward as well as for outward roll.

These are just a few examples that finding a universal method to define rollover propensity and handling poses a great challenge. This is made even more difficult by the fact that control systems can change the rollover propensity or handling characteristics of a vehicle.

A popular manoeuvre to measure rollover resistance is the Fishhook Manoeuvre and the **National Highway Traffic Safety Administration (2002)** describe two variants of the manoeuvre namely the Fixed Timing Fishhook (FTF) and the Roll Rate Feedback Fishhook (RRFF). The single difference between the two manoeuvres is that the dwell times between steering inputs are fixed for the FTF manoeuvre and that it is determined by the roll motion of the vehicle in the case of the RRFF manoeuvre. For these tests the vehicle is driven at a speed slightly higher than the desired entrance speed, the accelerator is then released and when the vehicle reaches the desired speed the steer robot engages the manoeuvre. The steer robot will give a steer input 6.5 times the steer input needed to obtain 0.3g lateral acceleration at 80km/h then after the determined dwell time it will give a countersteer input. All steer inputs should be done at 720 degrees per second. The Steering input and roll rate feedback for the RRFF manoeuvre is shown in Figure 6. The entry speed is increased until rollover takes place which is defined as 2 wheels lifting more than 51mm of the ground for more than 0.5 seconds. This test requires a wide enough track so that the manoeuvre can be performed without the risk of going of the track. Due to the lack of a wide enough track it was not possible to perform the Fishhook Manoeuvre during this study.

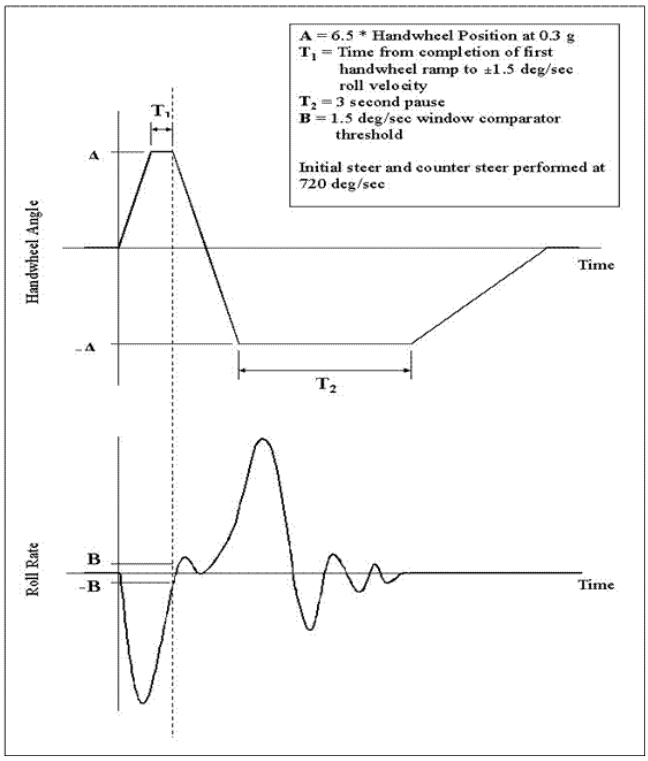

Figure 6 **NHTSA RRFF manoeuvre description (National Highway Traffic Safety Administration, (2002)**

2.2 Handling

The quality of the handling of a vehicle is determined by the ease with which a human can control the vehicle, in other words a vehicle that is easy to control has good handling and a vehicle that is hard to control has poor handling. There is currently no universally accepted method that can quantify the controllability of a vehicle seeing that various human beings will experience the controllability of a vehicle in different ways.

Uys et al. (2006a) investigated the possibility of a single, unambiguous objective criterion for handling. It is shown from literature that there is no single criterion to define handling, and experimental work is done where four drivers of different ages and gender drive three different vehicles. A one to one relationship is observed between the lateral acceleration and the roll angle in the case of all the test drivers. It is concluded that roll angle is a favourable criteria to optimise the suspension settings for a prescribed road, to determine when to switch over between a hard and a soft suspension and to measure handling.

It was shown in 2.1 that that a reduction in roll angle can decrease the tendency to roll over for a vehicle with a high CG. Thus if an improvement in the roll angle is obtained during a handling manoeuvre this will also indicate an improvement in the roll over tendency of the vehicle.

The handling of a vehicle can be divided into two categories namely steady state handling and dynamic handling. Steady state handling is somewhat easier to quantify than dynamic handling but does not give a

very good indication of how the vehicle will handle in a dynamic situation. Steady state handling can be tested with a constant radius test. It is however important that this test is used as a comparative test and that these tests are done around the same circle on the same surface. During this test the vehicle is driven around a circle maintaining a constant radius by changing the steer angle. The speed is increased until the vehicle can no longer keep to the prescribed path. The steering angle vs. speed indicates whether the vehicle under steers or oversteers. **Gillespie (1992)** recommends a minimum radius of 30m for the circle as shown in Figure 7.

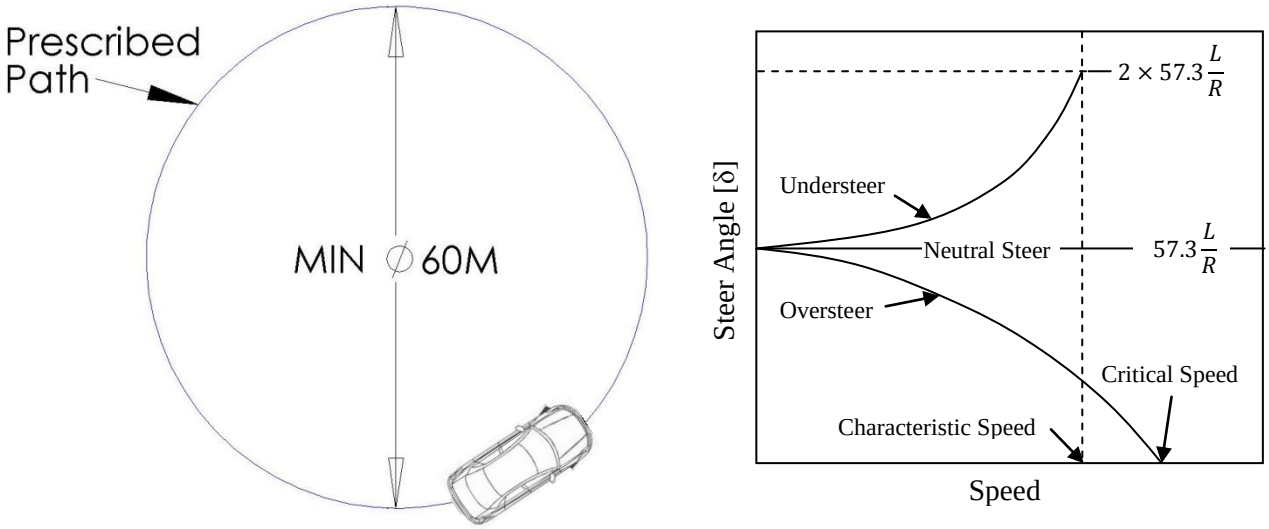

Figure 7 Constant Radius Test (Gillespie, 1992)

Steering characteristics such as over- and understeer can be derived using a simplified bicycle model. In this model the difference between the steer angles of the front wheels is seen as negligible. Thus the two wheels are represented as one wheel with a cornering force equal to the sum of the forces of both wheels at a steer angle δ. The same assumption is made for the rear wheels (see Figure 8). Body roll and lateral load transfer is ignored. The steer angle (in degrees) is then given by the following equation:

$$\delta = 57.3\frac{L}{R} + \left(\frac{W_f}{C_{\alpha f}} - \frac{W_r}{C_{\alpha r}}\right)\frac{V^2}{gR} \quad (3)$$

Where:

$C_{\alpha f} = Cornering\ stiffness\ of\ the\ front\ tires$
$C_{\alpha r} = Cornering\ stiffness\ of\ the\ rear\ tires$
$g = Gravitational\ acceleration\ constant$
$K = Understeer\ radient$
$L = Wheelbase$
$R = Raduis\ of\ turn$
$V = Forward\ speed$
$W_f = Load\ (Vertical\ Force)\ on\ the\ front\ axle$
$W_r = Load\ (Vertical\ Force)\ on\ the\ rear\ axle$

$$\alpha_f = \frac{W_f}{C_{\alpha f}} = Tire\ slip\ angle\ front$$

$$\alpha_r = \frac{W_r}{C_{\alpha r}} = Tire\ slip\ angle\ rear$$

$\delta = Steer\ angle\ at\ the\ front\ wheels$ (deg)

Neutral-, under- and Oversteer can now be defined as:

i) Neutral steer is when the no change in the steering angle is necessary to stay on the prescribed path (constant radius turn) as the speed increases or decreases.

$$\frac{W_f}{C_{\alpha f}} = \frac{W_r}{C_{\alpha r}} \rightarrow K = 0 \rightarrow \alpha_f = \alpha_r \quad (4)$$

ii) Understeer is when the steering angle needs to increase during a constant radius turn as the speed increases.

$$\frac{W_f}{C_{\alpha f}} > \frac{W_r}{C_{\alpha r}} \rightarrow K > 0 \rightarrow \alpha_f > \alpha_r \quad (5)$$

iii) Oversteer is when the steering angle needs to decrease with an increase of speed during a constant radius turn.

$$\frac{W_f}{C_{\alpha f}} < \frac{W_r}{C_{\alpha r}} \rightarrow K < 0 \rightarrow \alpha_f < \alpha_r \quad (6)$$

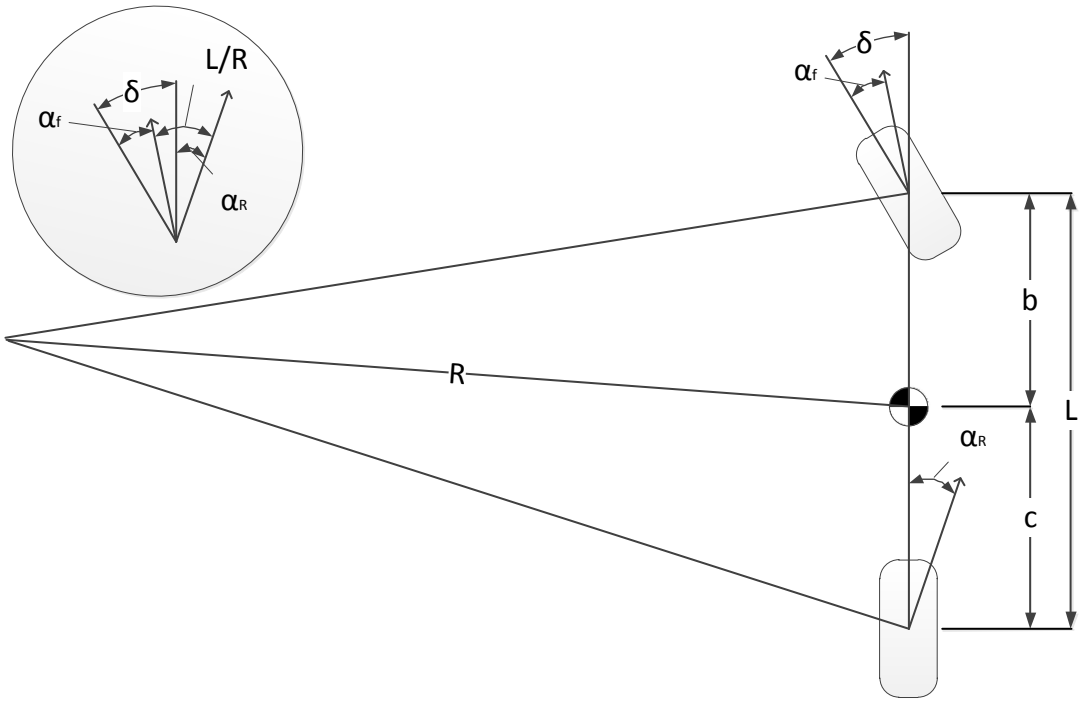

Figure 8 **Cornering of a bicycle model (Gillespie, 1992)**

The vehicle's handling characteristics (oversteer and understeer) can be changed by increasing the front or rear load transfer as indicated previously (Par. 2.1 and Figure 5) load transfer decreases lateral force. For example more lateral load transfer at the rear axle will result in a bigger rear slip angle and thus more oversteer, a vehicle that understeers will understeer less, a neutral vehicle will oversteer and a vehicle that oversteers will oversteer more **(Gillespie, 1992) & (Cronjé, 2008)**. Thus by controlling the suspension characteristics the vehicle can be forced into over- or understeer. The geometry and roll stiffness also play a role and as a result of the CG being far above the roll axis in an SUV, the CG causes a moment around the roll axis and this causes the vehicle body to roll outwards excessively. The inclination of the roll axis will also affect the lateral forces on the front and rear wheels. Having a roll axis that is lower at the front will decrease the lateral force on the rear wheels and increase it at the front wheels, this will help to obtain a vehicle that understeers rather than to oversteer **(Higuchi et. al., 2001).** Controlling the inclination of the roll axis might improve handling during dynamic manuoevres where the inclination can change.

Dynamic handling is often quantified using the Severe Double Lane Change (DLC) manoeuvre. The DLC manoeuvre is defined by the **International Organisation for Standardisation (1975)** as: "A dynamic process consisting of driving a vehicle from its initial lane to another lane parallel to the initial lane as fast as possible, and possibly returning to the initial lane.". Similar to the constant radius test this test is to be used as a comparative test where all the tests are done on the same surface. The track dimensions and cone placements are shown in Figure 9 and Table 1.

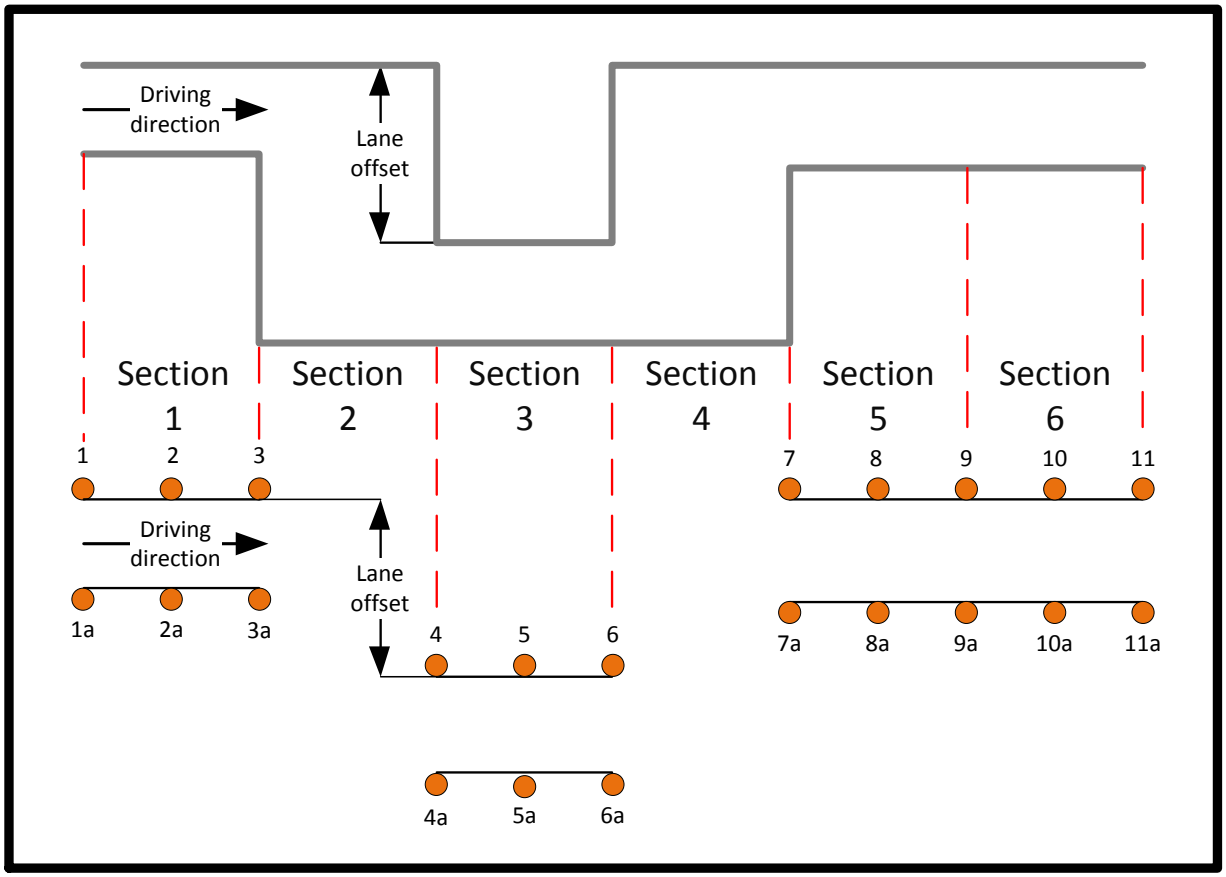

Figure 9 **Lane change track and cone placement (International Organisation for Standardisation, 1975)**

Table 1 Lane change track dimensions (International Organisation for Standardisation, 1975)

Section	Width	Length
1	1.1 x vehicle width + 0.25m	15m
2	Not Applicable	30m
3	1.2 x vehicle width + 0.25m	25m
4	Not Applicable	25m
5	1.3 x vehicle width + 0.25m	15m
6	1.3 x vehicle width + 0.25m	15m
Lane offset	3.5m	

The standard requires the test to comply with the following requirements:

- The lane change track must be marked by cones as shown in Figure 9
- The track limit must be tangential to the base circle of the cone as shown in Figure 9.
- The measuring distance starts at the beginning of section 1 and finishes at the end of section 5.
- The lane change must be done by a skilled driver.
- A passage is faultless when none of the cones positioned as specified have been displaced. **(International Organisation for Standardisation, 1975)**

Note that the lane change indicated in Figure 9 is mirrored from that given in the standard because it is applied to a right hand drive vehicle.

Several other handling tests exist as well, for example: The J-turn and Sine Sweep.

Other methods to quantify the handling of a vehicle is also possible for instance to measure the biological reactions of the driver, and then to use this to determine the workload the driver is experiencing. This test method was used by **Abe and Manning (2009)** to determine the controllability of a vehicle with oversteer characteristics compared to that of a vehicle with understeer characteristics. It was found that a vehicle with moderate understeer characteristics is easier to control. This test method does however require some medical knowledge as well as the appropriate equipment and is not easily executable without the appropriate expertise.

2.3 Methods to improve rollover and handling characteristics

There are various methods to improve handling including changes to the physical dimensions or aerodynamics of the vehicle. The handling can also be improved by changing the suspension characteristics either passively, semi-actively or actively. SUV's drive relatively slow and aerodynamic downforce is largely dependent on the speed of the vehicle therefore this will not be considered here. Changing the physical dimensions of the vehicle will also not be considered seeing that most of these dimensions are constrained due to some requirement other than handling.

Thus methods to improve handling that do not necessarily require changes to the geometry of the vehicle will be considered here. Any factor influencing the cornering force will directly affect the directional response of the vehicle. The suspension is one of the primary contributors to these influences. One of these influences is the load transfer that is largely determined by the suspension and can increase or decrease the lateral force possible **(Dukkipati et al., 2008)**. Optimising a passive suspension for handling

results in a vehicle with poor ride comfort and similarly good ride comfort results in poor handling, for this reason the tendency is to implement some form of control on suspensions to give good ride comfort and good handling in the relevant circumstances.

Shim and Velusamy (2010) categorises active roll control in the following four main categories: four wheel steering, active suspensions, active roll bars and differential braking.

2.3.1 Four wheel steering

Shaout et al. (2000) developed a nonlinear controller for a four wheel steering (4WS) vehicle. A single track nonlinear vehicle model is used and a linear quadratic regulator model is used to control the 4WS. It is concluded that the control is robust and effective in the presence of noise and shows an improvement in handling. No experimental data is given and no comment is made on the improvement of handling compared to a two wheel steer (2WS) vehicle.

Hakima and Ameli (2010) modelled a four wheel steer vehicle with an electronic stability program using the brakes to generate a corrective yaw moment using a 3 degree of freedom model. The steering is controlled using a fuzzy logic controller. The simulation results show that the system can improve the vehicle's handling and directional stability significantly. No experimental verification is given.

2.3.2 Passive interconnected suspensions

Interconnected suspensions are a popular method to overcome the ride handling compromise. **Smith. and Walker (2005)** defines an interconnected suspension as a system where a displacement at one wheel station can produce forces at other wheel stations. Concepts of hydraulic interconnected suspensions (HIS) is found as early as 1927, **(Hawley, 1927)**, and interconnected suspensions were widely used during 1950 to the 1970s for ride comfort improvement. In the later years the emphasis of these suspension systems moved to vehicle roll. Most of these systems were based on two wheel interconnections however, having a drawback due to the loose coupling between modal pairs. The advantage in four wheel interconnected systems lies in their ability to provide features such as increased roll stiffness together with reduced articulation stiffness and decoupled roll and bounce damping in a passive system. **Wilde et al (2005)** simulated and tested a kinetic suspension using a fishhook test. The performance was determined by the maximum speed the vehicle can maintain during the manoeuvre without a rim touching the ground or two wheels lifting more than two inches (51 mm) of the ground. The vehicle's speed improved from 43mph (69 km/h) to 60 mph (97 km/h). Figure 10 shows the different flow distributions on a schematic of the kinetic suspension used. **(Smith and Zhang, 2009)**

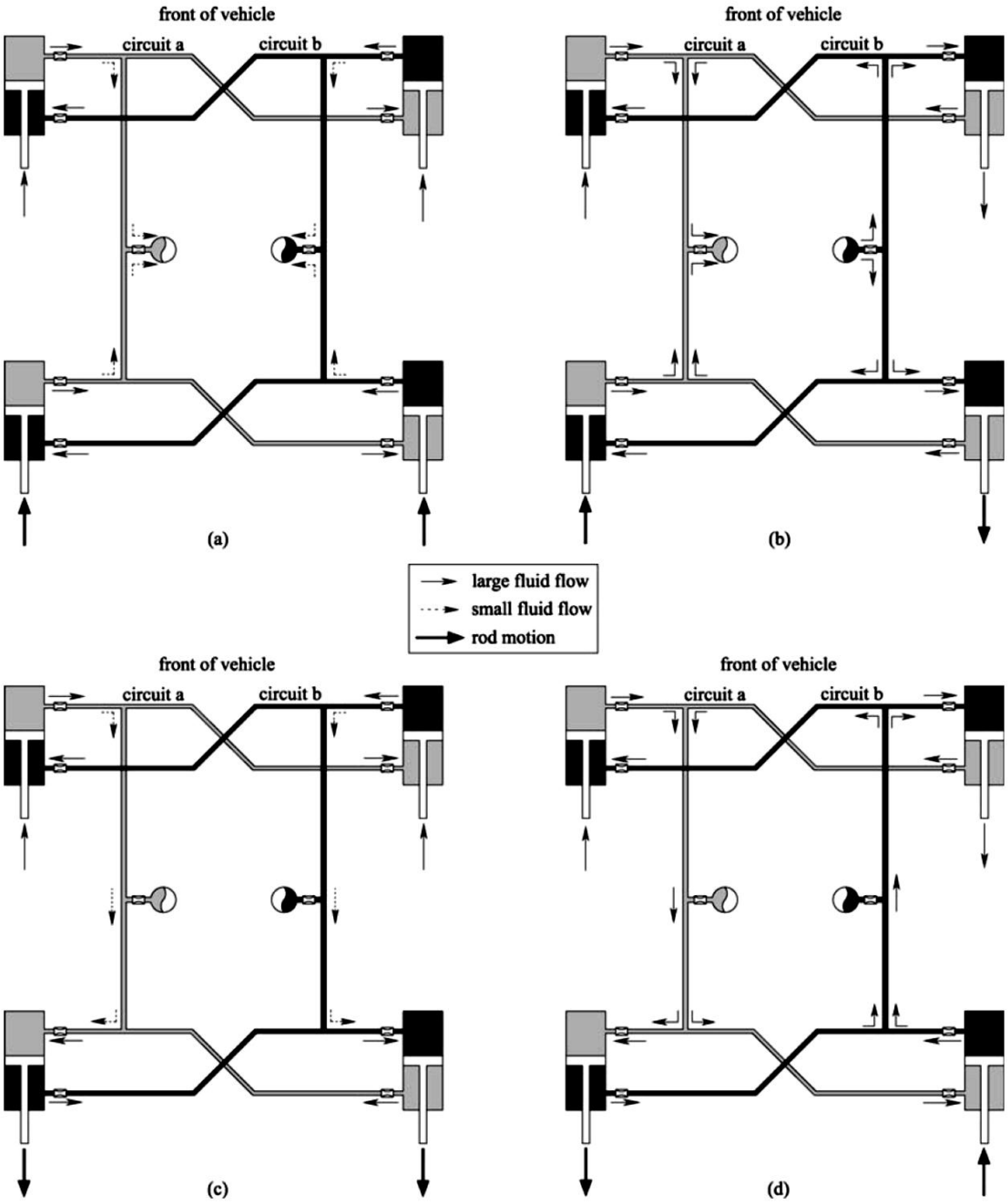

Figure 10 **Nominal fluid flow distribution in an idealised suspension modes (a) bounce, (b) roll, (c) pitch, and (d) articulation (Smith and Zhang, 2009)**

2.3.3 Semi-Active and Active Suspension Systems

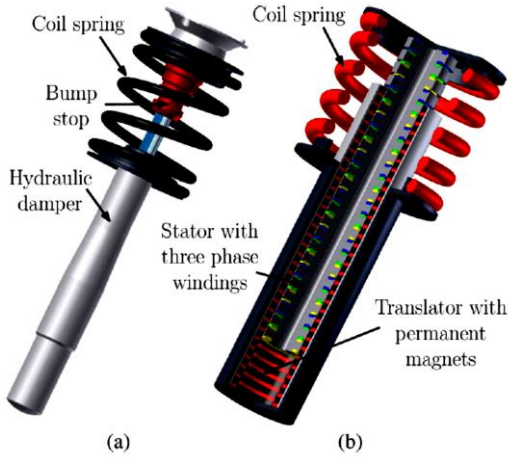

Figure 11 **(a) Conventional passive suspension system. (b) Electromagnetic suspension system. Geysen et al (2010)**

According to **Fischer and Isermann (2004)** it is important to keep the unsprung mass resonance frequency near 10Hz to increase the tire's contact with the road and thus increase the handling. On the other hand it is preferable to have the sprung mass resonant frequency at 1Hz for good ride comfort. This means that a passive system always results in some compromise between handling and ride comfort. Active and semi-active suspensions attempts to solve or reduce this compromise. Semi-active suspension systems adapts the damping or suspension stiffness to the demand where active suspension systems provides an extra force input in addition to the possible passive system. Active suspension systems have high power requirements. **Semi-active dampers** conventionally consist of a damper with a bypass that can be opened and closed to provide different states of damping. One variation of active or semi-active dampers are **magneto-rheological (MR) dampers**, these dampers offer stable hysteretic behaviour over a broad temperature range, a broad bandwidth and can have fast response times. **Active suspension systems** can be hydraulic, hydro-pneumatic, pneumatic, electro-mechanical, etcetera. Due to their complexity, high costs and high energy demand the commercial availability of these systems are limited. Figure 11 shows a passive suspension compared to an active electromagnetic suspension.

2.3.3.1 Four State Semi-Active Suspension ($4S_4$)

According to **Theron and Els (2003)** a vehicle's passive suspension always has to make some compromise between handling and ride comfort. Good ride comfort will require a soft suspension with good wheel travel to minimise the disturbances carried trough from the wheels to the occupants. For optimal handling the suspension needs to be stiff to minimise body roll as explained in the previous section. With controllable suspensions the characteristics of the suspension can be changed while the vehicle is driving, this can vastly reduce or maybe even eliminate the compromise between ride comfort and handling. According to **Wallentowitz and Holdman (2010)**, two spring stages are sufficient to overcome this compromise. A soft spring is used to obtain optimal ride comfort while a stiff spring is used during handling manoeuvres and braking. This phenomenon is illustrated in Figure 12.

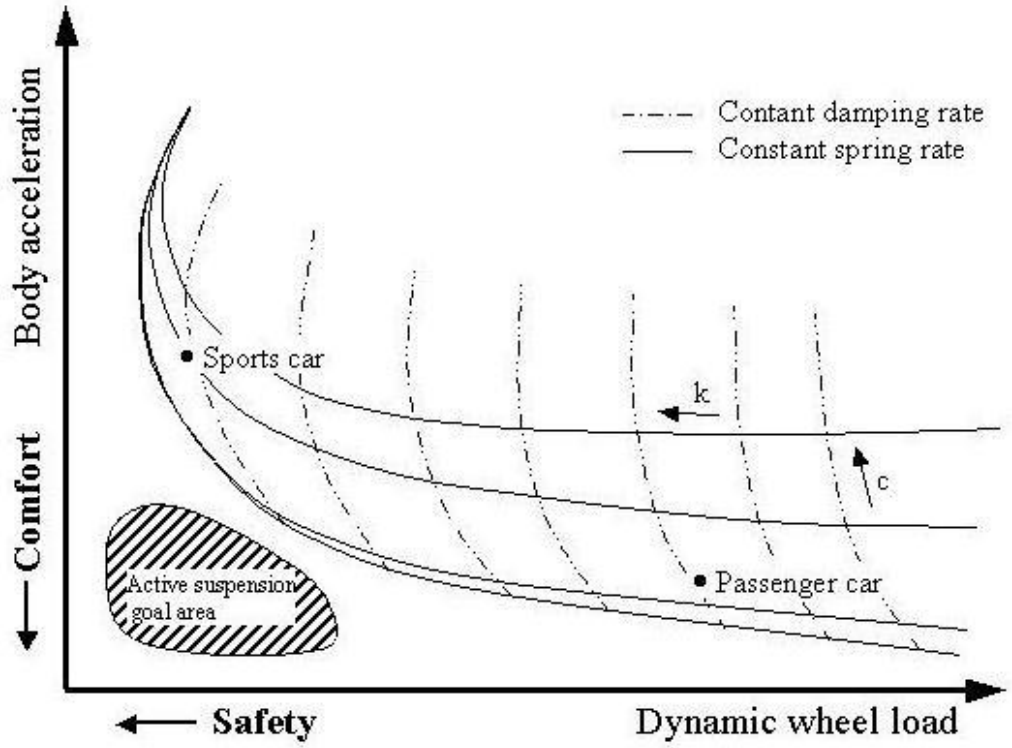

Figure 12 Suspension Design (Holdmann and Holle, 1999)

The four state semi-active suspension system ($4S_4$) was developed by **Els (2006)** which uses semi-active hydropneumatic springs and hydraulic dampers. The $4S_4$ was optimised to give optimal ride comfort (soft springs and low damping) and to give optimal handling (hard springs and high damping) on its specific settings. The ride comfort was optimised by minimising the vertical acceleration and the handling by minimising the body roll angle when performing a DLC. The $4S_4$ can switch between hard and soft spring settings and between high and low damping in less than 100 milliseconds. This is done automatically based on acceleration measured on the vehicle body. The switching is done by opening or closing solenoid valves (See par. 3.3). A schematic diagram of a 4S4 unit can be seen in Figure 13. The wheel displacement relative to the vehicle body results in the displacement of the piston in the main strut which is filled with oil. The oil then flows through the damper packs or valves until the oil pressure and the pressure of the accumulator equalises. If valves 3 and 4 are closed the suspension is on the stiff spring setting where only the 0.1 litre nitrogen accumulator is used as a pneumatic spring. If valves 3 and 4 are open it is on the soft spring setting where both the 0.4 litre and the 0.1 litre accumulators serve as a pneumatic spring. If valve 1 and 2 are closed the system has high damping because the oil flow is forced to flow through the damper pack, and if they are open the system has low damping because the oil flow can flow past the damper pack through the open valves. Two valves were used at 3 and 4 due to the high flow requirement and a faster response time is possible using two smaller valves compared to that of a larger single valve.

The $4S_4$ can change the driving characteristics of the vehicle from ride comfort mode to handling mode in a fraction of a second. It also has the added advantage that the power required is mainly that of the solenoid valves which results in a fraction of the power requirement of a fully active suspension. This suspension has been implemented successfully on a Land Rover Defender 110 at the University of Pretoria and experimental results of a DLC has shown improvements in the roll angle as high as 78% for the handling setting compared to the baseline vehicle. The comfort setting gave a 50 % to 80% improvement in ride comfort compared to the handling setting when driving over a Belgian paving. The suspension characteristics for the different settings of the $4S_4$ are shown in Figure 14 and Figure 15

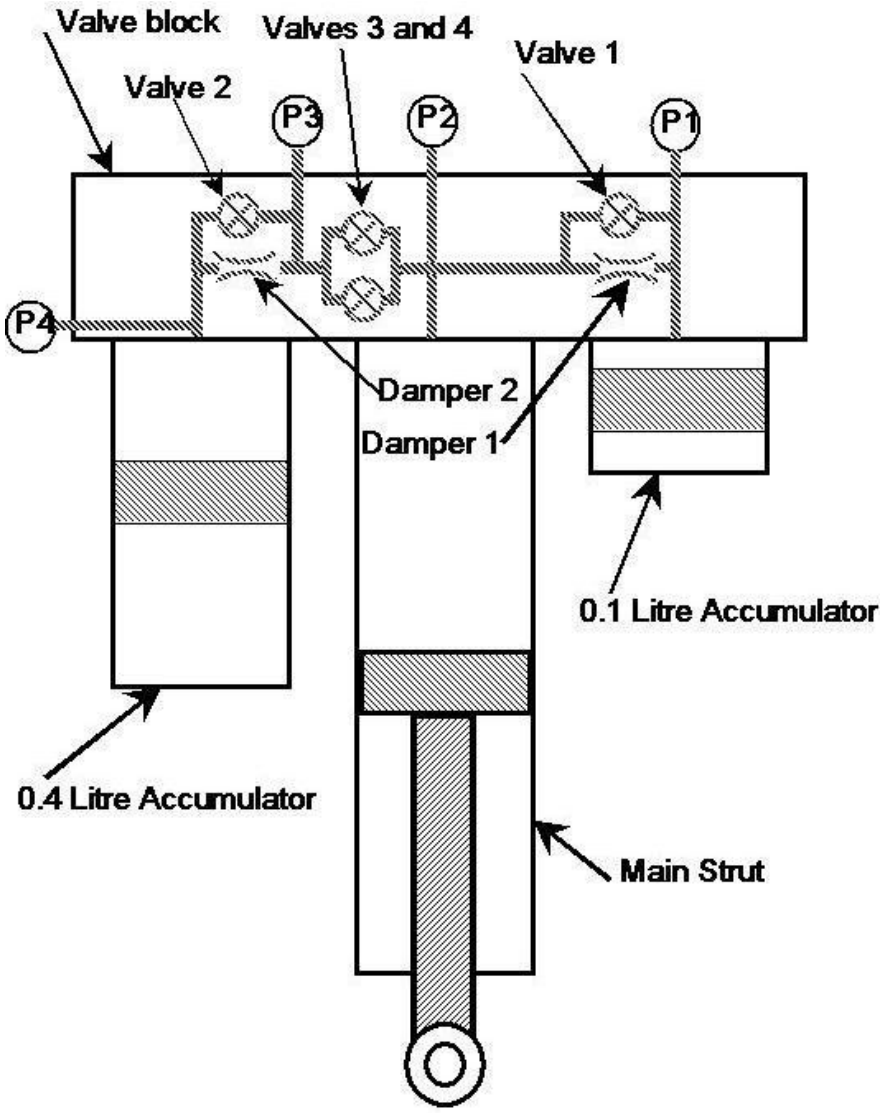

Figure 13 Schematic diagram of the $4S_4$ (Els, 2006)

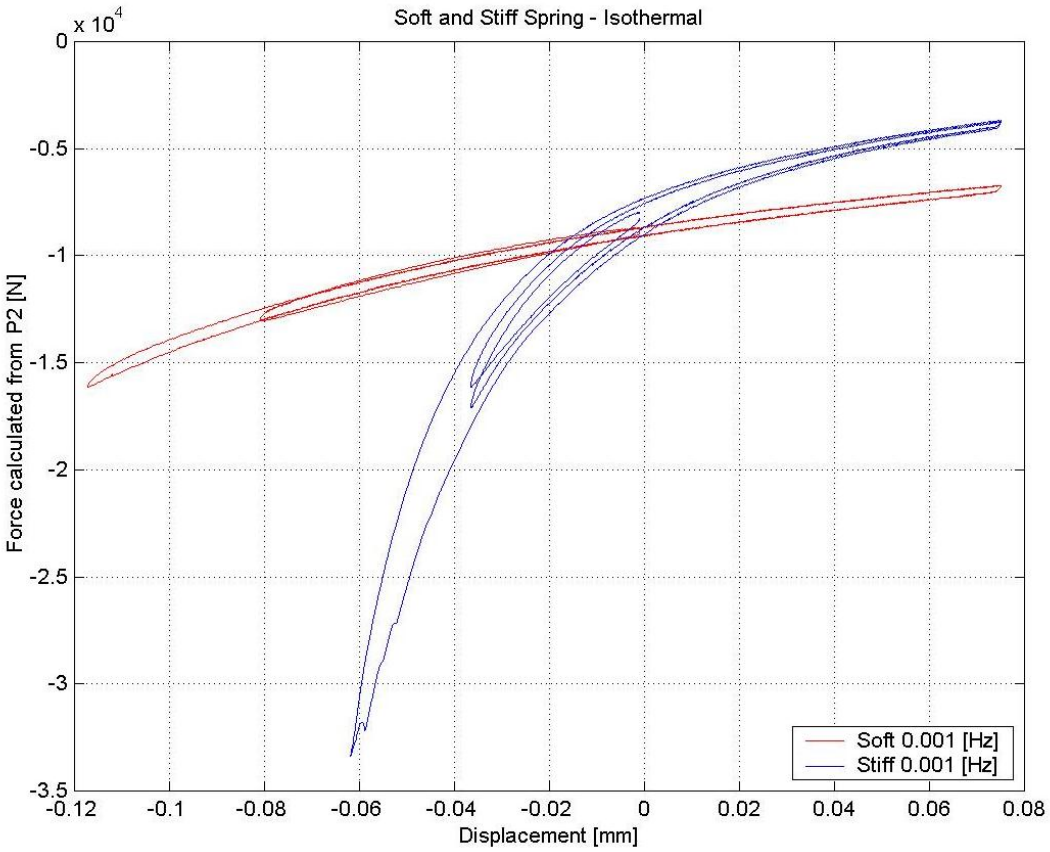

Figure 14 **Soft and Stiff spring characteristics of the $4S_4$ (Els, 2006)**

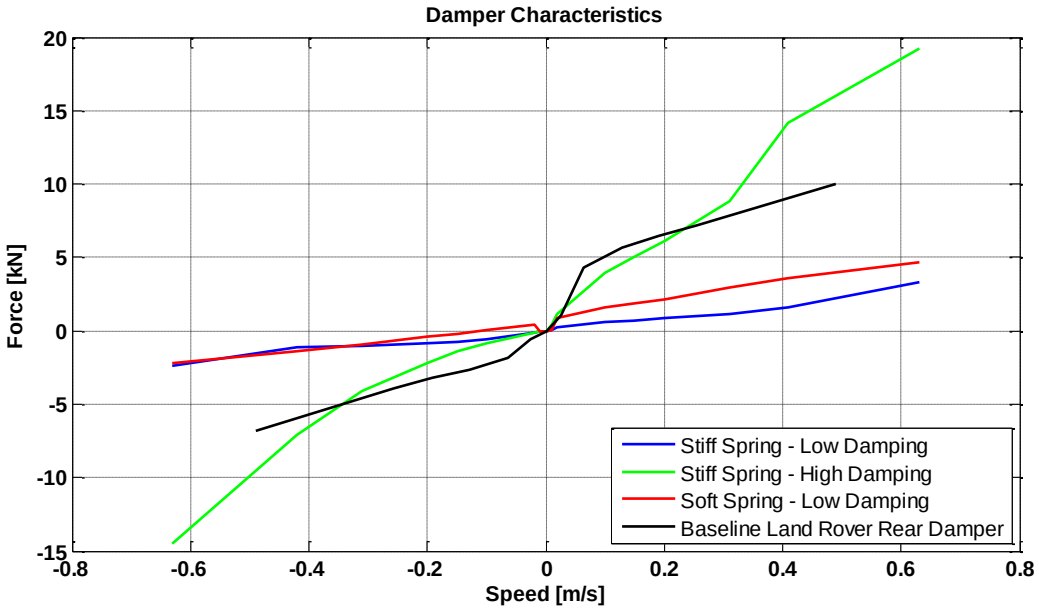

Figure 15 **Damper characteristics of the $4S_4$ (Els,2006)**

2.3.3.2 Other Semi-Active Systems

Choi et al. (2001) carried out field tests on a semi active electro-rheological (ER) suspension system. It is unclear what type of springs was used but the vehicle was fitted with ER dampers. The results showed an improvement in the ride quality over bumps and a reduction in roll angle during a sinusoidal test which shows that the steering stability has increased.

Nell and Steyn (2003) describes the development of a two-state semi-active translational damper implemented on a 6x6 high mobility off-road vehicle. The semi-active dampers consisted of the vehicle's original dampers fitted with a controllable bypass valve to provide a second state. Experimental tests included driving over Belgian paving and a rough suspension track for ride comfort and for handling the severe double lane change manoeuvre was performed. Experimental results showed an improvement in ride comfort as well as handling for the low and high damping settings respectively. The speed through the double lane change was improved by 9.4%, the roll velocity decreased by 9.6 % and the yaw velocity increased by 6%.

Ha et al. (2009) used a 6 degree of freedom model to simulate the dynamics of a 6 wheeled military vehicle. The vehicle, equipped with gas springs and semi-active MR dampers, is compared to the vehicle with its passive suspension. It is concluded that the steering stability can be improved and an improvement in body roll angle is also shown when driving over a random road surface and a bump at 50 km/h. No validation of the simulation results is given.

Dong et al. (2010) concludes that the performance of a MR damper is highly dependent on the algorithm used to control the damper. And thus good hardware without proper control will not necessarily improve the vehicles handling.

2.3.4 Active Systems

Geysen et al (2010), states that active hydraulic systems are commonly used due to their high force density, availability and the maturity of the technology but hydraulic systems can have relatively low efficiencies (pressure losses and flexible pipes) and a small operational bandwidth. An alternative to a hydraulic system is an active electromagnetic suspension system which allows for both the elimination of the road disturbances and active roll and pitch control. If a mechanical spring is used it also does not require continuous power as with a hydraulic system and can operate over a larger bandwidth. These systems however require a relatively high current at 12 V and are expensive to implement. (See Figure 11)

De Bruyne et al. (2011) use advanced vehicle state and parameter estimation to obtain the necessary parameters to implement skyhook control on an active suspension. The states and parameters are estimated using 4 suspension displacement sensors, 3 vertical accelerometers on the vehicle body and some longitudinal and lateral accelerometers. It was found that a significant reduction in body roll is possible during a slalom manoeuvre.

2.3.4.1 Active Anti Roll Bar on the $4S_4$

Anti-roll bars (ARB) control the roll stiffness independent of the vertical stiffness of the vehicles suspension. An Active Anti-Roll Bar (AARB) is an anti-roll bar that is controlled by some means to actively increase or decrease the roll stiffness of the vehicle when necessary. This enables the control of the of the body roll angle of the vehicle as well as the load transfer during cornering.

Cronje (2008) implemented a hydraulically controlled AARB on a Land Rover Defender test vehicle at the University of Pretoria. The AARB was controlled using a hydraulic actuator with a MOOG hydraulic servo valve with a maximum flow rate of 19 l/min. The displacement of the actuator was measured using a string displacement meter and the displacement data was then used to control the AARB. The servo valve was controlled with a Zwick Roell K7500 servo controller.

In conjunction with the $4S_4$ (See par. 2.3.3.1) it was possible to test the effect of the AARB on soft and hard suspension settings. It was found that a significant improvement in the body roll angle is possible using an AARB in during a DLC (See Figure 16) and a constant radius test (see Figure 17). The AARB was designed to keep the body roll angle at a minimum up to 0.4g where after body roll is allowed to warn the driver that the vehicle is reaching its limits. It was also found that the AARB had no significant effect on the ride comfort of the vehicle when driving over a rough road as can be seen in Table 2. Cronje concluded that an AARB can dramatically improve the handling of an off-road vehicle without sacrificing the ride comfort.

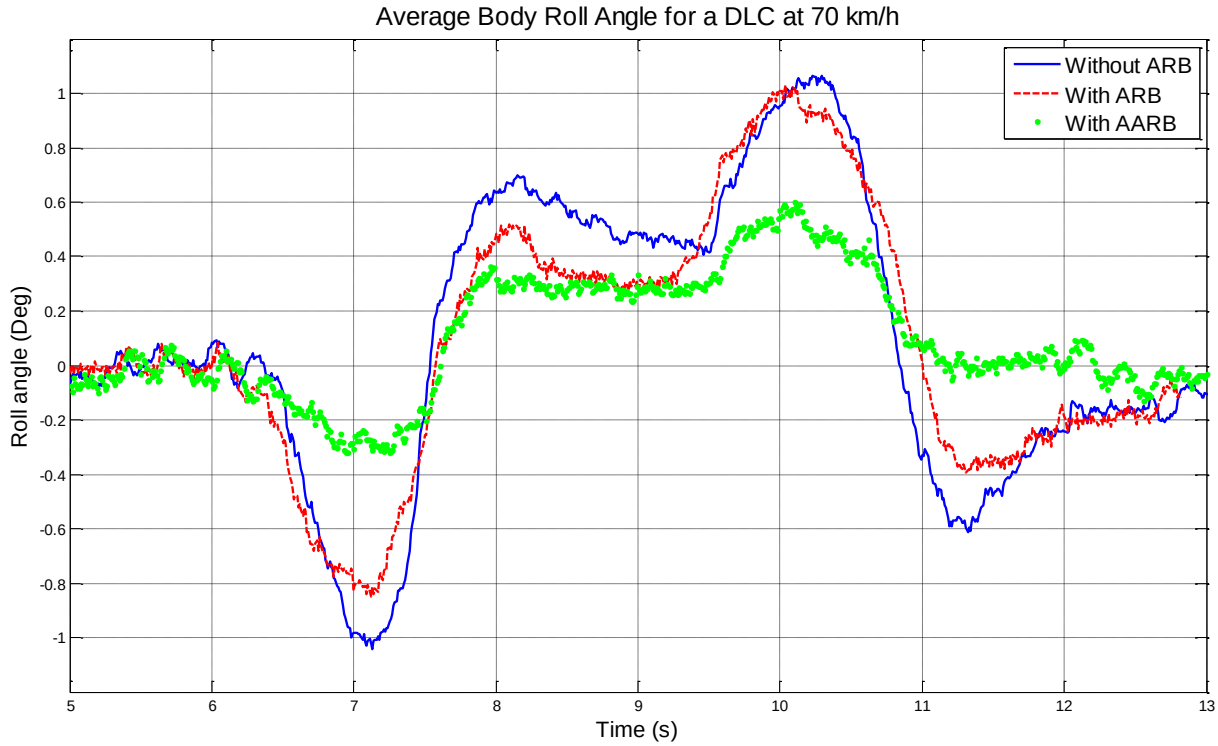

Figure 16 **Average body roll angles for different ARB settings on the stiff suspension during a DLC at 70 km/h (Cronje, 2008)**

Table 2 **Weighted RMS of vertical acceleration for test runs on a Belgian paving (Cronje, 2008)**

Suspension setting	ARB setting	Weighted RMS:
Soft	Disconnected	1.43 m/s^2
Soft	Connected (Passive)	1.41 m/s^2
Soft	Active	1.44 m/s^2

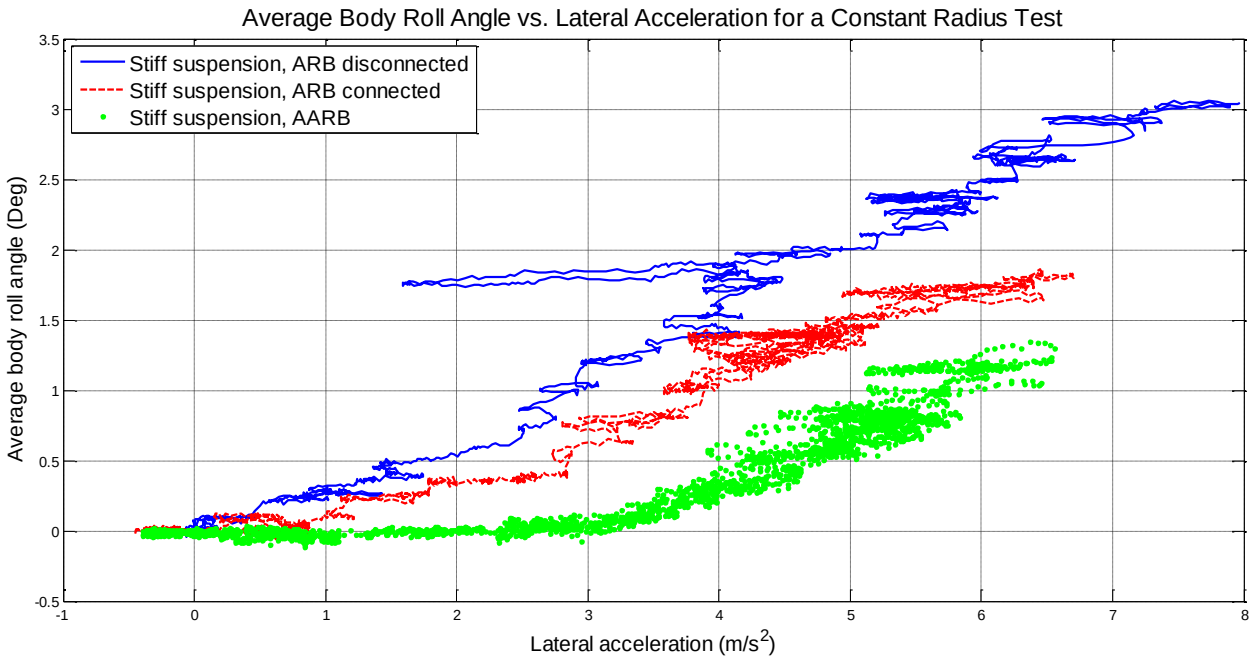

Figure 17 **Average body roll angle vs. lateral acceleration during a constant radius test (Cronje, 2008)**

2.3.4.2 Other Active Anti Roll Bars

Sampson and Cebon (2003) designed an active roll control system that can generate a roll moment between the sprung and unsprung mass at each axle. It consists of a stiff U-shaped anti roll bar connected to the trailing arms of the suspension and to the vehicle frame via a pair of double acting hydraulic actuators. A lumped mass is added to the truck to simulate a fully laden trailer. It is concluded that an improvement of between 26% and 46% in roll stability is possible over a passive suspension. Only simulation results are presented here and no experimental validation is given.

Cimba et al (2006) designed an active torsion bar system that utilises an anti-roll bar actuated by a hydraulic actuator. The system cancels the body roll up to a lateral acceleration of 5g where the system reaches saturation and the vehicle body will begin to roll at a rate similar to a passive suspension. Simulations were done and some of the results were then verified with experimental tests. The results show that an overall reduction in body roll of up to 73% may be possible.

2.3.5 Stability Control

Jo et al. (2008) investigates the use of a vehicle stability control system to prevent accidents from occurring. This system uses the vehicle's differential brake system to generate a yaw moment to improve the vehicle stability. Other control systems such as four wheel steer, active front wheel steer, rear wheel steering and differential traction is also mentioned. The satisfactory performance of the system is verified with a CarSim model as well as with experimental results. During the experimental test a single lane change at 90km/h with a SUV is done and a significant improvement in the yaw rate was obtained with the control system.

2.3.6 Tilting Vehicle

Gohl et al. (2004) implemented Steering Tilt Control (STC) on a narrow tilting vehicle. Tilting the vehicle moves the centre of gravity to the inside of the corner during cornering. This reduces the vehicles tendency to roll over due to the moment around the outside wheels being reduced. Without the STC the vehicle tipped over and with it was stable during cornering, thus it improved the stability of the vehicle but no quantitative value is given. It is however stated that this principle is more effective on narrow vehicles. Figure 18 shows an example of a tilting vehicle.

Figure 18 Tilting Vehicles (Rotpod, 2012)

2.4 Effect of height control on suspension characteristics

A passive suspension is designed to give some compromise between ride, handling and rollover for the range of different vehicle loads. Throughout the load range the suspension should allow enough travel for the suspension in both directions to avoid hitting the bump stops that have a negative effect on ride comfort. A linear passive suspension has a constant spring constant k, and the natural frequency ω_n is given by:

$$\omega_n = \sqrt{\frac{k}{M}} \tag{7}$$

From the equation it becomes clear that if the mass M increases, the natural frequency becomes lower or in other words the suspension becomes softer (see Figure 19). Not only does this have a negative effect on the handling but it also decreases the suspension travel and therefore increases the possibility of hitting the bump stops of the suspension. Therefore this suspension will always operate under some form of compromise depending on the load of the vehicle. The hydropneumatic suspension shares the favourable

characteristic of that of a pneumatic suspension that the force increases nonlinearly as the displacement increases.

To address the problem of changes in vehicle mass level control can be used. This can be done with different approaches. Mechanical level control exists but is rarely used. Level control on pneumatic suspensions is done by increasing the amount of gas where in hydropneumatic suspensions the amount of oil is changed. In both cases the pressure of the gas increases but in the case of the pneumatic suspension the volume of the gas stays constant while the mass increases. In the case of the hydropneumatic suspension the mass of gas stays the same and the volume decreases. For this reason there is a progressive behaviour in the spring rate vs. the sprung mass (Figure 20) for hydropneumatic suspensions (higher mass means higher spring rate). The advantage of doing level control with a hydropneumatic suspension is that the flow required is much lower than that of a pneumatic suspension due to the ideally incompressibility of the oil. **(Bauer, 2011)**

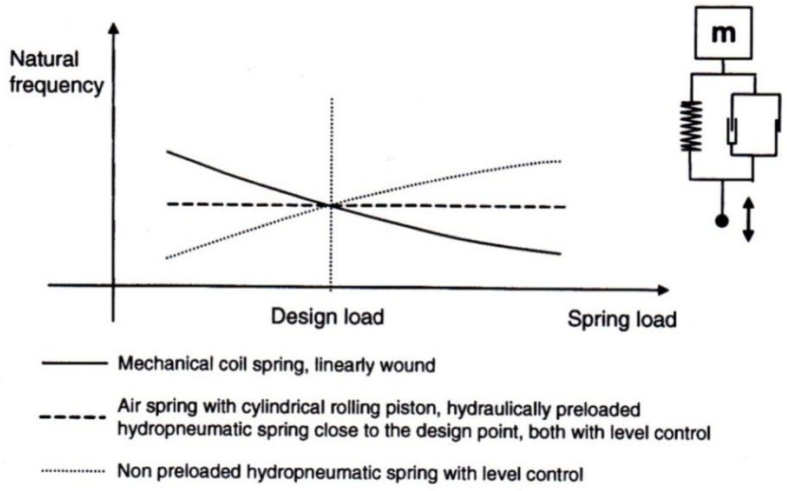

Figure 19 **Natural frequency as a function of spring load for for a mechanical, pneumatic and a hydropneumatic suspension (Bauer, 2011)**

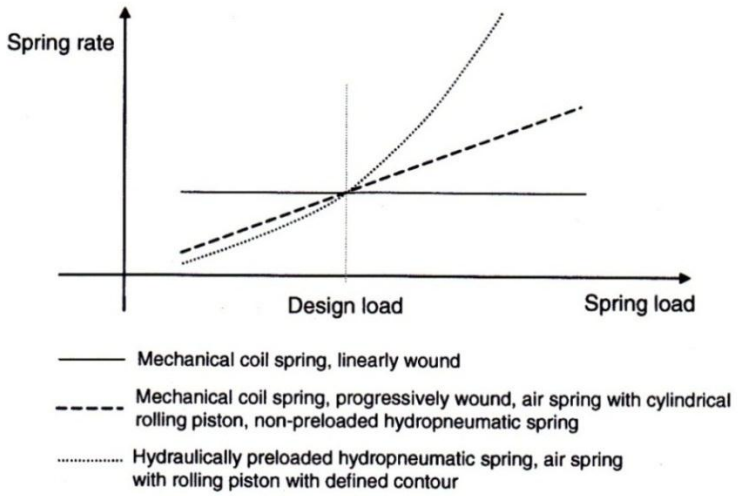

Figure 20 **Spring rate as a function of spring load for a mechanical, pneumatic and a hydropneumatic suspension (Bauer, 2011)**

2.5 Conclusion

There are various methods to improve the handling and rollover propensity of a vehicle. Four wheel steer is a feasible alternative but requires a robust algorithm to be able to use it for commercial purposes. It will also require a rear steering system which will add extra weight and costs. Tilting might also improve the vehicles rollover propensity to some extend but is less effective on normal vehicles. Stability control is another feasible alternative but is already widely in use commercially and many new vehicles are sold standard with stability control.

Cronje (2008) obtained satisfactory results for handling improvement using an AARB and found that it had a negligible effect on the ride comfort, but this is an expensive solution due to the expensive servo valve and servo controller. The AARB also has the downside that extra components and weight needs to be added on to the vehicle and it can only control the roll stiffness and lateral load transfer on the rear axle, thus it has highly limited uses.

It might be possible to achieve the same by controlling the suspension displacement utilising the existing height control on the $4S_4$ suspension. **Bauer (2011)** concluded that handling can be improved for different load cases with level control (similar to slow active suspension displacement control) on a hydropneumatic suspension. Not only will this be less expensive than an AARB, it will also require less extra weight and equipment, give the possibility to control load transfer in all directions, control the CG height and allow for tilting.

From the literature it became clear that active suspension has many advantages but that their large power consumption is a shortcoming. Using slow active suspension displacement control where the suspension is a single acting hyropneumatic actuator, will reduce the power requirement seeing that power will only be required to pump oil into the suspension. Oil will be drained form the suspension utilising the pressure difference between the oil in the suspension and the atmosphere. Slow active suspension control seems like a feasible method with added advantages over active suspension control and will be investigated in this study.

The simulation model, theoretical development and simulation results used to determine the feasibility of slow active suspension control are given in Chapter 3, while the experimental results and a comparison between the experimental and simulation results are given in Chapter 4. A conclusion is given in Chapter 5 and recommendations for future work in Chapter 6.

3. Simulation Results

The test vehicle used in the following simulations is a Land Rover Defender 110, fitted with the $4S_4$ suspension as described in par. 2.3.3.1.

In order to determine the feasibility of slow active roll control, using height adjustment of the $4S_4$ struts, several simulations have been done. In the simulations the aim was to minimise the displacement of each suspension unit by pumping oil into the system from a pressurised accumulator when the suspension is compressed, and to allow oil to flow out of the suspension to atmospheric pressure when the suspension unit is extended. Initial simulations were done with simple suspension models and as the project progressed the models were updated and improved to incorporate additional parameters.

In this chapter the vehicle model, some key requirements for slow active suspension control and the results of the initial simulations will be discussed. All the simulation result shown in this chapter were simulated using an ideal gas suspension model and the valve characteristic of the SV10-24 valves as described in par. 3.3, seeing that none of the final system specifications was available at the time. The baseline and controlled runs were done with the same model each time to make sure that the improvement is not due to other model parameters, but due to the suspension control.

3.1 Full Vehicle Model

A full vehicle model of the Land Rover Defender 110 test vehicle used in this study was developed by **Thoresson (2007)** in ADAMS/View **(MSC.Software, 2011)**. This model has 15 unconstrained degrees of freedom. It also has 16 moving parts, 6 spherical joints, 8 revolute joints, 7 Hooke's joints and a motion defined by the steering driver. The model was modified by **Uys et al (2007), Cronje (2008)** and **Botha (2011)** to add the additional changes made to the test vehicle. The ADAMS/View model is linked with Simulink and Matlab **(MathWorks, 2012)** using the ADAMS/Control interface. Adams/View exports the vehicle dynamics variables to Simulink **(MathWorks, 2011)**. These variables are then used to do calculations and the relevant variables are sent back to ADAMS/View (See Figure 21). An example of this is the suspension forces that are calculated using a Matlab model and then sent back to ADAMS via Simulink.

An extensive amount of work has been done to get an accurate model that verifies well with experimental results. The Hydro-pneumatic $4S_4$ suspension units fitted to the test vehicle has been modelled as an adiabatic process using the ideal gas law. It also takes into account non-linear friction, damping and the bulk modulus of the oil derived from experimental results. The model makes use of the Pacejka 89 tyre model **(Pacejka, 2002)**. The longitudinal behaviour of the tyre and vehicle is not taken into account to make the model less computationally expensive. The more important vertical and lateral dynamics is however taken into account. The body torsion is taken into account by dividing the vehicle body in two rigid bodies and connecting them with a revolute joint and a torsional spring. The bump and rebound stops are modelled as non-linear force elements. The suspension bushings are modelled using kinematic joints with torsional spring characteristics. The CG, and moments of inertia has been determined experimentally and is also incorporated in the model (Uys et al, 2006b). See Figure 22 to Figure 25 for the suspension layout in the ADAMS model.

The model has been fully validated against 16 measured channels during experimental testing and very good correlation was obtained. The vertical verification was done by driving over discrete bumps and the dynamic verification was done by performing a DLC at 65km/h. Some of the relevant results are shown in Figure 26.

A validated model as described above is extremely valuable for the initial development of a new project. This model will be modified to determine the feasibility of slow active suspension control on a SUV.

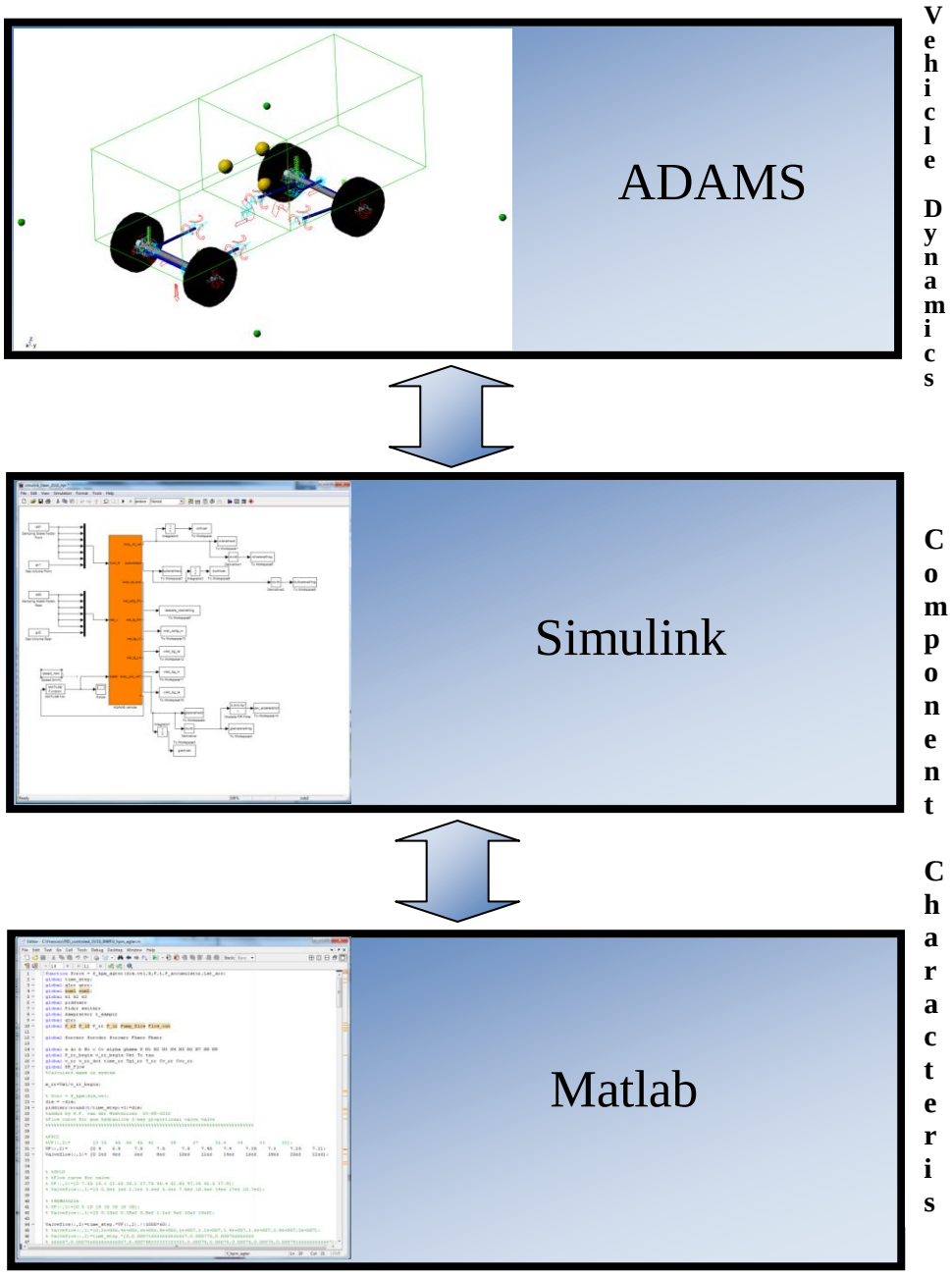

Figure 21 Simulation model interaction (Cronje, 2008).

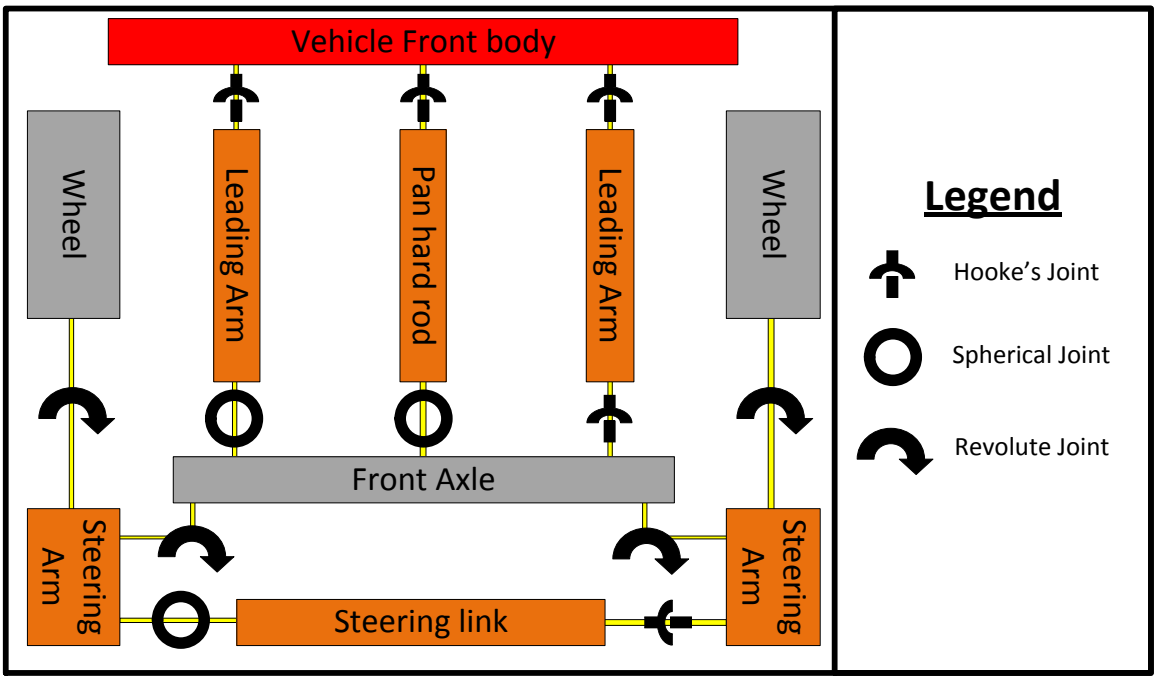

Figure 22 **Schematic of the front suspension (Thoresson, 2007).**

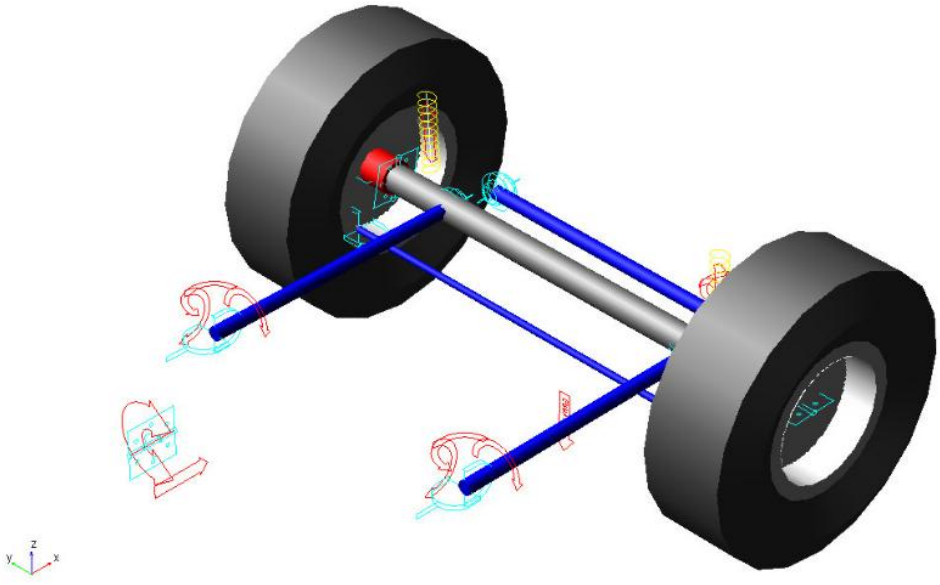

Figure 23 **Front suspension in ADAMS model (Thoresson, 2007).**

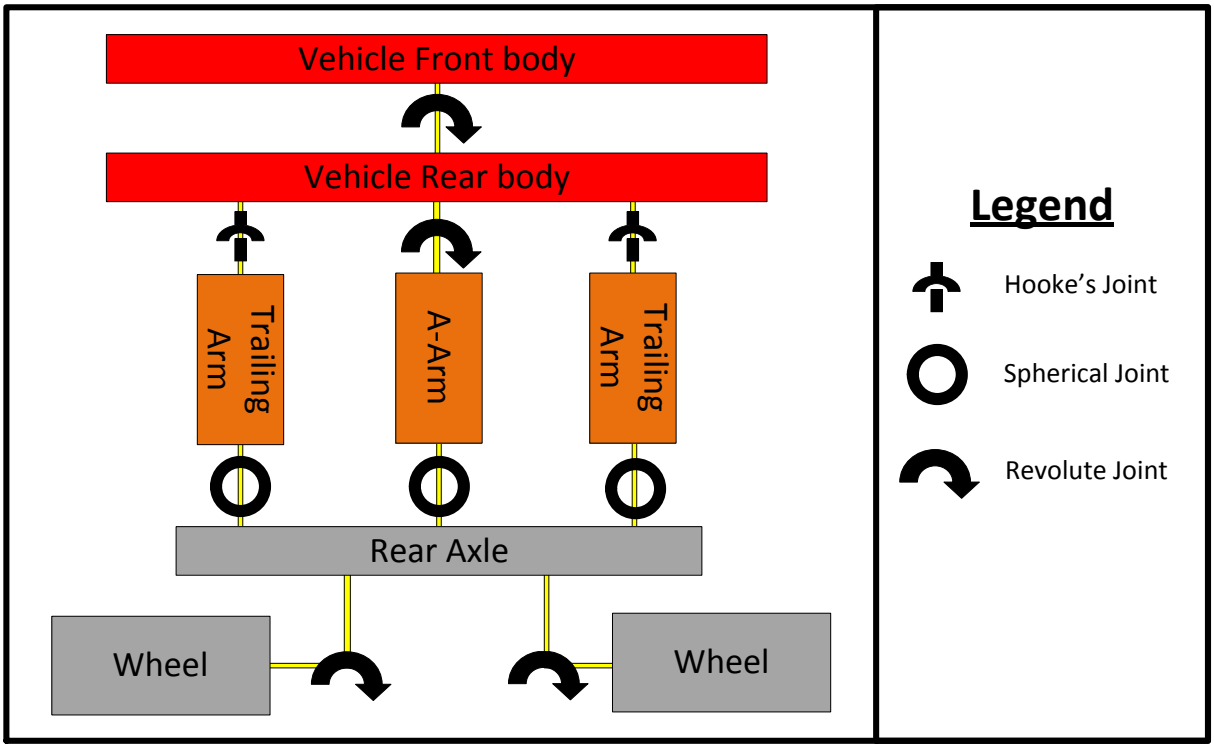

Figure 24 **Schematic of the rear suspension (Thoresson, 2007).**

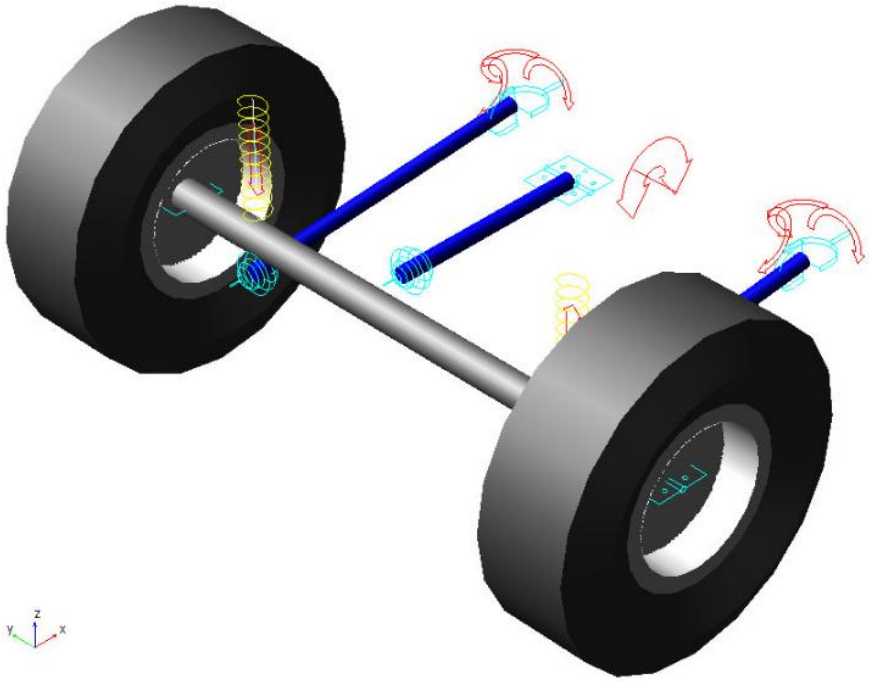

Figure 25 **Front suspension in ADAMS model (Thoresson, 2007).**

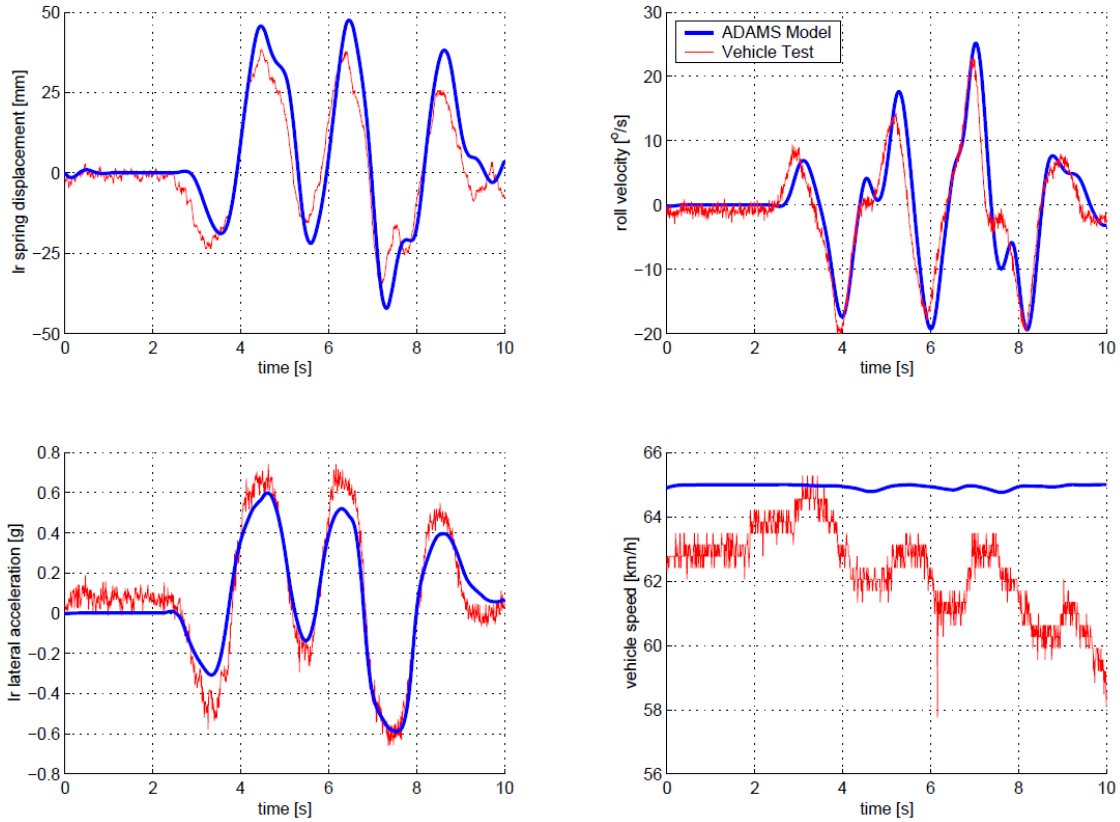

Figure 26 **Validation of the ADAMS model's handling dynamics for a DLC at 65km/h (Thoresson, 2007)**

3.2 System Requirements

Before any simulations were done a worst case flow requirement was calculated using the model described in par. 3.1. To determine the maximum flow needed to keep the suspension level on the stiff suspension setting the maximum vertical velocity of the suspension was obtained for a DLC at 80 km/h. The right front wheel had the highest maximum velocity of $V_{max} = 0.08\,m/s$. The flow of the oil is then obtained from this velocity by multiplying it with the piston area of the $4S_4$ which equates to 14.1 l/min.

To determine the system requirements, the maximum pressure in the suspension during the double lane change at 80 km/h was determined. It was found that the right rear wheel reached the highest pressure during the manoeuvre namely $P_{max} = 3.7\ MPa$.

It was decided to use a system pressure of 20 MPa so that a pressure difference in excess of than 16 MPa will exist. To determine the return flow from the suspension to the oil reservoir the minimum pressure in the suspension during the manoeuvre was determined as $P_{min} = 1.6\ MPa$.

This will give a minimum pressure difference of 1.5 MPa between the atmosphere and the suspension.

Repeating the same analysis for the soft suspension setting a $Q_{max} = 39.67\ l/min$ was found.

It must be noted that these are the peak flow requirements that are necessary only for a short amount of time when the suspension velocity is at its highest. The oil flow requirement should decrease once the suspension is controlled because the control would counter the movement of the suspension. Taking this into account the values seemed reasonable to continue with the design of the slow active roll control system.

3.3 Hydraulic Circuit

The hydraulic circuit for a single suspension unit is shown in Figure 27 and the full circuit is shown in Figure 31. Oil is supplied by a Stone KP40 gear pump **(Stone Hydraulics, 2012)** at 12 l/min, the pressurised oil is then stored in a $10l$ bladder type accumulator which supplies oil to the suspension when the strut is extended. The SV12-33 directional valves can connect the suspension strut with either the accumulator to add oil or the reservoir to drain oil. The FPCC is a proportional valve used to control the in and out flow and is opened relative to the magnitude of the lateral acceleration of the vehicle. The SV10-24 valves were kept open during the suspension control. It would be preferable to remove these valves to reduce the flow losses, but these valves are integrated in the suspension units and could therefore not be removed. P_2 on the diagram corresponds to P_2 in Figure 13 and is the pressure generated by the vertical wheel force. P_5 depends on the pressure the pump is able to supply (Max 12.5 MPa with the battery setup in the test vehicle but the pump can supply up to 20 MPa). The pump is switched on and off using the accumulator pressure as a decision value.

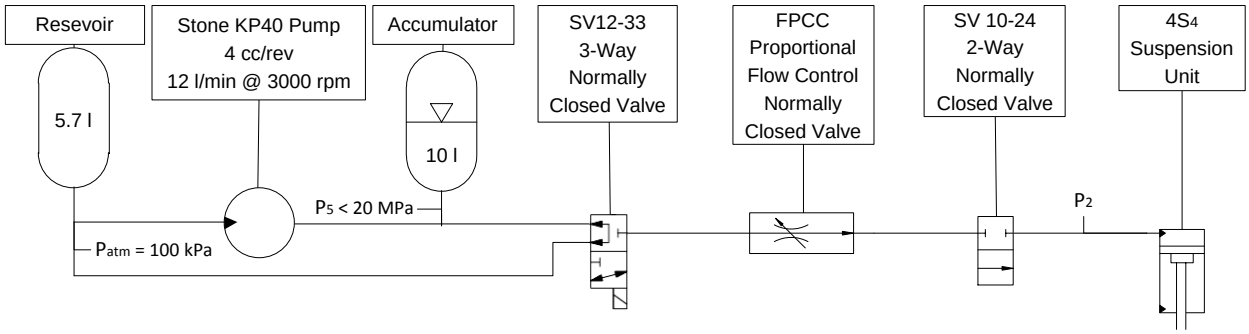

Figure 27 Hydraulic circuit for a single suspension unit

The SV10-24 valves are manufactured by **HydraForce (2012)** and are solenoid operated, 2-way normally closed valves. The performance graphs, as given by the manufacturer, are shown in Figure 28. From the given graphs, Figure 29 was generated to obtain a flow rate for the specific pressure drop in the suspension model. This graph was then used to determine the flow through the valve during the initial simulations. Later during the simulations it became clear that, although these on-off valves will work, they will only function optimally under certain circumstances (for a specific lateral acceleration) and therefore it was decided to introduce the proportional valves.

The SV12-33 valves are manufactured by **Hydraforce (2011)**. These valves can handle oil flow of over 56 l/min and have a reaction time of 100 ms. These valves have a leakage of 410 cc/min at 24 MPa.

The FPCC valves are manufactured by **Sun Hydraulics (2011)** and can control oil flow between 0.8 and 28 l/min. Laboratory tests have shown that these valves have a response time of 30ms. These valves

have a maximum leakage of 100 cc/min at 21 MPa. The graphs shown in Figure 30 were used in the model to simulate the SV 12-33 and FPCC valves (Figure 77 in par. 4.6.1.3 shows the valves in the test vehicle).

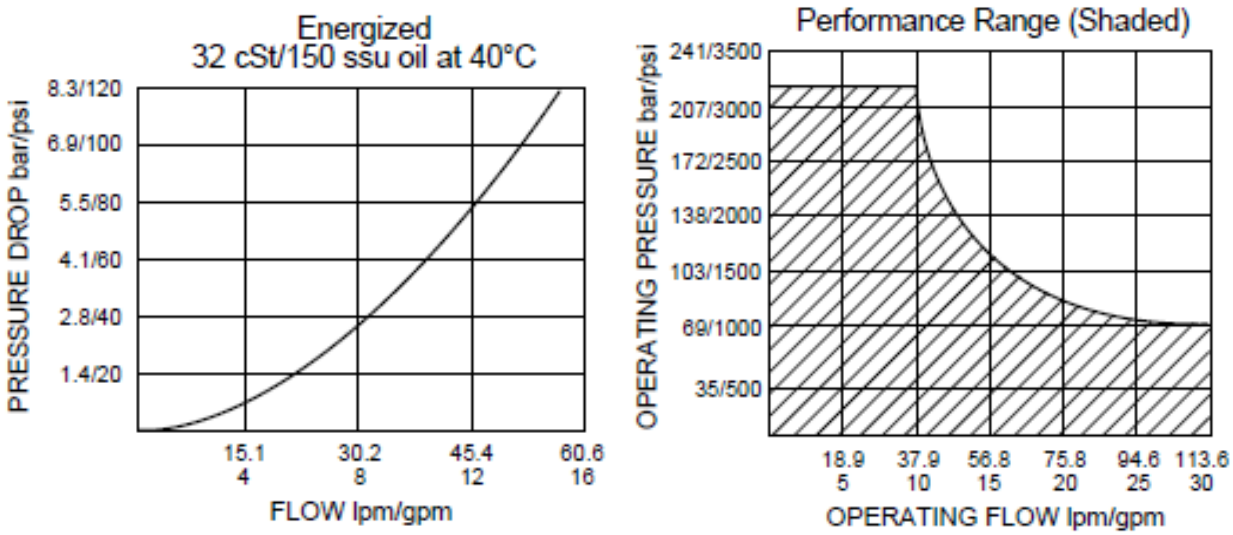

Figure 28 **Performance graphs for SV10-24 valve (Hydraforce, 2012)**

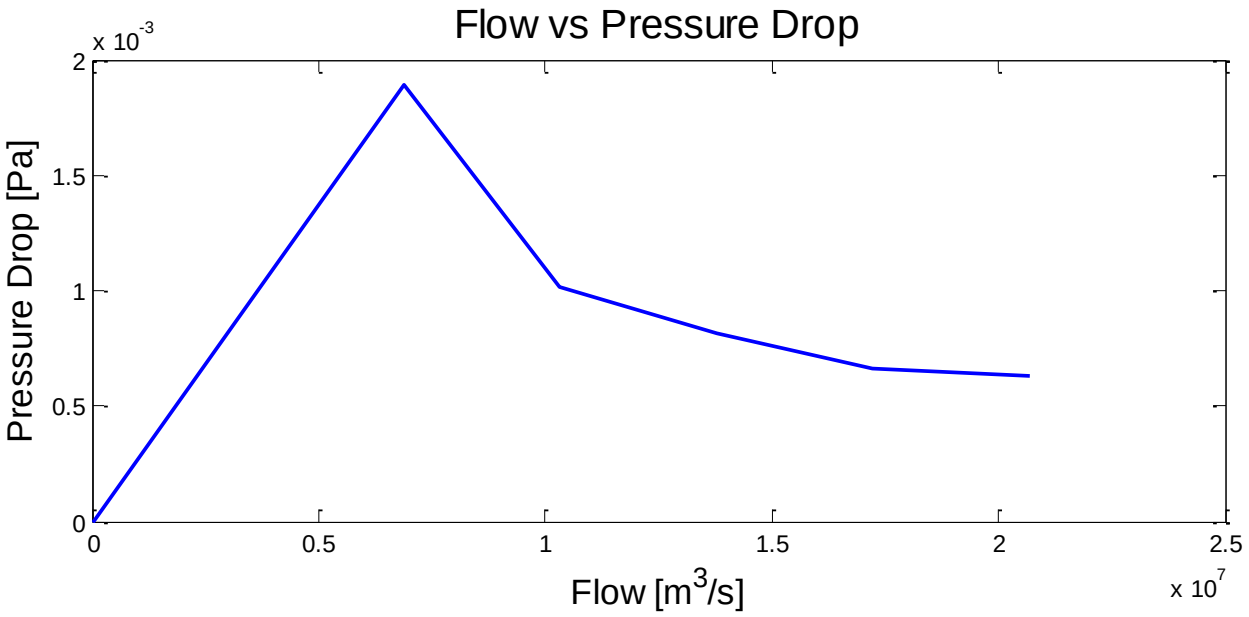

Figure 29 **Flow vs Pressure Drop for SV10-24 valve**

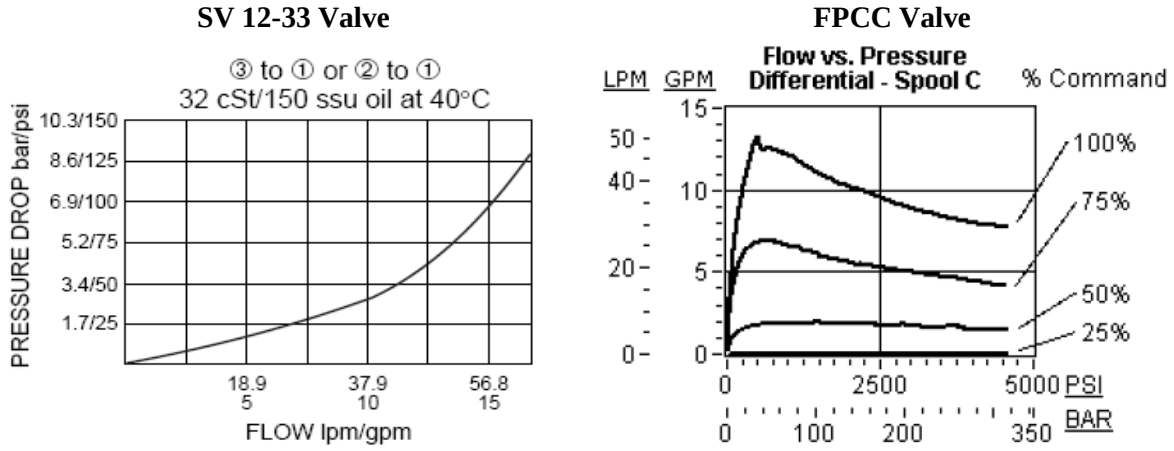

Figure 30 **Flow vs Pressure graphs for the SV12-33 (Hydraforce, 2011) directional valve (left) and the FPCC (Sun Hydraulics, 2011) proportional valve (right)**

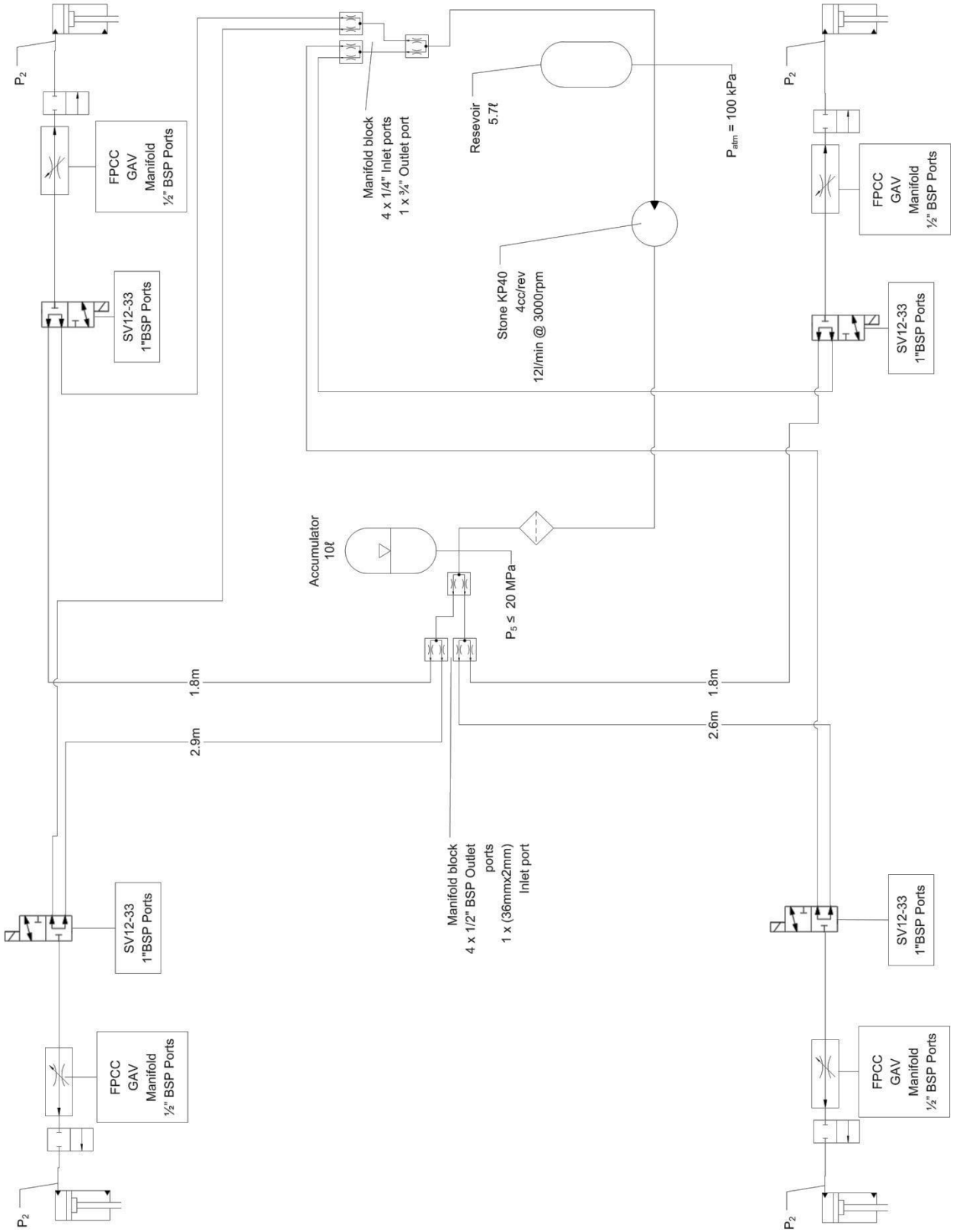

Figure 31 **Flow diagram of the hydraulic setup in the test vehicle**

3.4 Suspension Model

The suspension is modelled using MATLAB **(MathWorks, 2012)**/Simulink **(MathWorks, 2011)** and provides the ADAMS **(MSC.Software, 2011)** vehicle model with a suspension force. The total suspension force consists of four forces namely: damper force, friction force, spring force and the bumpstop force (see Figure 32). The damper force is defined using piecewise quadratic approximations giving damping force as a function of velocity. Friction is determined using a lookup table giving friction as a function of velocity. The force generated by the gas spring is calculated using either the ideal gas equation or the Bennedict Webb Rubin (BWR) real gas equation. The gas model receives a displacement value from the ADAMS vehicle model and then calculates the spring force. The effect of the bump stops are modelled using first order polynomials giving the bumpstop force as a function of displacement.

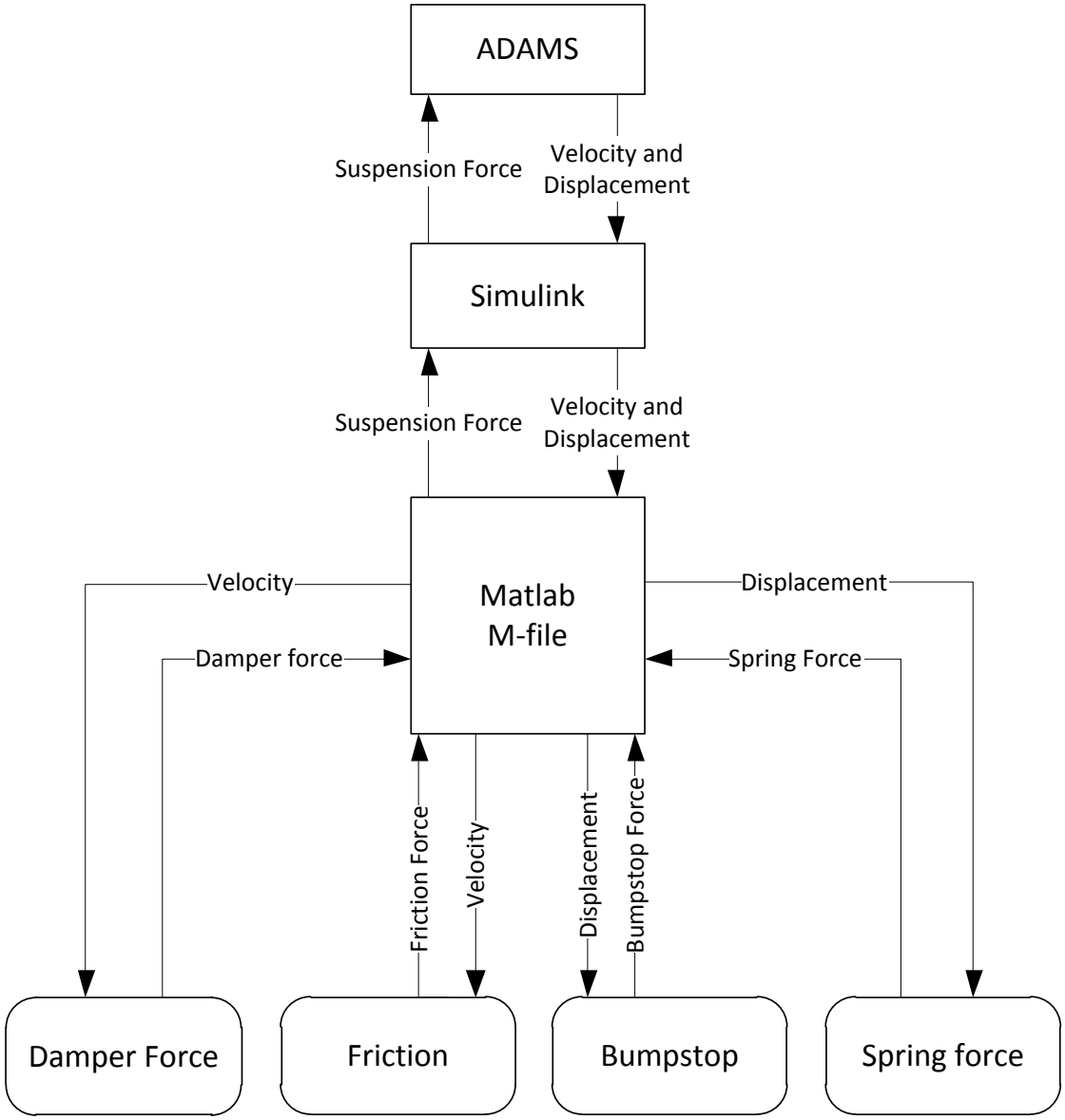

Figure 32 Suspension model interaction

3.4.1 Ideal Gas Spring Model

For the initial feasibility study the ideal gas suspension model was modified so that oil can be pumped into or drained from the suspension units. The flow into and out of the suspension is proportional to the pressure difference between the accumulator and the suspension unit's cylinder. A ΔP is determined between the accumulator and the suspension for the inflow and between the suspension and atmospheric pressure for the outflow. A lookup table of the valve's characteristics is used to determine the flow (Figure 29).

The added or drained oil is simulated using the ideal gas law which states:

$$PV = mRT \tag{8}$$

Which can be rewritten as follows

$$P = \frac{mRT}{V} \tag{9}$$

From equation 9 one can see that reducing the volume will increase the pressure and will result in increased suspension force.

It is assumed that the oil is incompressible and when oil is pumped into the suspension the volume for the gas in the suspension is reduced by the amount of oil added to the suspension. Similarly when oil is allowed to flow out the volume for the gas is increased by the amount of the oil that has flown out. For each time increment a new flow rate is determined using the internal pressure (P2 in Figure 31) and the external pressure which is 20 Mpa for the inflow and 100 kPa for the outflow. The flow rate is determined using the lookup table of Figure 29 or Figure 30 and is then multiplied by the time increment to obtain the volume of oil that was pumped in or out for that time increment. In Figure 33 one can see that if d decreases, F will increase. When F increases the mass will move up to increase d until F=Mg. Using this principle the suspension model obtains parameter values from the ADAMS model via Simulink and then calculates a force which is then sent back via Simulink to the ADAMS model (see Figure 32).

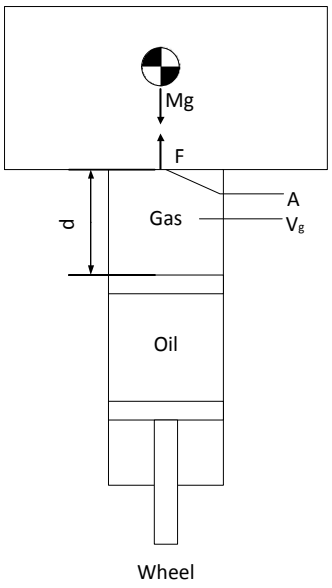

$$V_g = dA \qquad (10)$$

$$F = PA \qquad (11)$$

Replacing 10 & 11 into 8 we get:

$$F = \frac{mRT}{d} \qquad (12)$$

$A = Nett\ area\ in\ which\ pressure\ exerts\ a\ upwards\ force$
$d = Displacement\ of\ the\ gas\ accumulator's\ piston$
$F = Upwards\ force\ exerted\ by\ pressurised\ gas$
$g = Acceleration\ due\ to\ gravity$
$M = Mass\ of\ the\ vehicle's\ body\ on\ the\ suspension\ unit$
$V_g = Volume\ of\ the\ gas$

Figure 33 Main principle of the suspension model

3.4.2 BWR Spring Model

During the first experimental testing concerns about the accuracy of the ideal gas law in this application arose. Subsequently the Benedict Webb Rubin (BWR) real gas equation was introduced. This model works on the same principle as the ideal gas model but here the gas in the suspension as well as the gas in the accumulator is modelled using the BWR equation. Thus the accumulator pressure is not a fixed value as in the case of the ideal gas model but takes into account the flow of the pump and the flow out of the accumulator to get a more accurate pressure difference to model the flow. This model is described in par. 4.1 and Appendices A and B.

3.5 Control Strategies

To determine a suitable control strategy for roll angle control, different ideas were implemented and simulated for a DLC manoeuvre at 60 km/h. All these simulations were done using the Ideal gas suspension model and the $4S_4$ in handling mode. One of the main challenges is the non-linearity caused by the fact that the $4S_4$ is only a single acting cylinder. This means that an increase in ride height can be well controlled, but a decrease is heavily reliant on the pressure in the suspension strut.

3.5.1 Control Strategy 1

In control strategy 1, oil is drained from the suspension units that experiences positive displacement (extended), and when a unit experiences a negative displacement (compressed) oil is pumped in. The oil is added and drained with valve opening directly proportional to the magnitude of the suspension displacement up to 50mm positive or negative displacement and from there on it is added or drained at maximum rate. The results are shown in Figure 34 and Figure 35. The suspension control was only activated after 0.8 seconds, after the vehicle has reached 60km/h.

The working principle of the algorithm is shown below:

$$
\begin{aligned}
&if\ |x| \leq 50 \\
&\quad \%valve\ opening = \left(\frac{|x|}{50}\right) \times 100 \\
&else \\
&\quad \%valve\ opening = 100\% \\
&end
\end{aligned}
$$

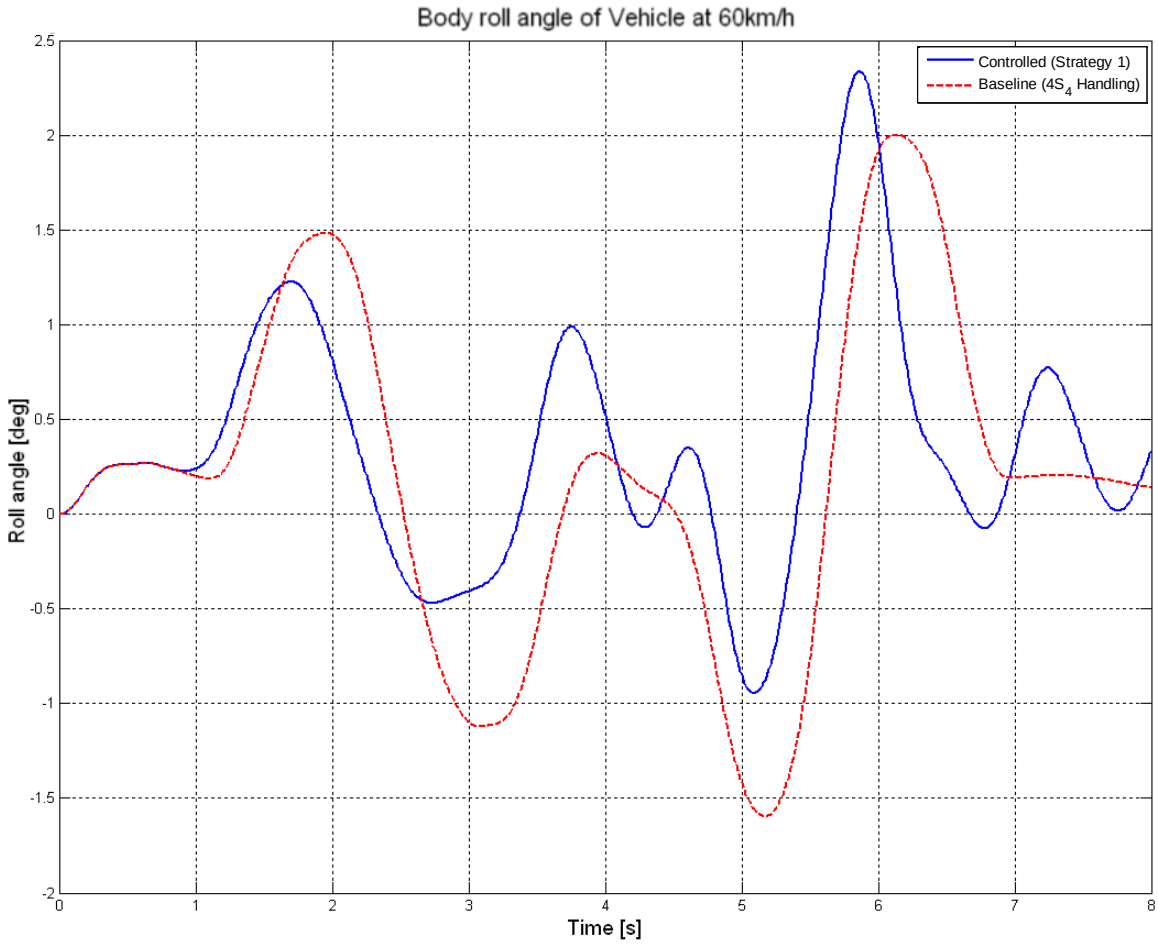

Figure 34 Body roll angle for a DLC manoeuvre at 60 km/h

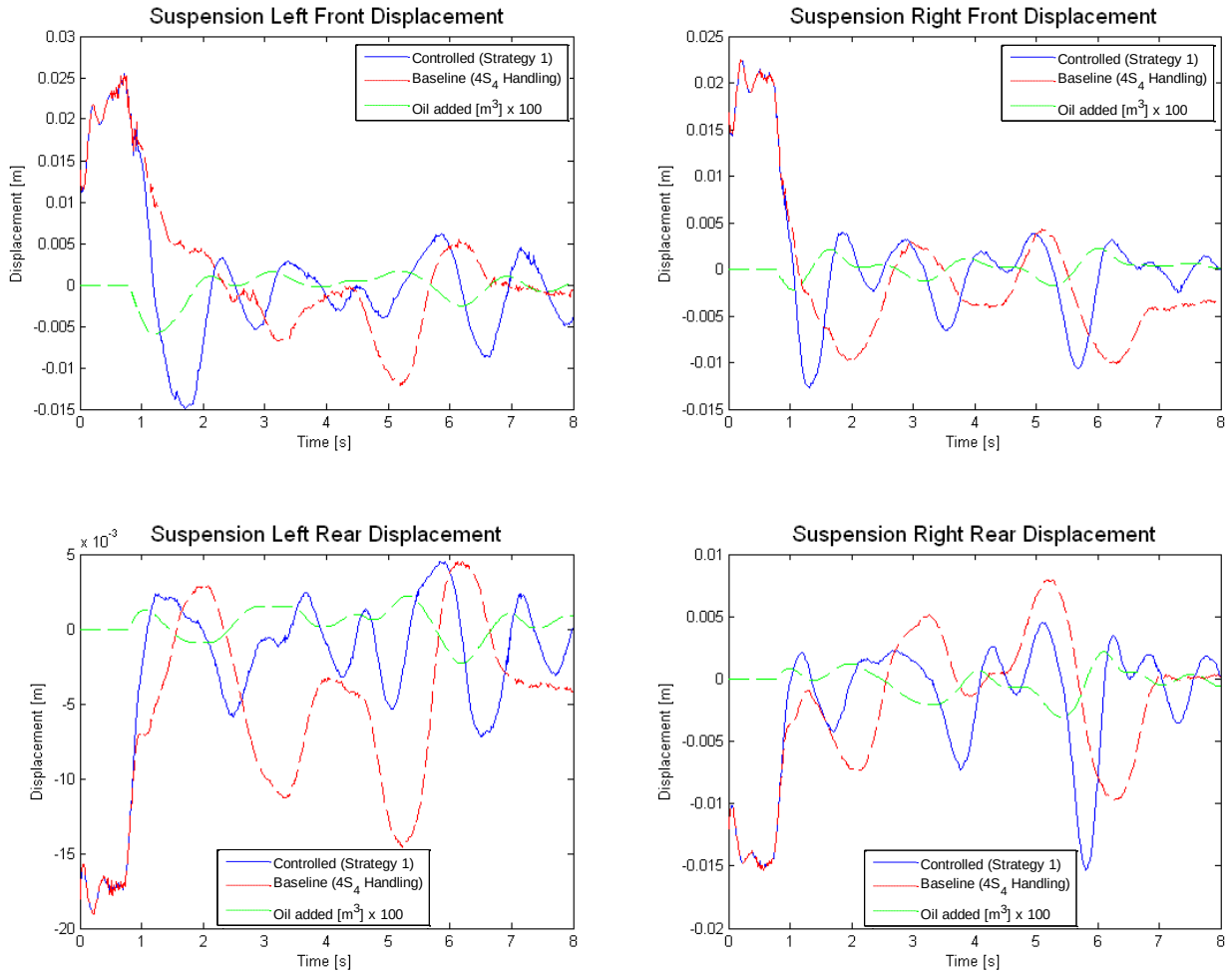

Figure 35 Suspension responses for a DLC manoeuvre at 60 km/h

Looking at the results it becomes apparent that a sudden shift of the vehicles weight, to the side of the suspension where oil has previously been drained, results in large body roll angles. The weight shifts too fast for the system to counter the compression of the units. A good example can be seen just before 6 seconds on the right rear suspension graph and on the roll angle graph (Figure 34) where the roll angle of the vehicle makes a very sharp and high peak.

3.5.2 Control Strategy 2

For this strategy the oil is only drained out of the suspension unit until the original amount of oil (when the vehicle is static) in the unit is reached. This simulation was run for 12 seconds to see if the suspension units settle down at a displacement of 0 after the double lane change. The results for the $4S_4$ in handling mode are shown in Figure 36 and Figure 37.

The working principle of the algorithm is shown below:

```
if x ≥ 0
    if volume of oil added ≥ 0
        if x ≥ 50
         %valve opening = 100%
        else
            %valve opening = (|x|/50) × 100
        end
    else
        %valve opening = 0%
    end
else
    if x ≤ −50
        %valve opening = 100%
    else
        %valve opening = (|x|/50) × 100
    end
end
```

Suspension Extended (Outflow Control)

Suspension Compressed (Inflow Control)

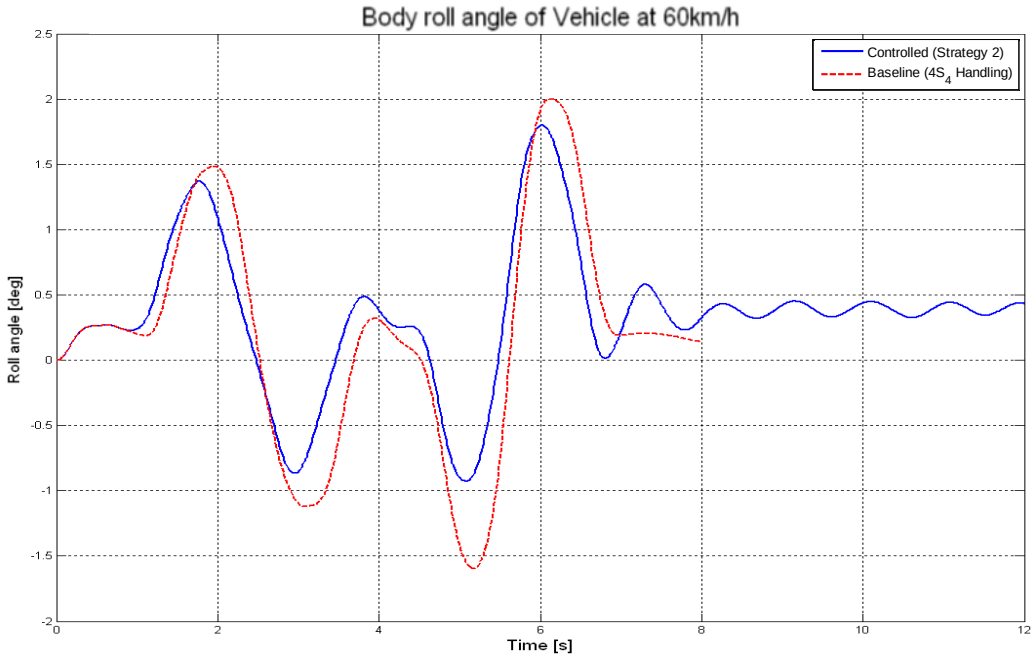

Figure 36 Body roll angle for a DLC manoeuvre at 60 km/h

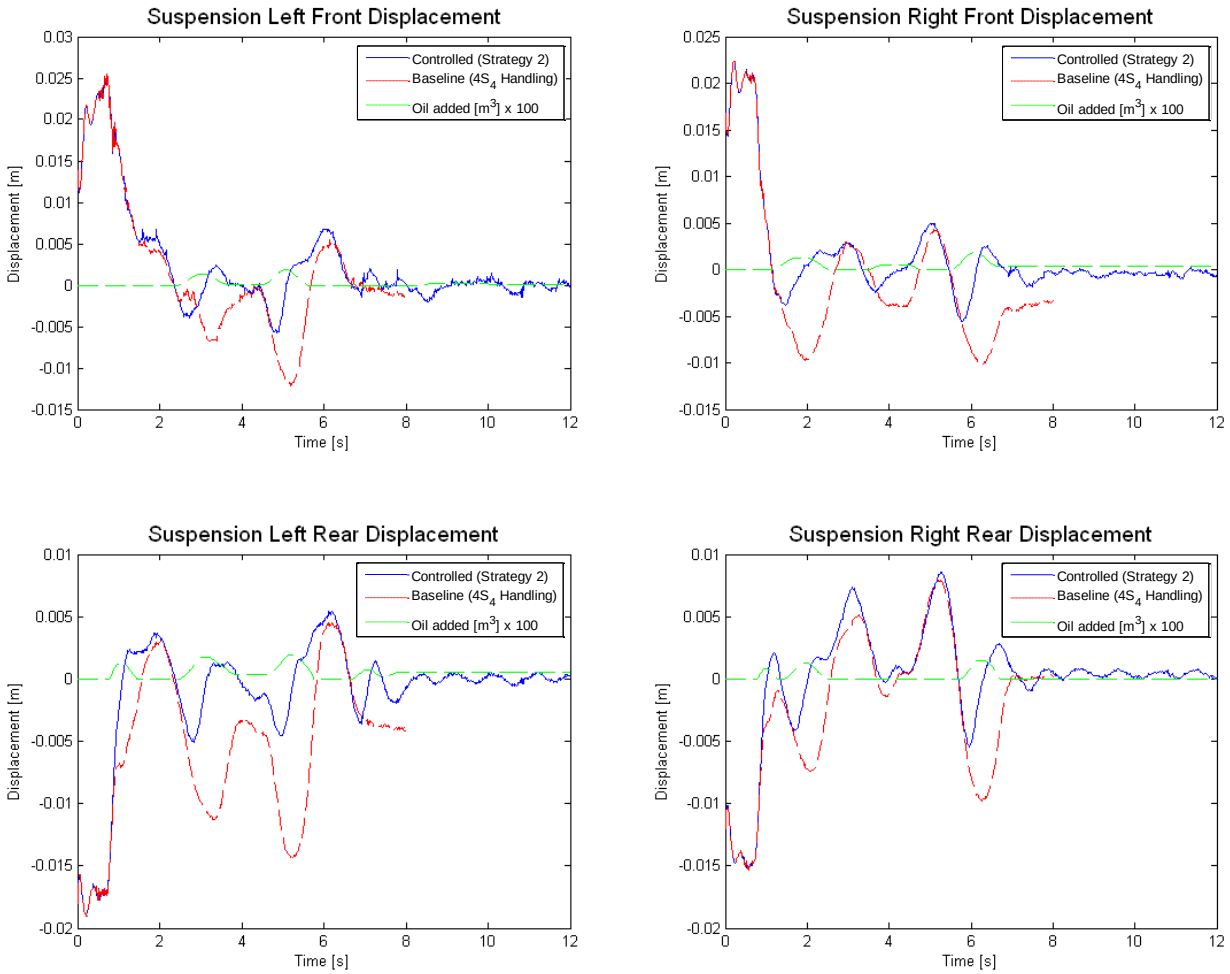

Figure 37 Suspension responses for a DLC manoeuvre at 60 km/h

The results for the suspension show a significant improvement. There is also an improvement in the body roll of the vehicle. Although these results show an improvement the on-going oscillation after 8 seconds in the body roll angle (Figure 36) is of some concern. Thus control strategy 2 does not give satisfactory results even though there is a significant improvement.

It is important to take note of the difference in the results between control strategy 1 and control strategy 2. To drain too much oil out of the system seems to have more losses than gains. This principle is shown in Figure 38 and Figure 39 where a Proportional–Integral–Derivative (PID) controller was used to control the flow. In the Figure 38 the oil was drained with no limit, where in the Figure 39 the oil was only drained until the amount of oil in the suspension unit was equal to that of the static position.

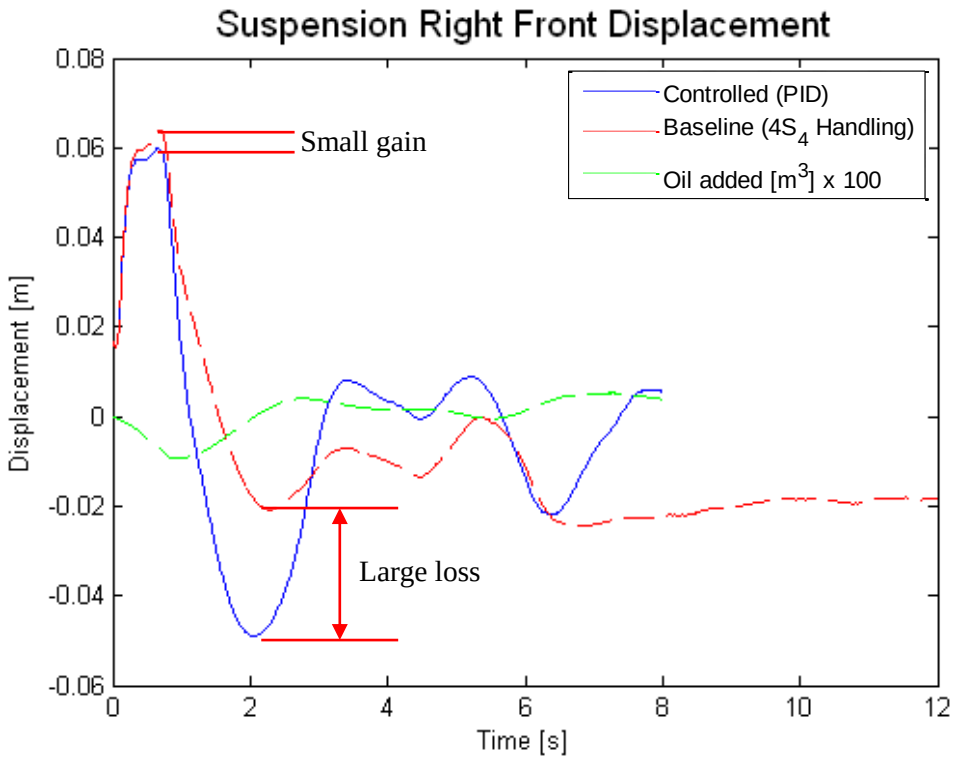

Figure 38 **Suspension responses for a DLC manoeuvre at 60 km/h for unconstrained outflow**

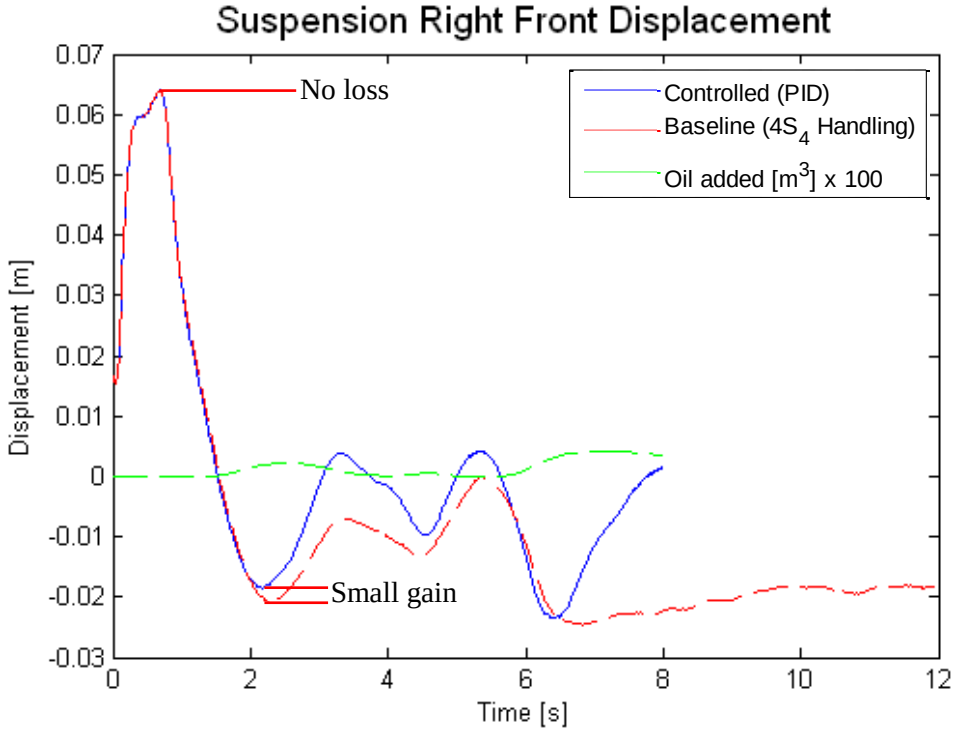

Figure 39 **Suspension responses for a DLC manoeuvre at 60 km/h for constrained outflow**

3.5.3 PID Controller

The PID controller made use of the following method to control the valve opening for oil inflow also using the volume limit on the outflow:

$$PID = k_1 x + k_2 \int x\,dt + k_3 \frac{dx}{dt}$$

if volume of oil added ≥ 0
  if $PID < 1$
    $\%valve\ opening = |PID| \times 100$
  else
    $\%valve\ opening = 100\%$
  end
else
  $\%valve\ opening = 0\%$
end
if $PID > -1$
  $\%valve\ opening = |PID| \times 100$
else
  $\%valve\ opening = 100\%$
end

Suspension Extended (Outflow Control)

Suspension Compressed (Inflow Control)

Where x is the displacement of the suspension unit with compression negative and extension positive. The aim is to keep the suspension displacement zero as this will result in zero body roll and pitch.

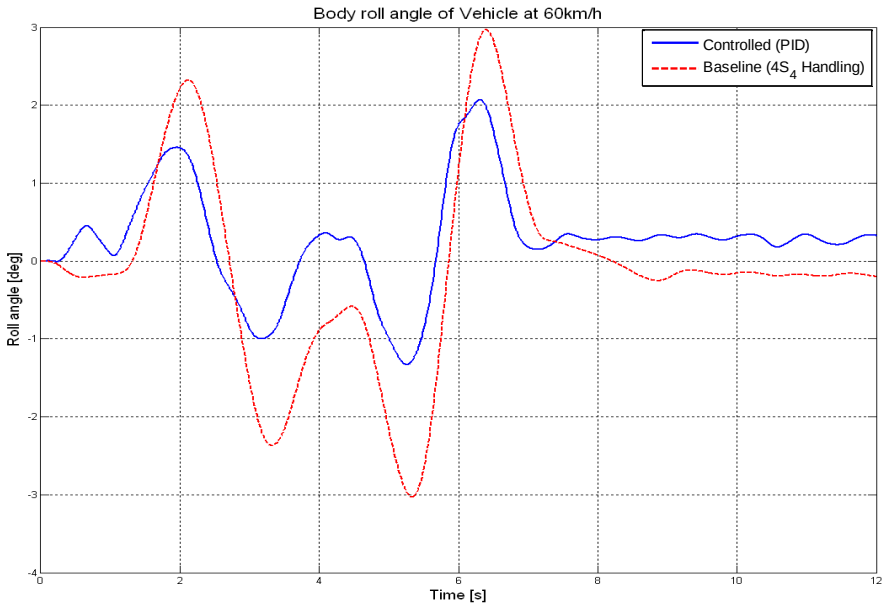

Figure 40 Body roll angle for a DLC manoeuvre at 60 km/h using a PID controlled proportional valve

To obtain the optimal results it was attempted to optimise the gains of the PID controller with an optimisation algorithm. The algorithm did however not converge satisfactorily but did show that the results improve with larger gains for k_1 and k_3. The optimisation was not investigated further because

this was not the final design, but the improvement with larger gains showed that the valves spend very little time being opened proportionally and are almost always fully open or fully closed. This means that on-off valves, which are generally cheaper that proportional valves, can be used.

The results for $k_1 = 8 \times 10^8$, $k_2 = 5$ and $k_3 = 1 \times 10^8$ is shown in Figure 40 and Figure 41. The PID controller gave satisfying results in terms of the body roll angle, but the displacement does not converge to zero due to the large gain on the derivative. Due to the PID decision value being low relative to the gains, the controller is insensitive to changes in the gains.

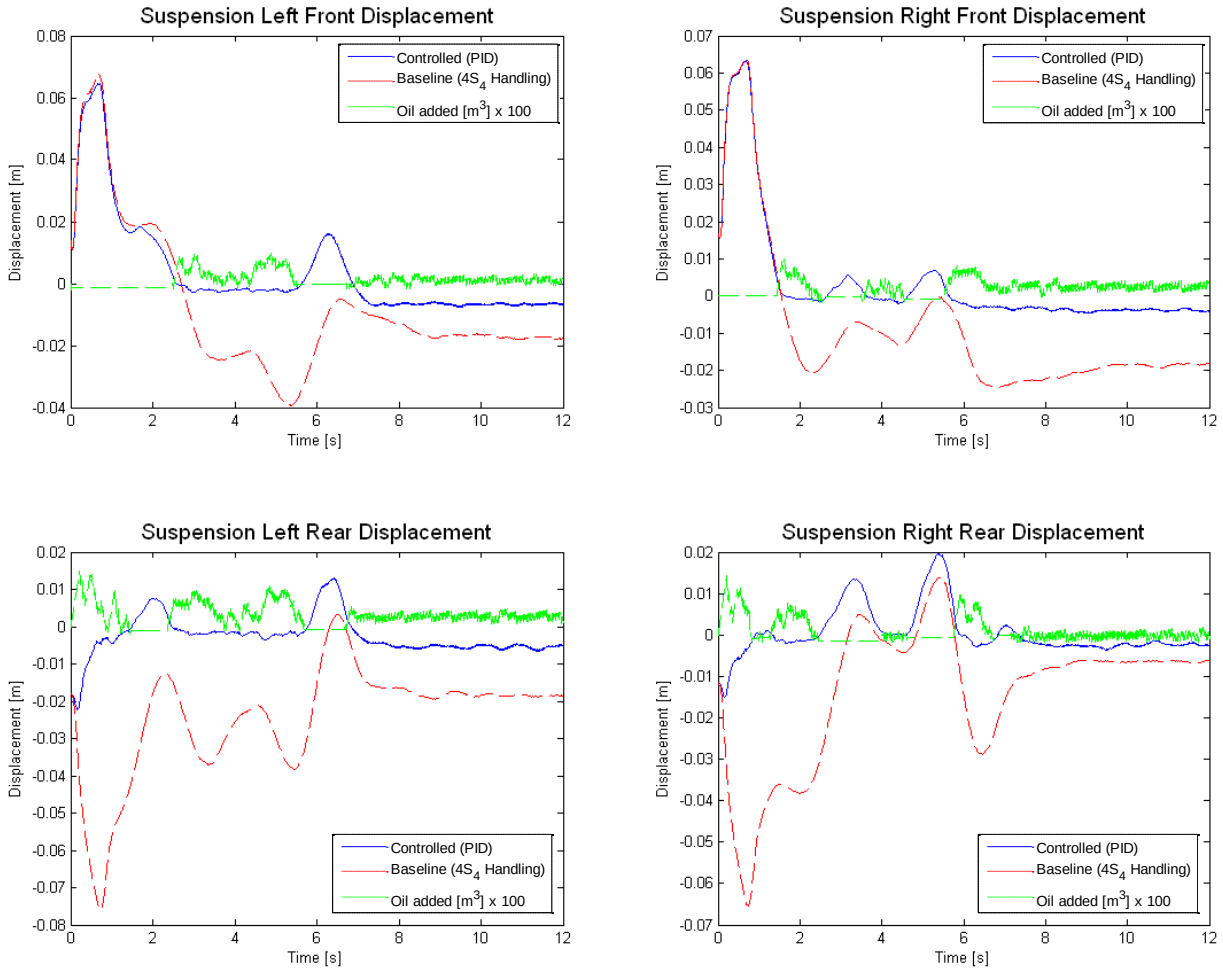

Figure 41 **Suspension responses for a DLC manoeuvre at 60 km/h for PID controlled proportional valves**

3.5.4 On-off valve control

The on-off PID controller makes use of the following method to control the on-off valve for oil flow:

$$PID = k_1 x + k_2 \int x\, \partial t + k_3 \frac{\partial x}{\partial t}$$

$$PIDavg = average\ of\ PID(sample\_time_{i-1})\ to\ PID(sample\_time_i)$$

```
if PIDavg > 0.5                                   } Suspension Extended
    if Amount of oil added > −0.005l              } (Outflow Control)
        Outflow valve is open                     }
    else                                          }
        Both valves are closed                    }
    end                                           }
end                                               }

if PIDavg < −0.5                                  } Suspension Compressed
    Inflow valve is open                          } (Inflow Control)
end                                               }

if |PIDavg| < 0.5                                 } Suspension Neutral
    Both valves are closed                        } (No Control)
end                                               }
```

The same gains as with the proportional valve is used namely, $k_1 = 8 \times 10^8$, $k_2 = 5$ and $k_3 = 1 \times 10^8$. It was however found that the improvement is small once the gains are larger than the decision value (0.5 in this case). Compression is taken as negative and extension as positive.

3.5.4.1 60 Millisecond sampling increments

The characteristics of the SV10-24 valves manufactured by **Hydraforce (2011)** are used in the model for these simulations. The valve response is not modelled but to compensate for the response time of the valves a sampling time of 60 milliseconds is used which is double the response time indicated by the manufacturer. This is done by obtaining an average value of the PID for the previous 60 milliseconds, and then this value is used as the parameter to determine the switching signal for the valves.

Figure 42 and Figure 43 shows that there is a significant improvement in the roll angle as well as the suspension displacements. This shows that at higher speeds and hard cornering proportional control is not necessary. The oscillation in the roll angle after 7 seconds is of some concern but has been improved by using one proportional valve to reduce the total flow to each valve as can be seen in Figure 44. This proportional valve was modelled to reduce the flow to 10% of the original after 7 seconds but a strategy to control the proportional valve should be investigated.

Figure 44 shows that the valves rarely need to switch within 60 milliseconds from the initial switch. This means that the response time of the valve should be sufficient for the control. The total volume and flow rate shown in Figure 45 and Figure 46 is also acceptable.

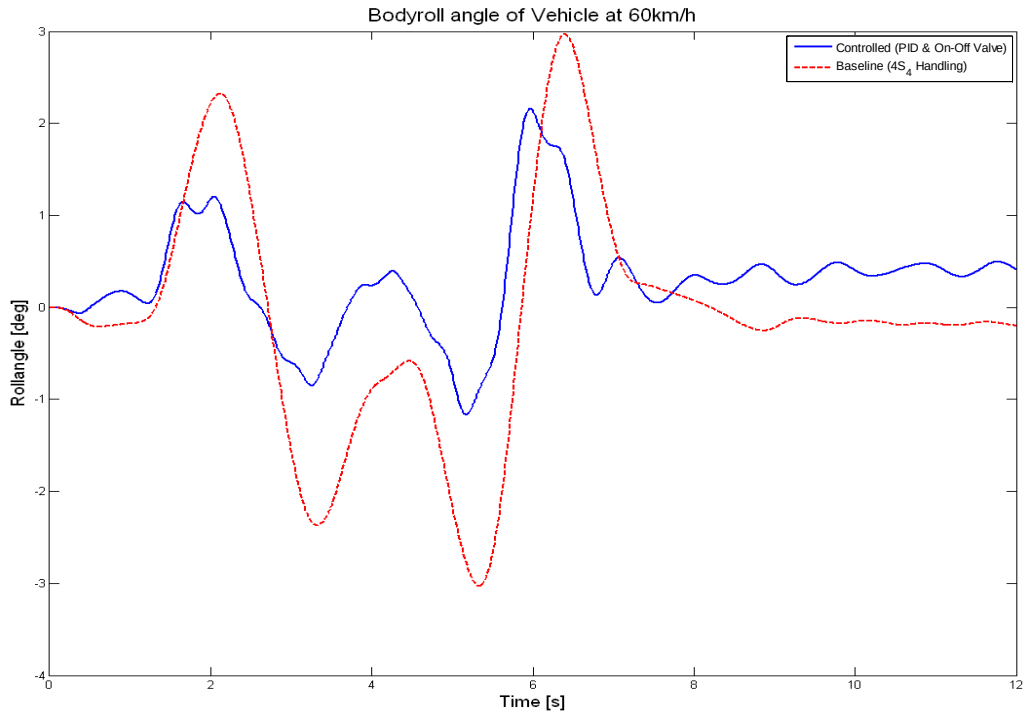

Figure 42 **Body roll angle for a DLC manoeuvre at 60 km/h using a PID controlled on-off valve**

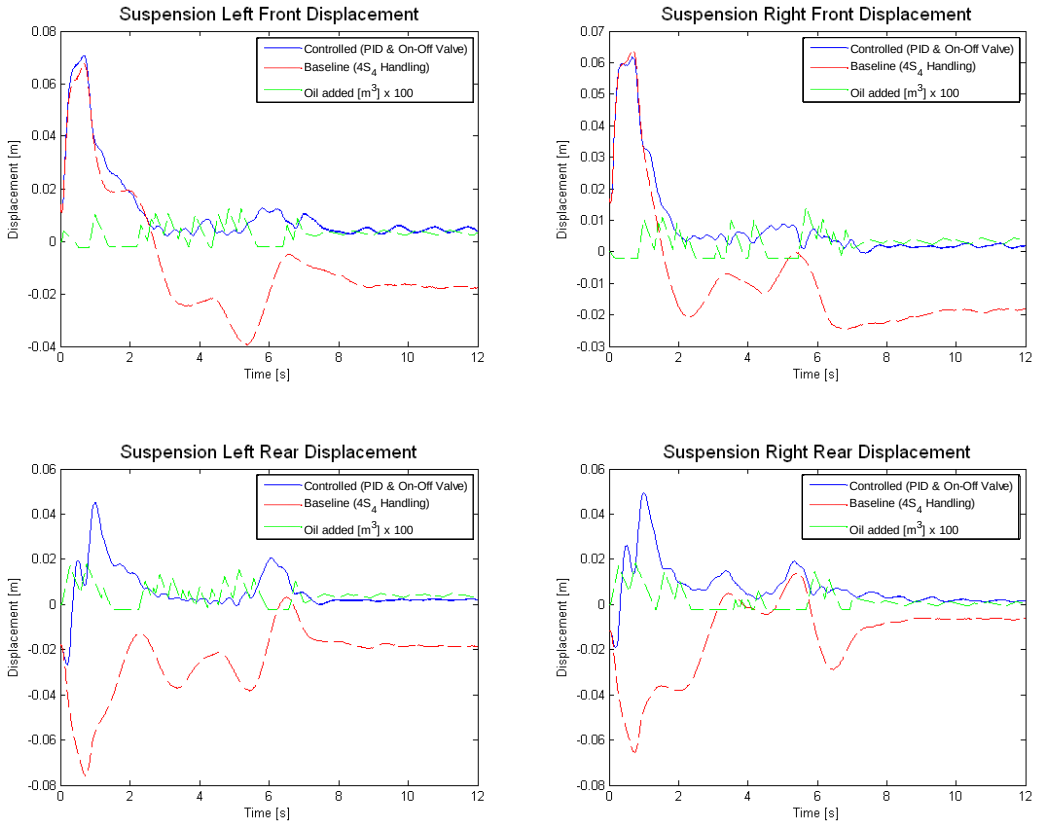

Figure 43 **Suspension responses for a DLC manoeuvre at 60 km/h for on-off valves**

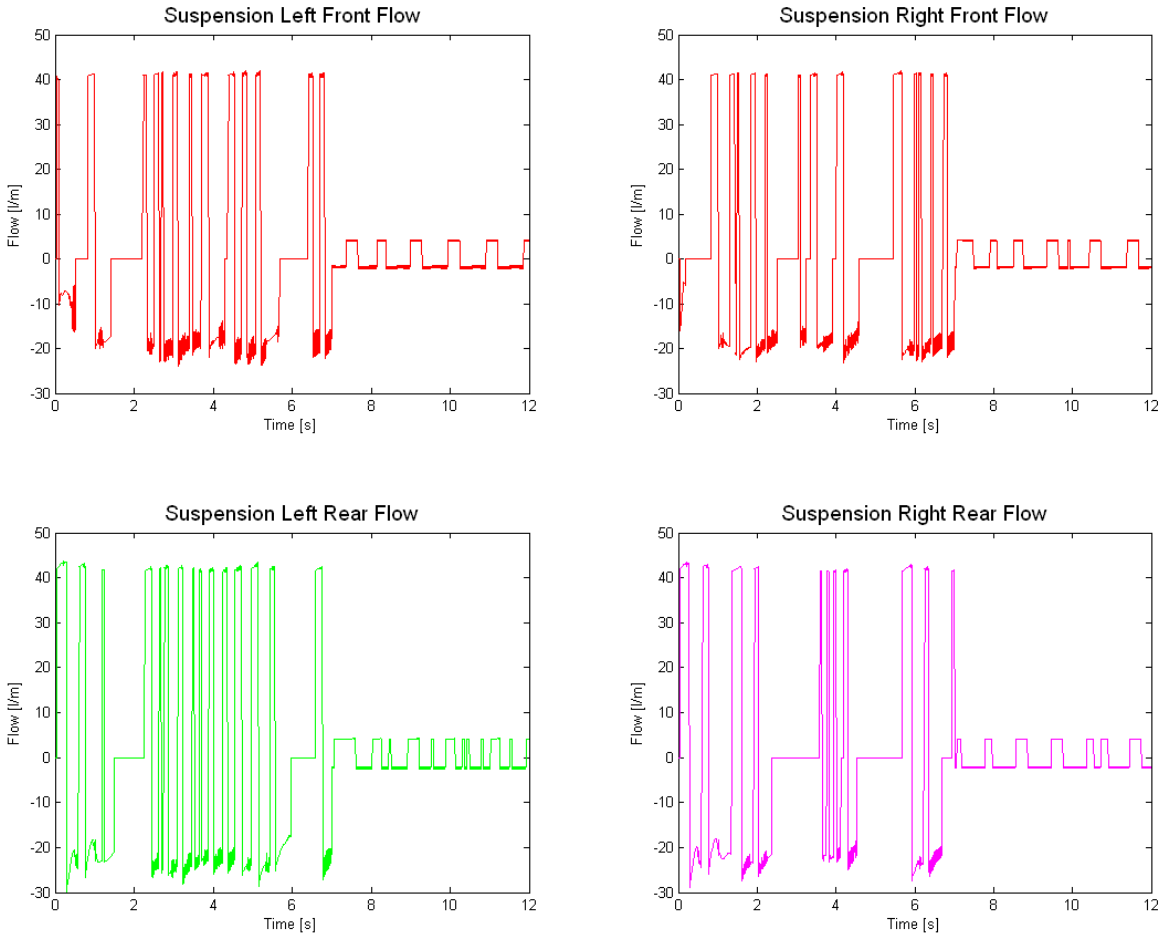

Figure 44 **Flow rates for each suspension unit**

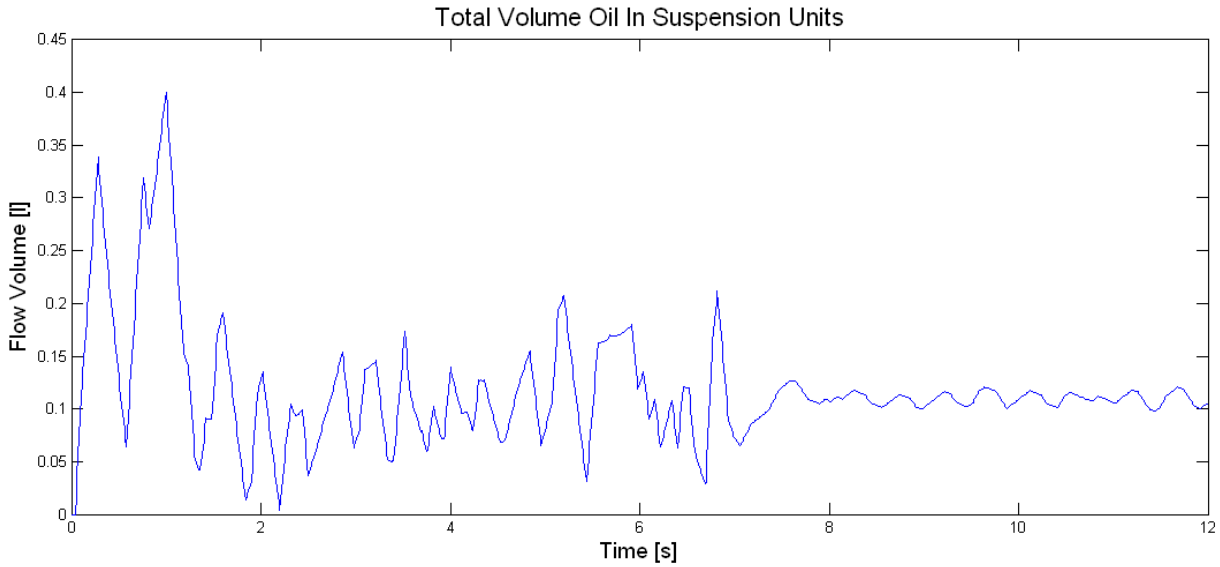

Figure 45 **Total volume of oil pumped into the suspension**

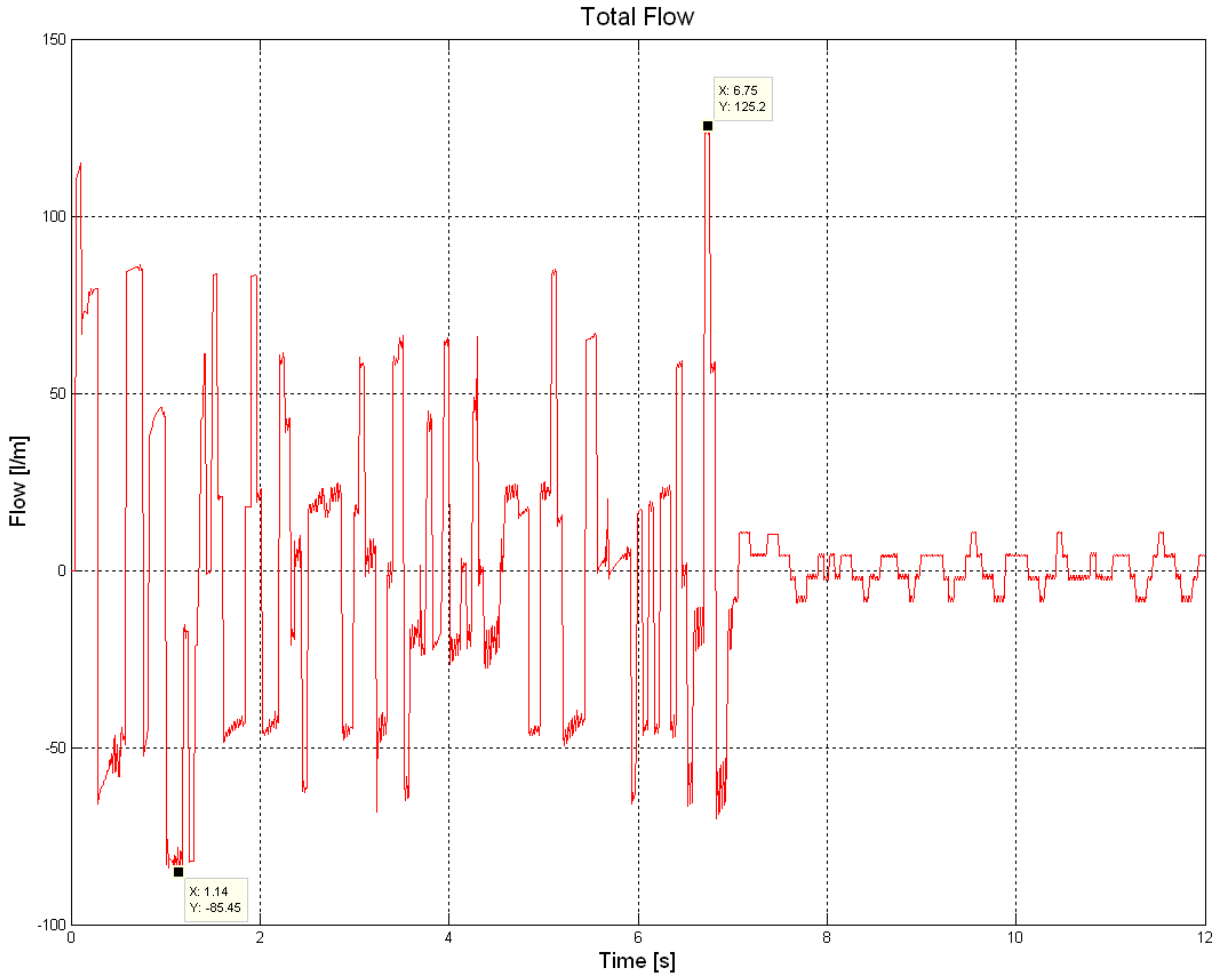

Figure 46 Total flow rate required

3.5.4.2 90 Millisecond sampling increments

To determine the effect if the valves responded slower a sample time of 90 milliseconds was taken which is 3 times the response time of the valves. In Figure 47 the second positive peak at 6 s is smaller where the negative peak has increased. This shows that the specific time at which the control signal is sampled will have an effect on the performance of the system. The results are still satisfactorily and the improvement is still significant. There is however a larger on going oscillation in the body roll angle due to the slower system response, as can be seen after 7 seconds. The response of the suspension (Figure 48) is not as good as with the lower sampling time but still results in a significant improvement over the baseline suspension. The flow requirements shown in Figure 49 to Figure 51 stay similar to that of the 60 ms sampling time.

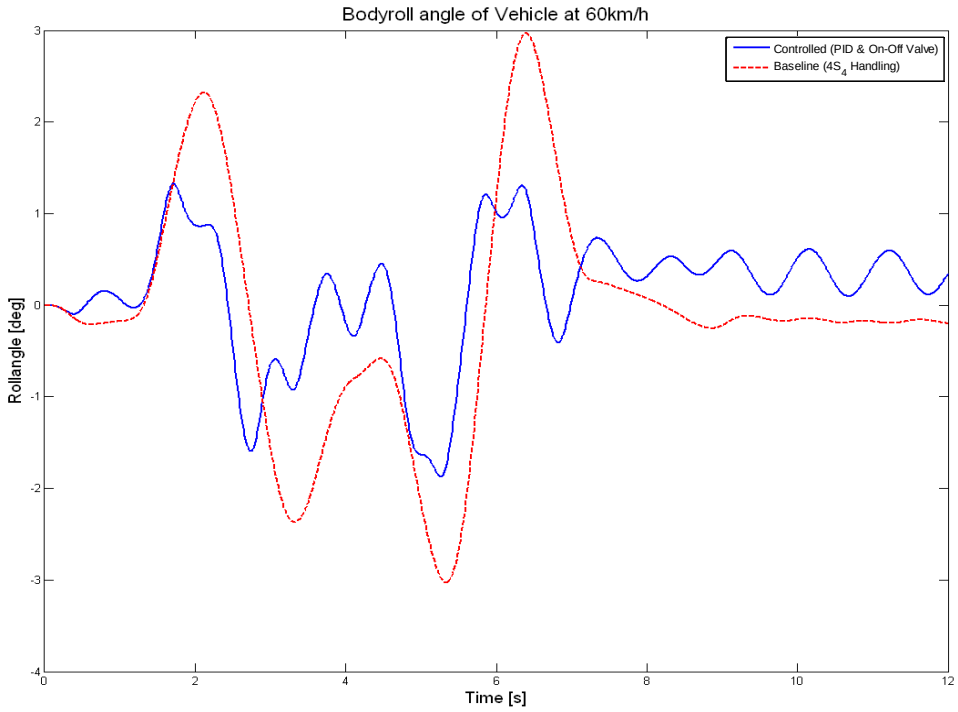

Figure 47 **Body roll angle for a DLC manoeuvre at 60 km/h using a PID controlled on-off valve**

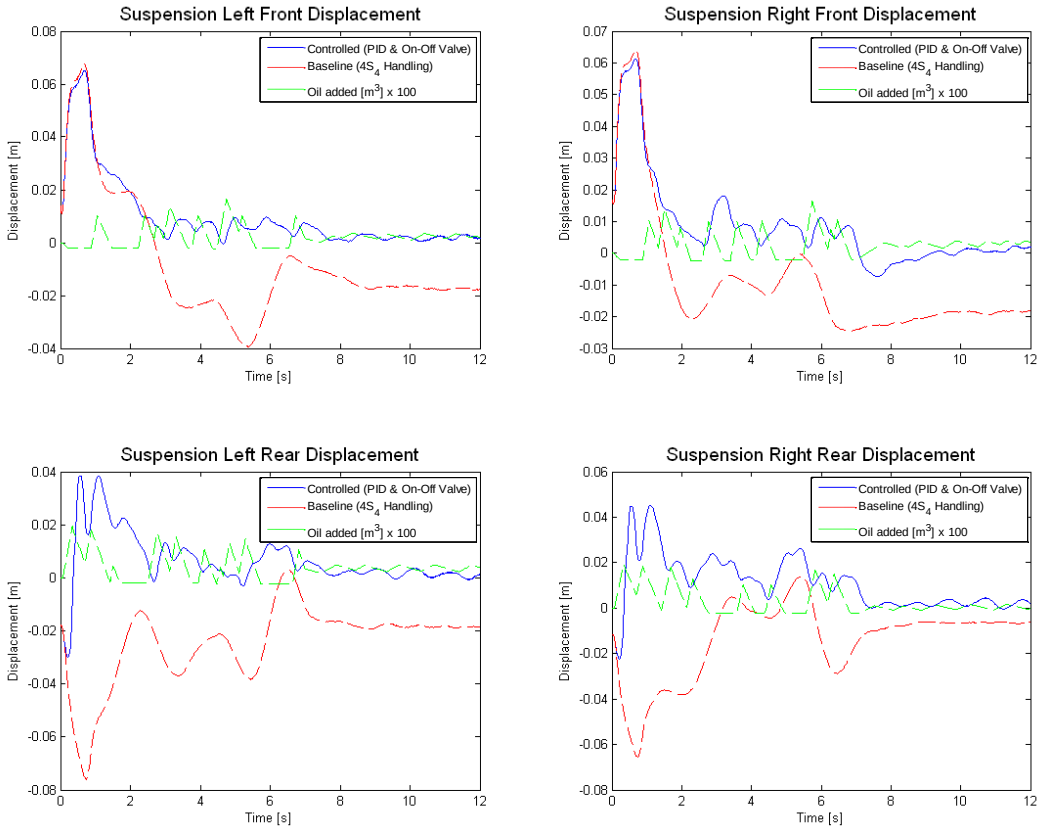

Figure 48 **Suspension responses for a DLC manoeuvre at 60 km/h for on-off valves**

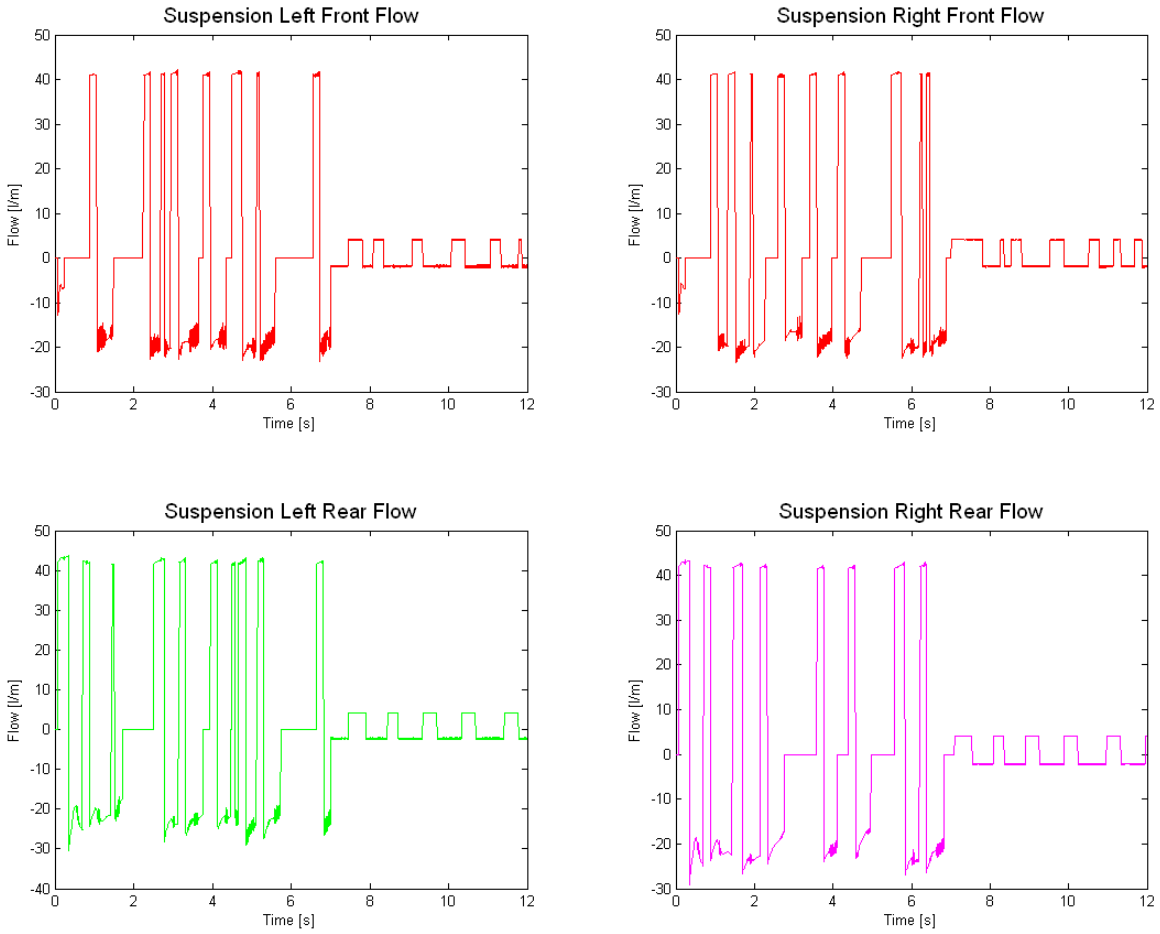

Figure 49 **Flow rates for each suspension unit**

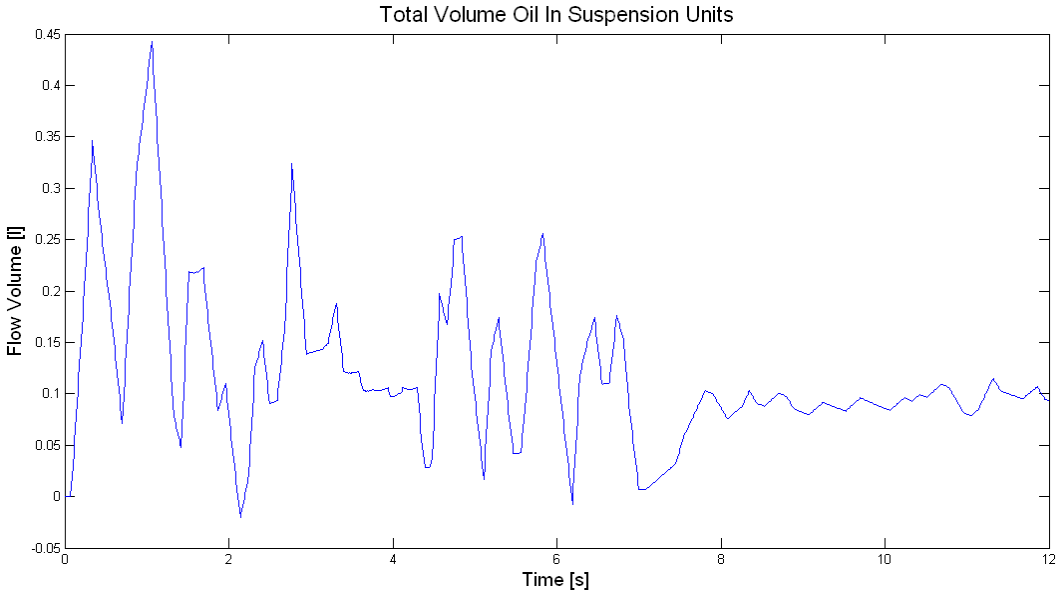

Figure 50 **Total volume of oil pumped into the suspension**

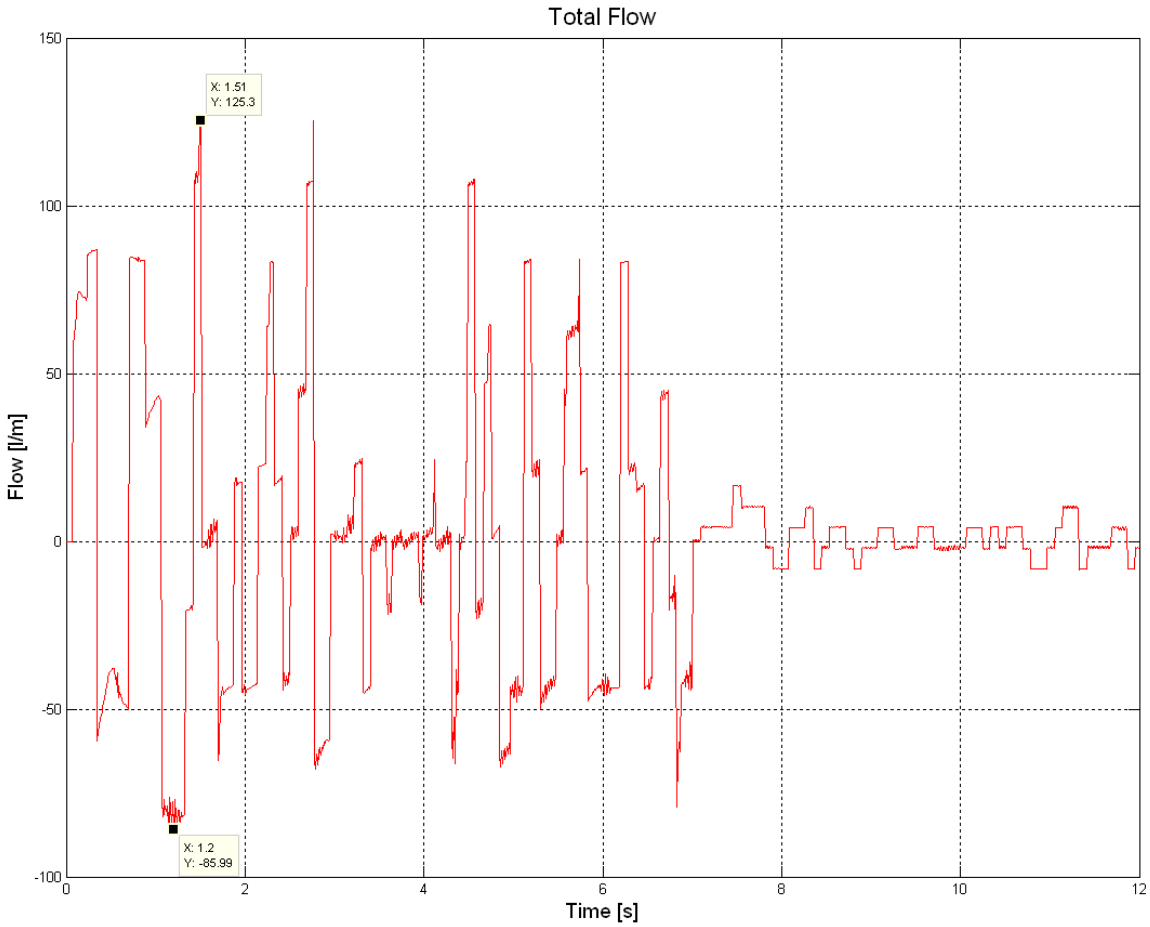

Figure 51 Total flow rate required

3.6 Conclusion

From the simulation results it seems feasible to continue to implement slow active roll control on a vehicle to improve the handling and rollover propensity of the vehicle. The flow requirements seem within reach and this system will allow for many other advantages over that of an AARB. Although the model is not yet given the correct input parameters due to most of it still being unknown, the improvement looks to be significant and therefore it was decided to continue with the hardware implementation of slow active suspension control on the test vehicle.

The experimental results and a comparison between the experimental and simulation results will be given in Chapter 4. A conclusion is given in Chapter 5 and recommendations for future work in Chapter 6.

4. Experimental Work and Results

In this chapter the system, proposed in chapter 3, is implemented and experimental tests are performed. The initial verification tests, voltage controlled current source developed and the valve characterisation is discussed in par. 4.1 to 4.5 where the vehicle is stationary in the lab. The problems experienced and the performance of the system during track tests is discussed (Par. 4.6) and the model is updated with the known parameters and then compared to the experimental results (Par. 4.7).

4.1 Initial Verification Tests

In order to obtain an indication to the accuracy of the model two verification tests were done where the displacement was measured to verify with the simulation results. The first test consisted of opening the valves of the front suspension units for 0.5s while the pump supplies oil at $\pm 12\,\mathrm{l}/min$ to raise the front, as is shown in Figure 52. For the second test the valves for all four suspension units were opened for 1.5 s to raise while the pump supplies oil at $\pm 12\,\mathrm{l}/min$, the valves were then closed for 1 second and opened to lower the suspension for 2 s (see Figure 56). Both these tests were done while the vehicle was stationary on a solid surface without any external disturbances.

During the initial simulations poor correlation with the experimental results were obtained, which initially looked like the gas is modelled too compressible, but the problem was narrowed down to be the friction in the model as well as the friction taken into account in the damping. As there is always some form of friction present in any system the force measurements done to determine the damping of the suspension also had a component due to friction. In order to improve the correlation the friction was removed from the model. The results are shown in Figure 52 and it is clear that the friction caused a greater deviation from the measured experimental results.

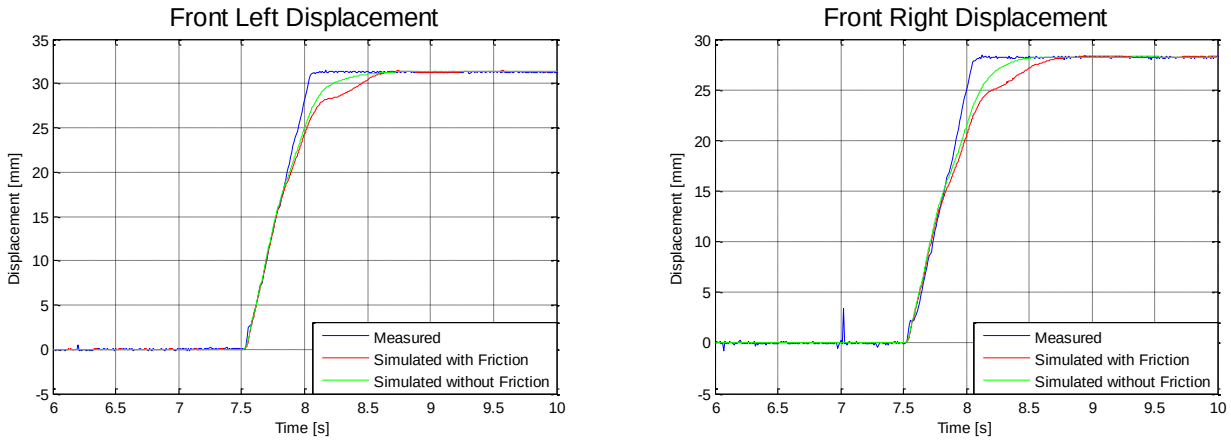

Figure 52 **Comparison between the measured results and the simulation results with and without friction**

Initial simulations were performed using the original ideal gas law suspension model, developed by **Thoresson (2007)**. These results showed that a significant improvement in body roll is achievable but some concerns regarding the accuracy of the ideal gas law in this application arose. The concerns were

that calculation errors could be introduced due to the fact that the ideal gas law does not take the intermolecular forces at small intermolecular distances into account. It therefore over estimates the compressibility at either high pressures or low temperatures, of which the former is present when working with hydropneumatic suspensions **(Sontag and Van Wylen, 1991)**. In the initial verification test the ideal gas model correlated well with the measured results, but this is done at low pressures while the vehicle is standing still (see Figure 53). Subsequently the BWR real gas equation was introduced **(Otis and Pourmovahed, 1985)** (See Eq. 13).

$$P = \frac{RT_g}{v} + \frac{B_o RT_g - A_o - \frac{C_o}{T_g^2}}{v^2} + \frac{bRT_g - a}{v^3} + \frac{a\alpha}{v^6} + \frac{c\left(1+\frac{\gamma}{v^2}\right)e^{\frac{-\gamma}{v^2}}}{v^3 T_g^2} \tag{13}$$

A new specific volume and temperature is calculated for each time step to enable the calculation of the pressure by means of the BWR equation (See Appendix A for the temperature equation and Appendix B for the BWR constants). During the simulation of the DLC the flow requirements for the ideal gas model was found to be much higher than that of the BWR model. This is likely due to the above mentioned problems and the BWR model is expected to deliver more accurate results.

The BWR model correlates well with the measured values as can be seen in Figure 54. The pump delivers $\pm 12\,l/min$ depending on the voltage of the battery and the flow losses in the system. It was found that both models correlate with the measured results at a flow of $12.8\,l/min$. Both models do however deviate quite substantially from the measurements if the displacement becomes negative. As described in par. 3.4 the damping is modelled as a function of the suspension velocity. Thus the model cannot distinguish between movement due to height control and movement due to road inputs. The damper effect can be modelled more accurately if the flow through the dampers is calculated using fluid mechanics, this is however computationally very expensive and it was therefore not implemented.

In the model the suspension is lowered by increasing the volume of the gas, this lowers the pressure which then gives a lower suspension force. In reaction to this the Adams model lowers the vehicle body at the suspension unit to obtain an equilibrium of forces. But due to the damping not being able to distinguish the nature of the movement it generates a force to resist the movement. The damping thus causes the suspension to lower more slowly than the rate at which the oil is removed (gas volume is increased). This causes the gas to expand more than in reality which then predicts a smaller suspension force than in reality. This happens for each time step and the net effect after a few time steps is that the suspension lowers more and faster than in reality. The effect of the damping on the specific volume can be seen in Figure 55 where the rapid increase in the specific volume of the gas can be seen once the displacement becomes negative (Figure 56). In Figure 56 it can be seen that the simulation results overshoot the measured results when the suspension is lowered.

There is some discrepancy between the measured and simulated results while the displacement is positive as well, this is also due to the damping. The oil is pumped into the suspension at the main strut (P2) in Figure 13. In the simulation it is modelled as the equivalent to the oil being pumped in at the accumulator (P1). This has the effect that the damping resists the displacement, where in reality it can allow for faster raising. The model is modelled in this way; because the ADAMS **(MSC.Software, 2011)** model requires a force input from the suspension m-file **(Mathworks, 2012)** as is shown in Figure 32 and Figure 33. Figure 57 shows the results where the damping in the system has been set to half its original value. An

improvement is visible at the end of the raising (8s) but during the raising process it becomes clear that the gas expands too much because there is less damping resisting it. Reducing the damping will give inaccurate results during a dynamic manoeuvre where the damping in the suspension plays a major role.

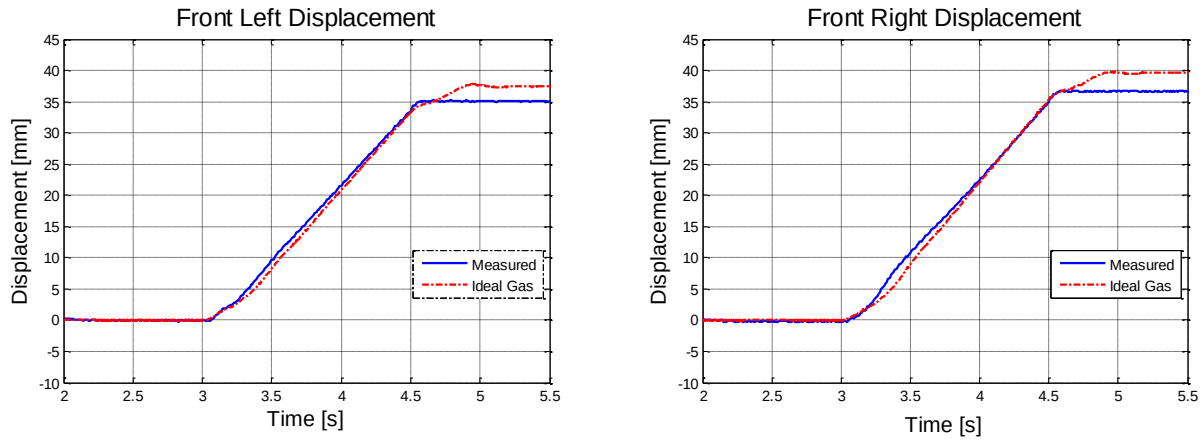

Figure 53 **Comparison between simulation results of the ideal gas model with flow 12.8l/m and experimental results**

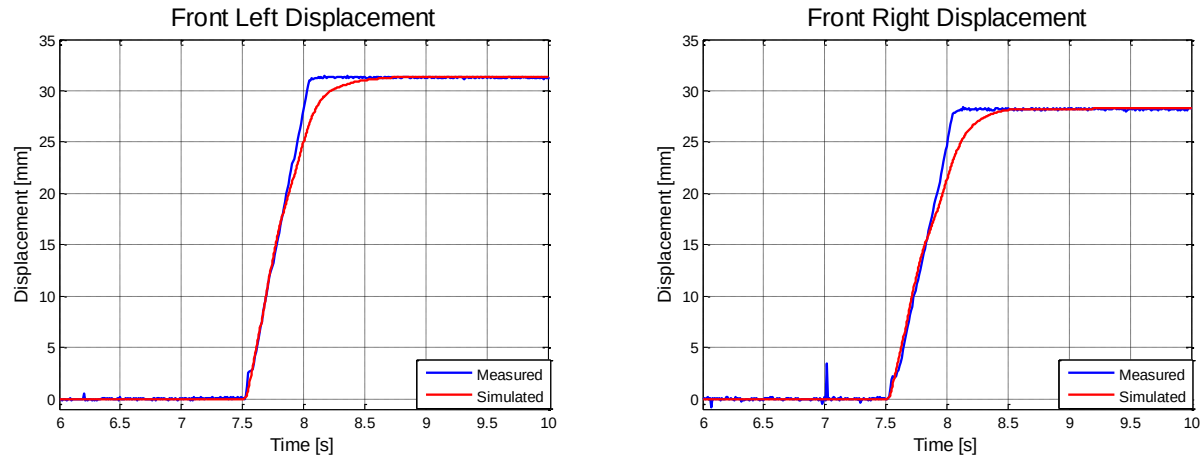

Figure 54 **Simulation results of BWR equation model with flow 12.8l/m**

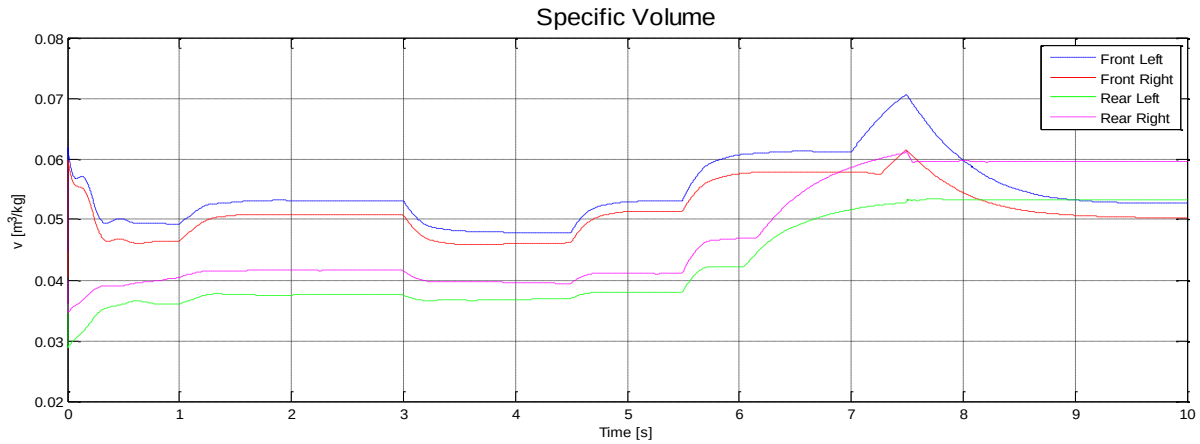

Figure 55 **Specific volume during the simulation**

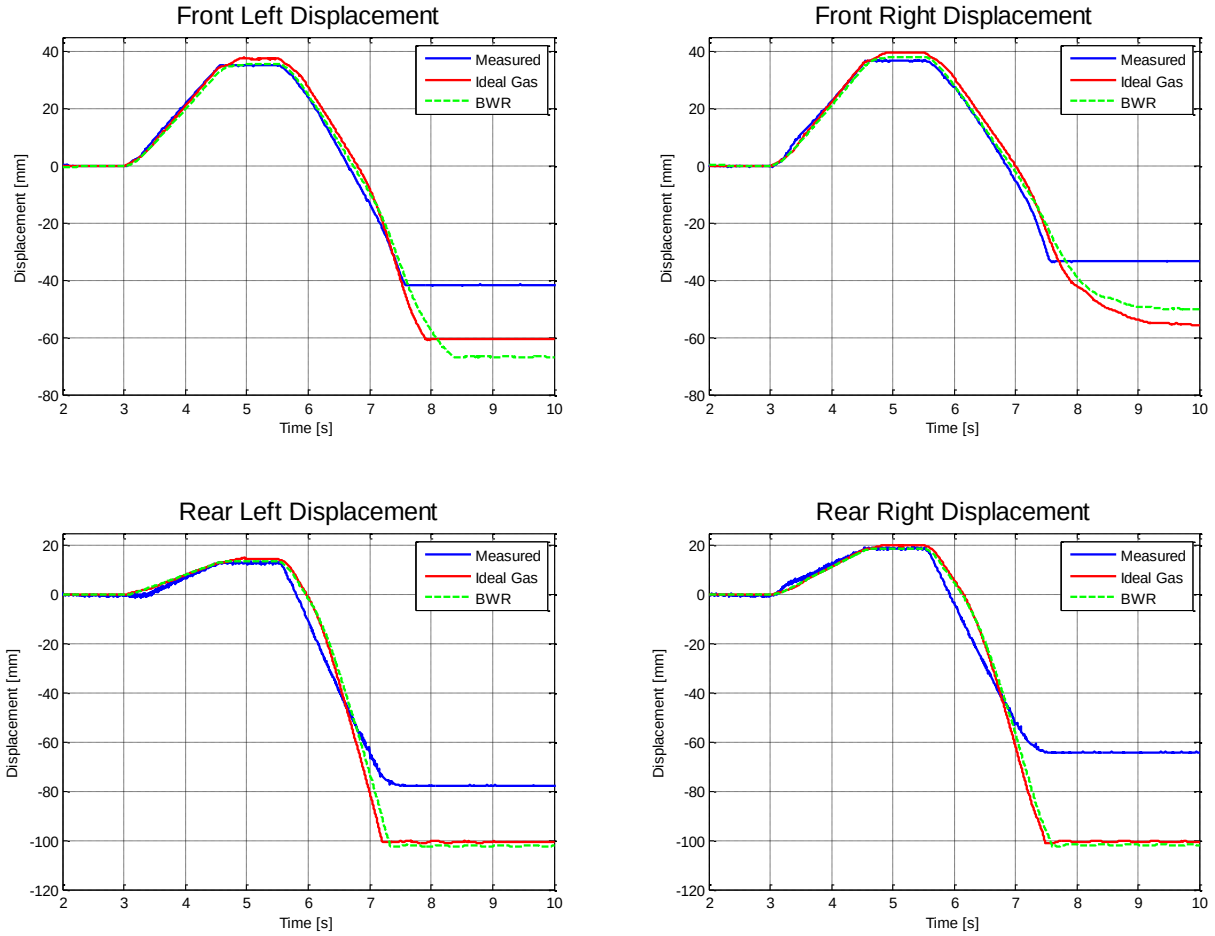

Figure 56 **Measured and simulated results for Ideal gas and BWR model**

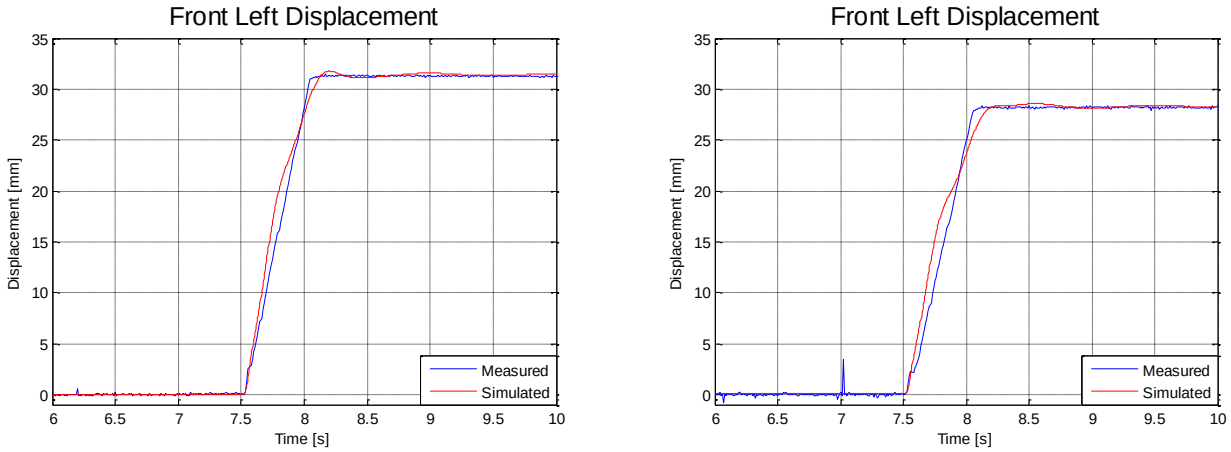

Figure 57 **Simulation results of BWR equation model with flow 12.8l/m (no friction & 50% damping)**

The lessons learned from the initial verification tests are now incorporated in the model and the BWR model is used to simulate a DLC manoeuvre at 60 km/h. The suspension displacement is controlled by adding or removing oil from each suspension unit. Oil is supplied from an accumulator (which is also modelled using the BWR equation) at a maximum pressure of 12.5 MPa. The maximum accumulator pressure was initially chosen as 20 MPa but initial tests on the vehicle have shown that the battery driven pump delivers a maximum pressure of 12.5 MPa. A PID controller as shown below is used to choose between pumping oil in, draining it or to close the valve. The gains used were the same as used in par 3.5.4. After looking at the data of the previous simulations it was found that the lateral acceleration becomes higher than 0.1g when entering a DLC. Thus in order to control the oil flow, the model selects between high or low flow using the lateral acceleration as input. Initial simulations showed that it has a negative effect on the handling to pump out too much oil from a suspension unit in order to keep the displacement zero. Therefore oil is only pumped out until a little less than the original amount of oil is left in the suspension. Simulations with this model again showed that a substantial improvement is possible on the body roll angle of the vehicle as can be seen in Figure 58. The working principle of the control algorithm used is shown below:

$$PID = k_1 x + k_2 \int x \, \partial t + k_3 \frac{\partial x}{\partial t}$$

$$PIDavg = average\ of\ PID(sample\_time_{i-4})\ to\ PID(sample\_time_i)$$

$if\ lateral\ acceleration < 0.1g$
  $valve\ opening = 10\%$
$else$
  $valve\ opening = 100\%$
end

$if\ PIDavg > 0.5$
  $if\ Amount\ of\ oil\ added > -0.005l$
    $Outflow\ valve\ is\ open$
  $else$
    $Both\ valves\ are\ closed$
  end
end

$if\ PIDavg < -0.5$
  $Inflow\ valve\ is\ open$
end

$if\ |PIDavg| < 0.5$
  $Both\ valves\ are\ closed$
end

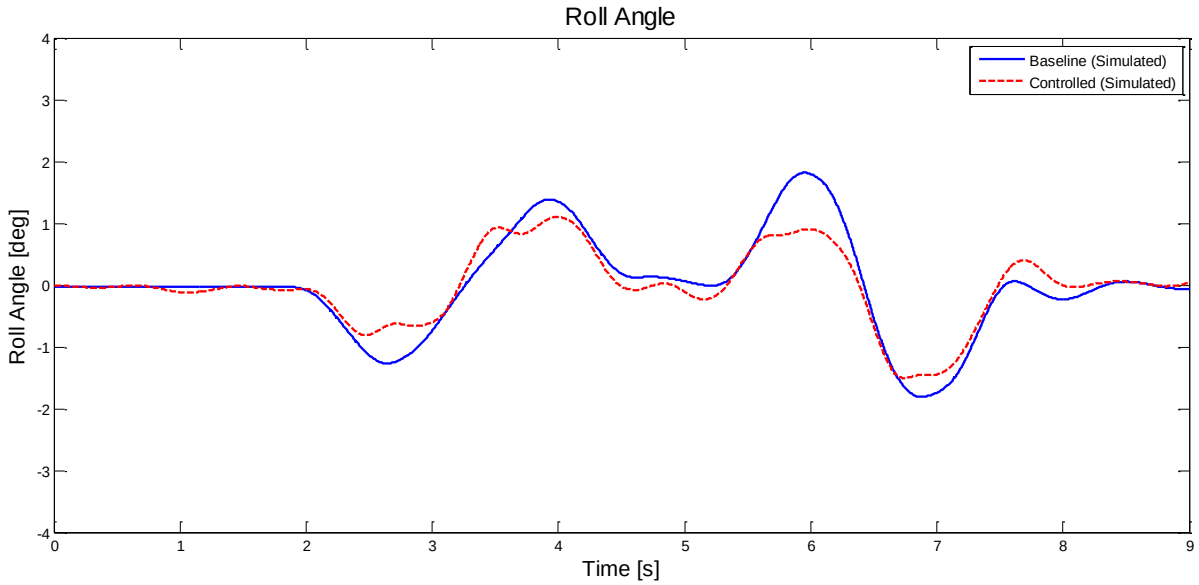

Figure 58 **Roll angles for a baseline and controlled DLC at 60km/h**

4.2 Voltage Controlled Current Source

In order to control the FPCC **(Sun hydraulics, 2011)** proportional valve (see Par. 3.3) using the PC/104 **(Diamond Systems, 2012)** available on the Land Rover test vehicle a voltage controlled current source is needed. An amplifier that serves this purpose is available from the valve manufacturer but it is expensive and the possibility of another solution was researched.

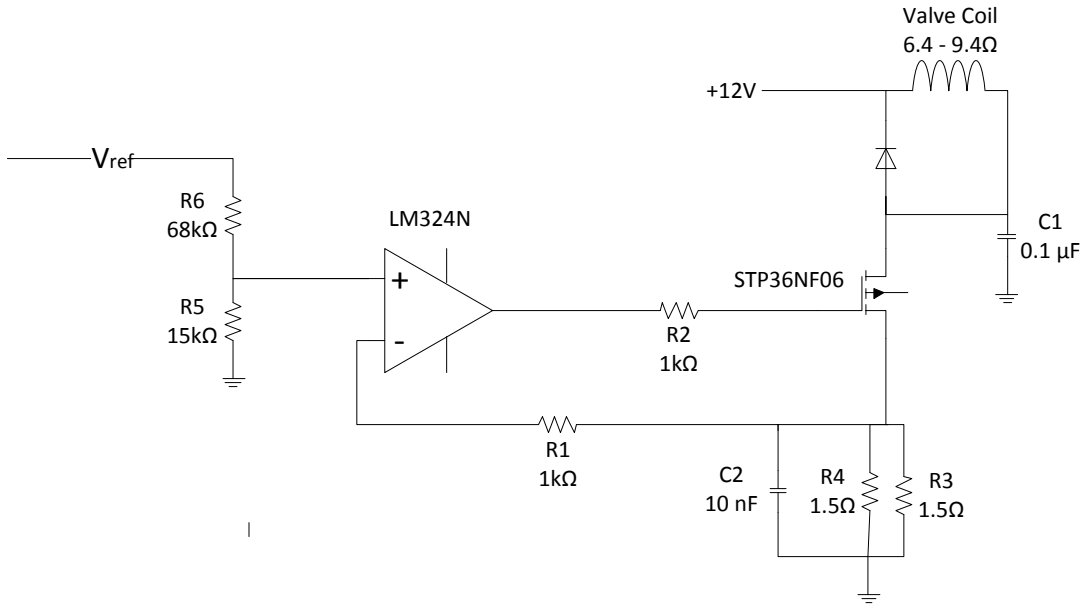

Figure 59 **Voltage controlled current source with a voltage divider in the reference voltage signal**

A voltage controlled current source was developed and tested in conjunction with another student who intends to use this current source to control a magneto-rheological (MR) damper. The PC/104 used in the test vehicle can deliver voltage between +5 and -5 volt on its analogue output channels, therefore it was decided that the current source should deliver a current of 0 - 1.15A for a voltage input of 0 – 5V. The coil of the valve can have a resistance as high as 9.4Ω when it heats up to 50ºC. Therefore a restriction on the maximum total resistance for R3+R4 of 1Ω was determined (see Figure 59), to enable sufficient current from the 12V power supply $\left(I = \frac{V}{R} = \frac{12}{1+9.4} \approx 1.15A\right)$.

In order to get the required input to output ratio the reference voltage to the operational amplifier is lowered by adding a voltage divider (R5 & R6) in the reference signal as can be seen in Figure 59. The resistors R5 and R6 has been given a high resistances so that the required current is low. The operational amplifier measures the voltage difference over R3+R4 and if the current is too low it closes the gate of the power MOSFET and if it is too high it opens the gate, thus controlling the current.

Due to the relatively high current passing through R3+R4 axial film resistors will have to be used in parallel due to their low power rating. A coil resistor, which generally has higher power ratings, can also be used. Using a single coil resistor will have the advantage that the manufacturing will be easier but the inductance of the coil might increase the response time. Comparative tests were done with axial film and coil resistors, and the results showed that there is no quantifiable difference between the response times and a coil resistor can be used (see Figure 60). The resistors used at R3 and R4 in the final design are 1.5Ω, 2W axial film resistors and were used due to availability at the time (see Figure 59).

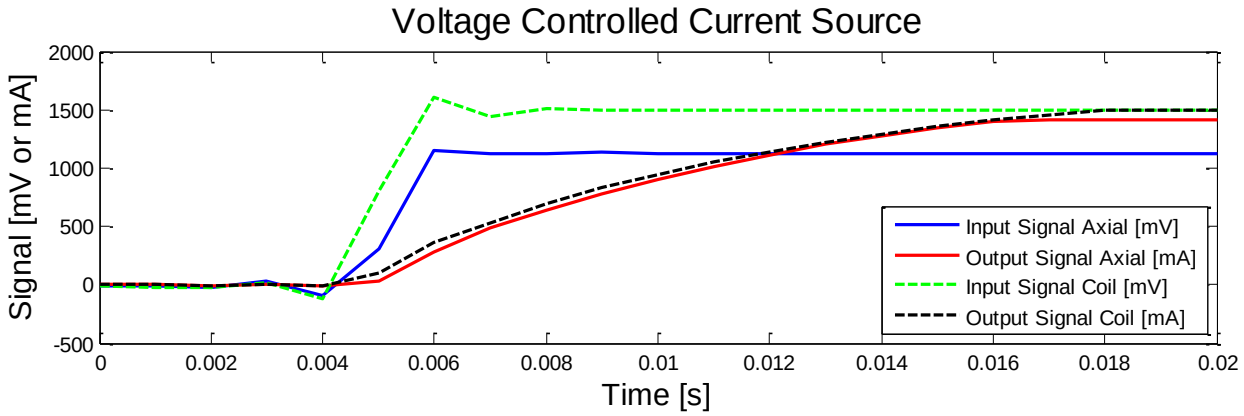

Figure 60 **Comparative test between a 1Ω-10W coil resistor at R3 and two 1.5Ω-2W axial resistors in parallel.**

The response for different input signals, and the valve coil as the load, is shown in Figure 62. The response show that there is a linear relationship between the input and output where 0V input will give a 0A output and a 5V input will give a 1.2A output. Although the sampling frequency (1000Hz) was too low in Figure 63 one can still see that the response time is under 4ms for maximum input command which is sufficient for the intended purpose.

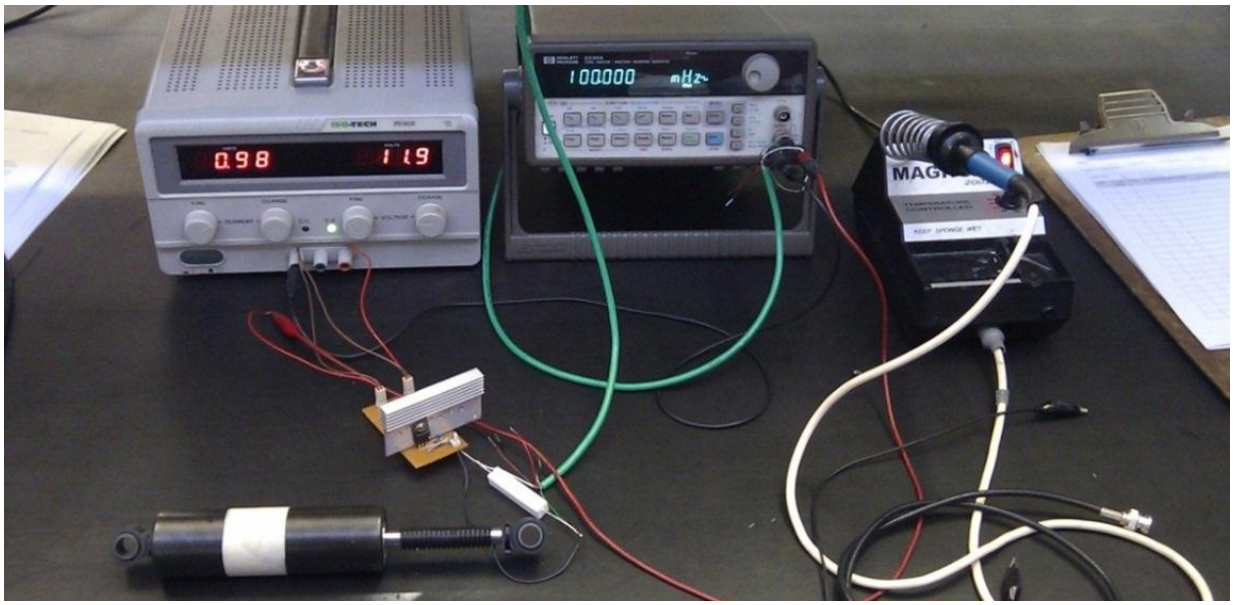

Figure 61 **Test setup with MR damper as load**

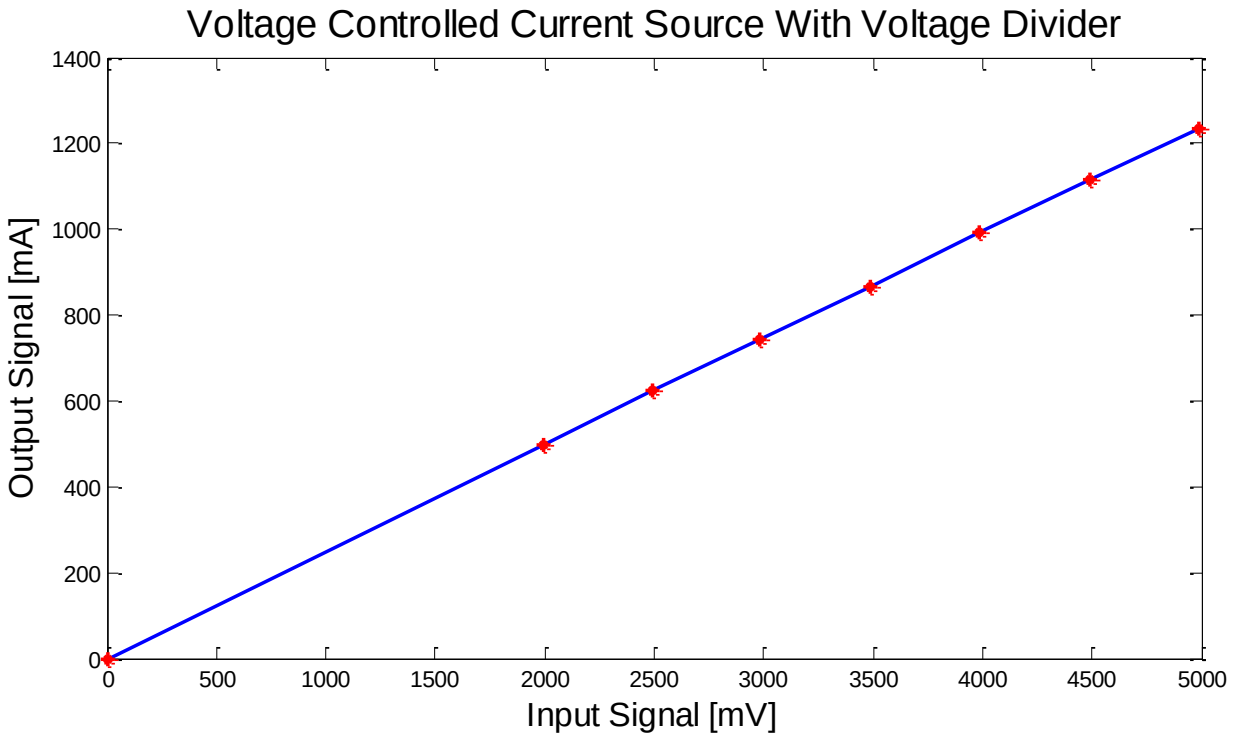

Figure 62 **Output signal for an input signal of 2-5V in 0.5V increments**

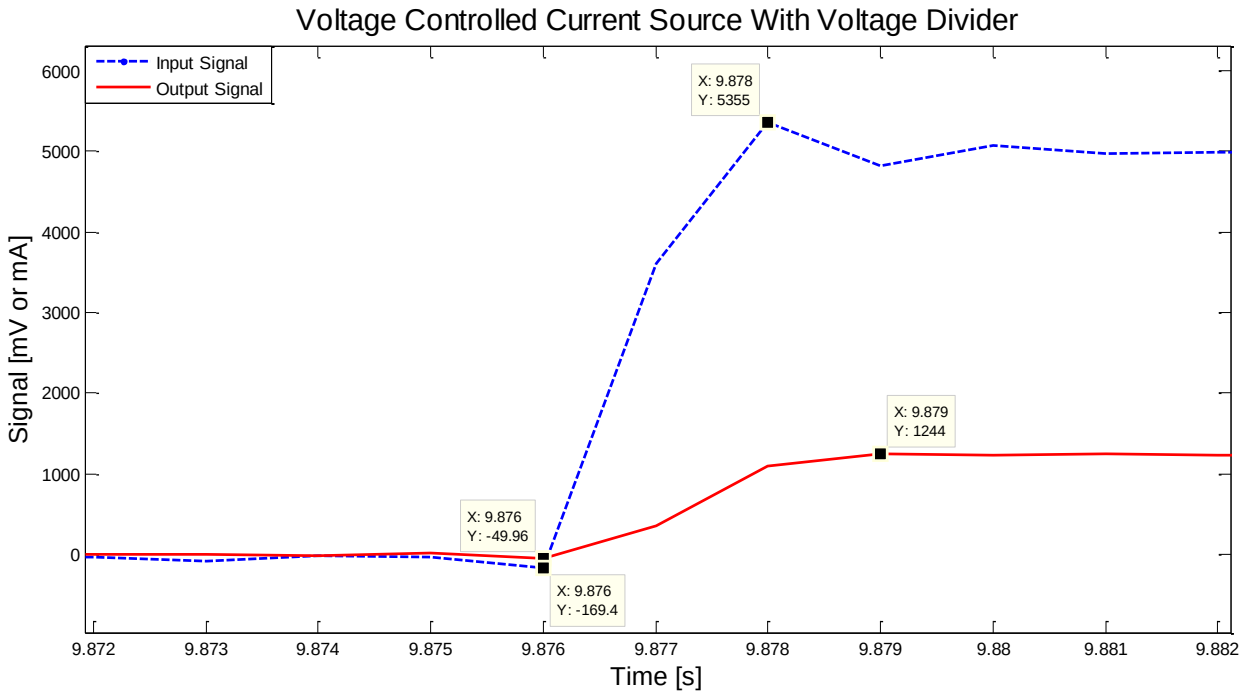

Figure 63 **Input and output signal for an input signal of 5V**

4.3 Proportional Valve Characterisation

To determine the flow obtained at different valve opening commands, the valve is given a determined percentage of its command input for 0.5 seconds to raise the suspension and then it is given the same command input for 1 second to lower the suspension. Using this data, the average flow can be determined as it is indicated in the legends of Figure 64 to Figure 67. From these results it is seen that the proportional valve responds faster than the directional valve and thus there is a slight increase in the height just before the suspension is lowered. This increase in height is due to the proportional valve opening before the directional valve was able to switch from inflow to outflow. This was rectified by adding a delay on the proportional valve so that it starts to open 70 ms after the directional valve so that both open fully at the same time. From the data one can also see that an input of less than 50% gives negligible small flow and therefore it was not included in the characterisation. Flow above 80% is more than 200% higher than the expected required flow and it will also not be included in this characterisation measurements.

Using the data in Figure 64 to Figure 67 for the inflow and the pressure data recorded of the suspensions and the accumulator, a pressure vs. flow graph is generated (see Figure 68). The data obtained here is not sufficient to get an accurate indication of the flow curve of the valve, the valve needs to be opened longer over a broader range of ΔP. This however is not possible with the valves installed in the vehicle and the characterisation will need to be done on a hydraulic test bench. The average flow does give a relatively good indication as to what flow to expect at different valve openings and it was decided that this will be sufficient.

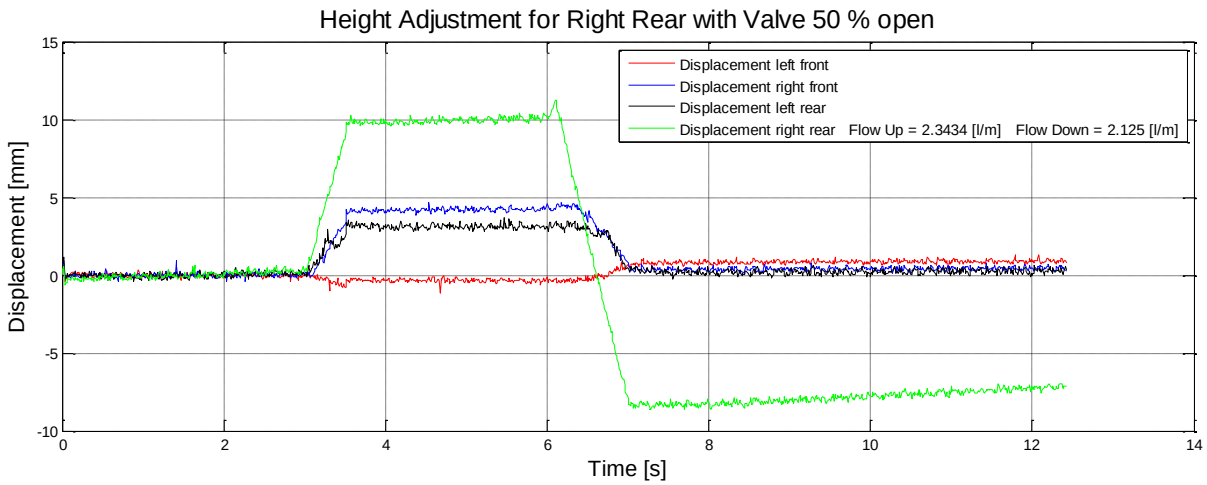

Figure 64 **Valve test with a 50% command input.**

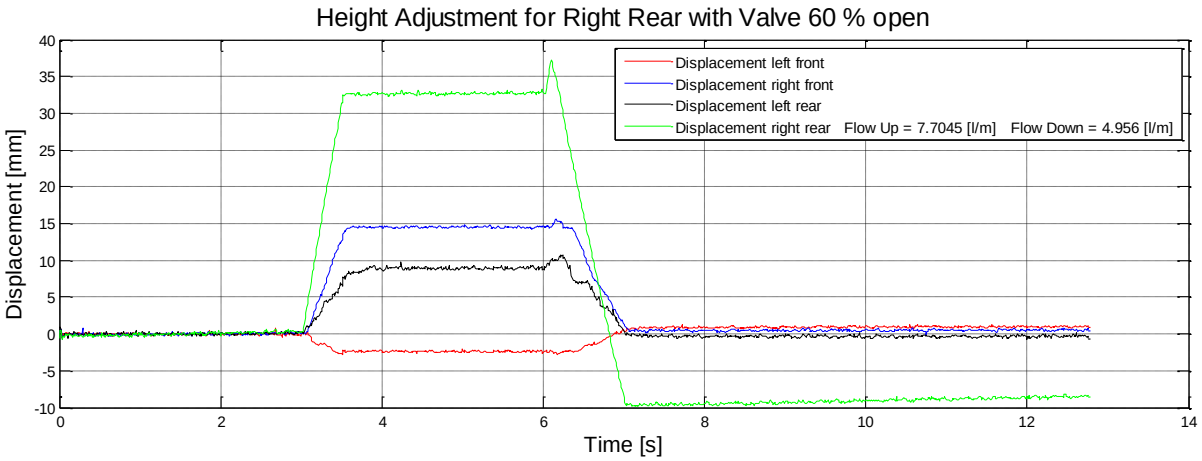

Figure 65 **Valve test with a 60% command input.**

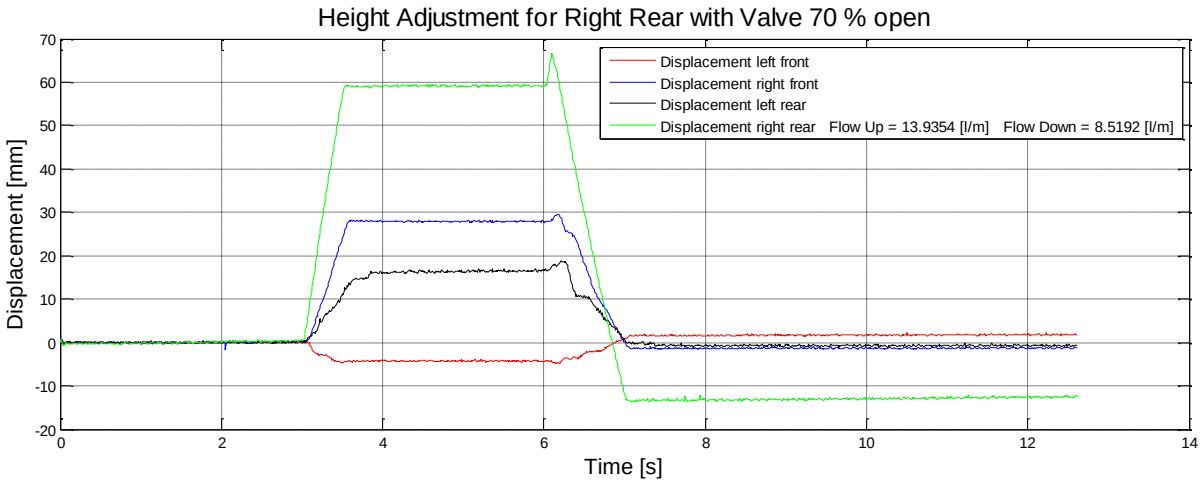

Figure 66 **Valve test with a 70% command input.**

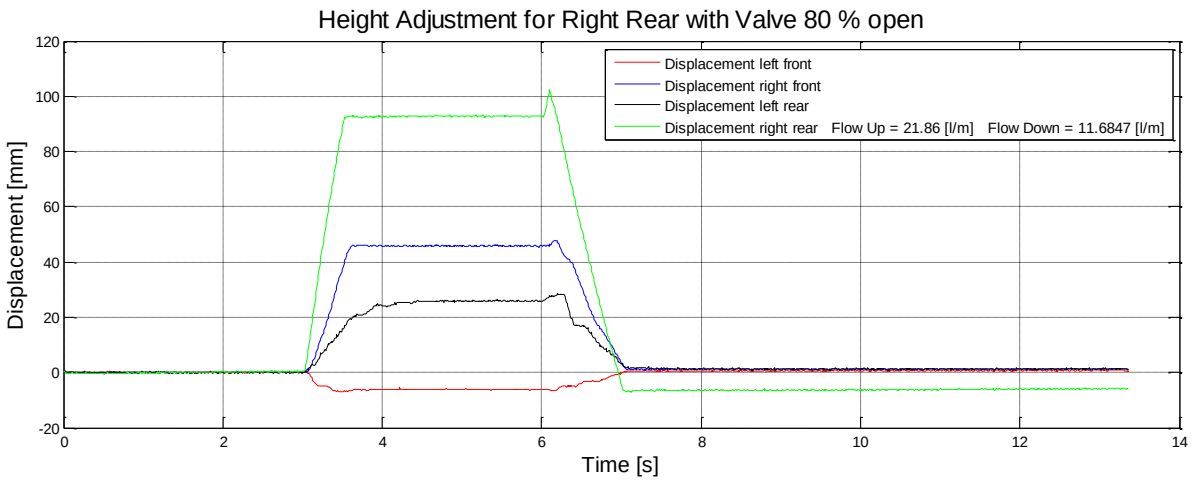

Figure 67 **Valve test with a 80% command input.**

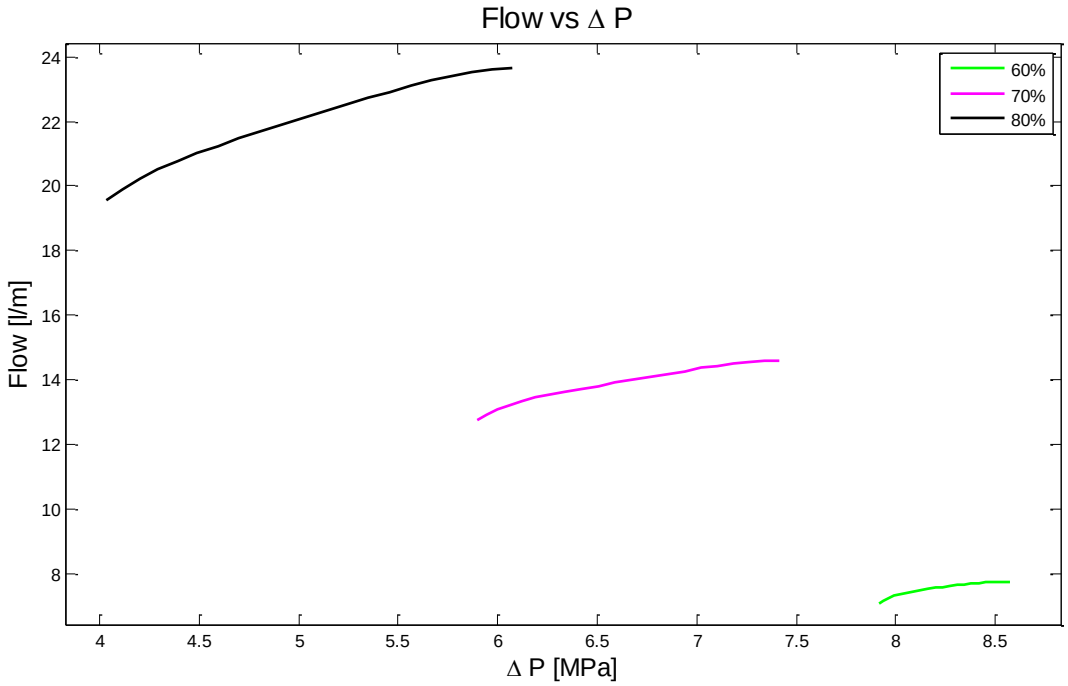

Figure 68 **Flow vs Pressure curve obtained for different valve openings.**

4.4 PID Control Algorithm

Initially when the control algorithm was first implemented (Par. 3.5) the PID controller was averaged over 5 terms. However, the derivative term gave erroneous values due to the noise present in the displacement signals, a typical signal is shown in Figure 69 where the noise is visible in the detail section. In Figure 70 the drift on the PID signals for a static test can be seen in the left figure. Therefore the displacement signals were filtered by taking the average over 5 terms. The derivative was then calculated from the filtered displacement and this was found to improve the results substantially as can be seen in the right figure of Figure 70.

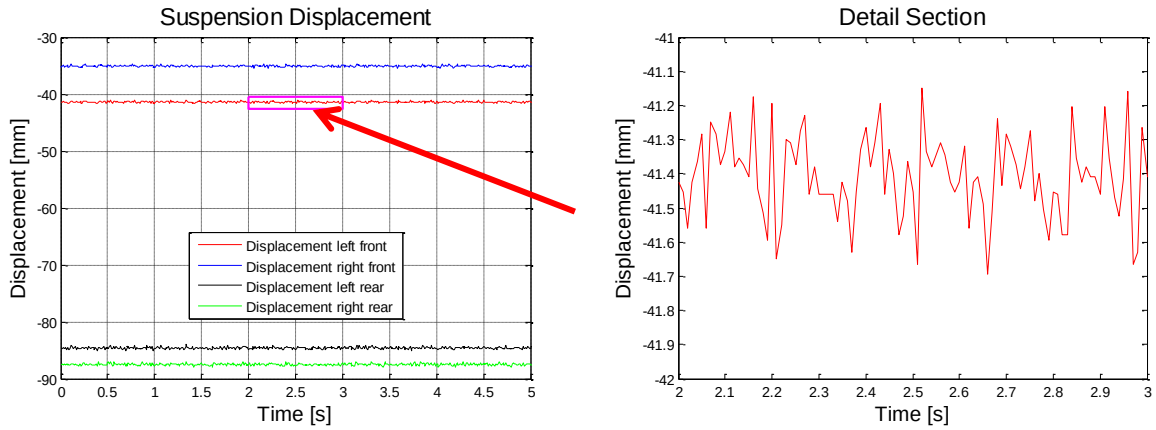

Figure 69 **Noise on the displacement Signals**

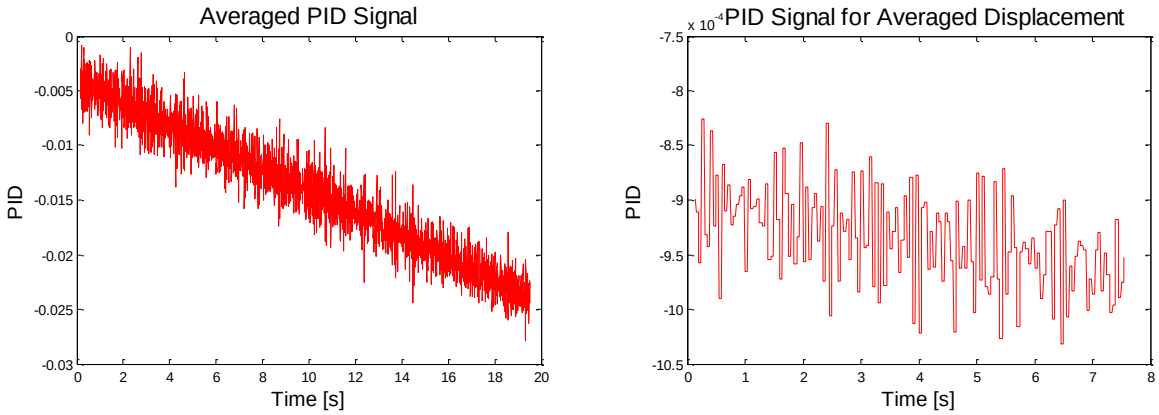

Figure 70 **PID signals for the averaged PID (left) and for the averaged displacement (right)**

4.5 Volume Estimation

The amount of oil in the suspension units are estimated to prevent the control algorithm from pumping out too much oil from the suspension, as this can have a negative effect on the suspension response. In order to estimate the amount of oil in each suspension unit the equation for the bulk modulus of fluid is used in combination with the ideal gas equation. The volume of the nitrogen is estimated using the ideal gas law while the compression of the oil is calculated using the bulk modulus equation (See Appendix C).

In order to get a better estimation the input signals to the volume equation is filtered with a low pass finite impulse response filter in real time. The filter has a pass frequency of 8 Hz and a stop frequency of 25 Hz. The filter is of the order 14 and has a step response of about 90 ms. This results in a delay of about 90 ms on the estimated volume signal. In order to get a minimum volume value where the algorithm should stop the outflow the volume of oil in the suspension is calculated while the vehicle is standing still and the roll control is active, the vehicle is left until the suspension settles and then the average of the predicted volume is obtained. Twice the standard deviation of the signal is taken and subtracted from the average to get a value that will include 97.8% of the signal values at the desired amount of oil. In the control algorithm of the suspension no more oil is pumped out of the suspension once the predicted

amount of oil in the suspension reaches this value. In Figure 71 it can be seen that the suspension has settled by the time it reaches 8s therefore the value is calculated from 8s to the end of the signal and is shown in Figure 72. To test if the estimation prevents the suspension from pumping out too much oil the vehicle was lifted at the front with a hydraulic jack and then dropped. The same was then done with the rear as is shown in Figure 73. The results look relatively good but there is some error in the prediction of the volume, possibly due to the friction in the suspension strut. The effect can be seen in Figure 74 at the right front and left rear wheels where the volume settles to a different value even though the displacement is at zero in both cases as can be seen in Figure 73. In a controlled environment like this it is expected that the suspension will settle close to the same value each time but due to the friction this is not the case in reality. It is however expected that during actual driving of the vehicle, the effect of friction will be less due to continuous suspension movement and the dynamic friction is significantly lower than the static friction. In Figure 74 one can see that the Left front and Right Rear had a large and definitive reaction to the suspension being extended, it was later found that these two suspension units had very little gas in their accumulators. Thus pressures nearing zero were measured and this gave the large change in the estimated volume.

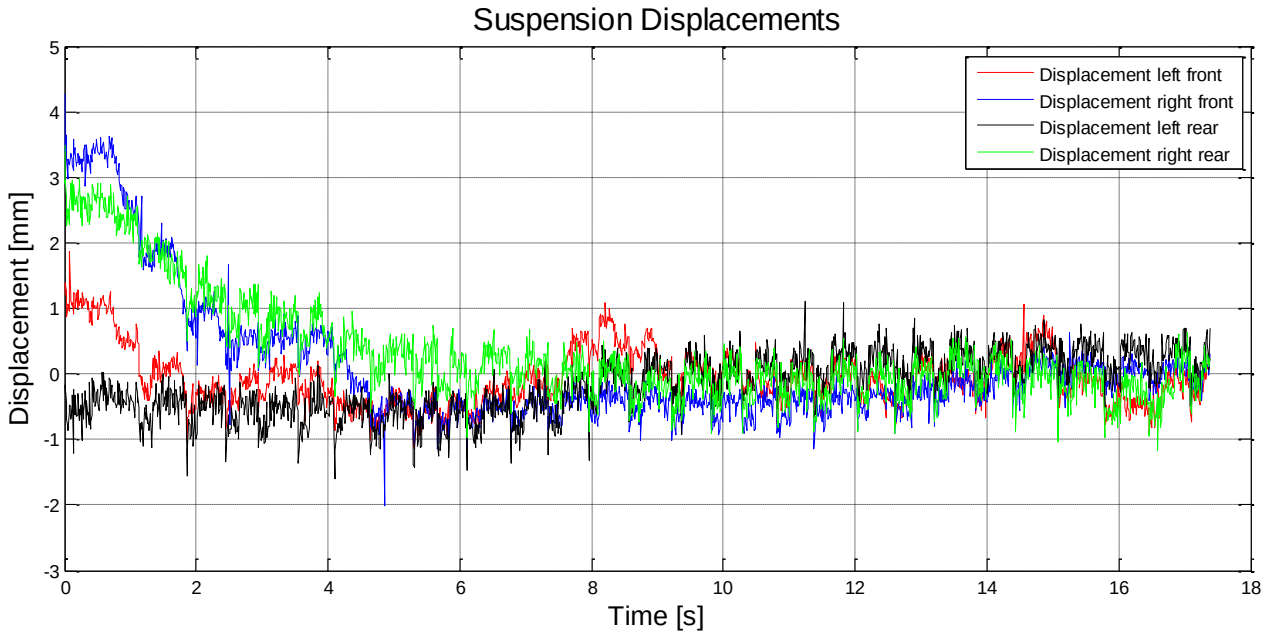

Figure 71 **Suspension displacements**

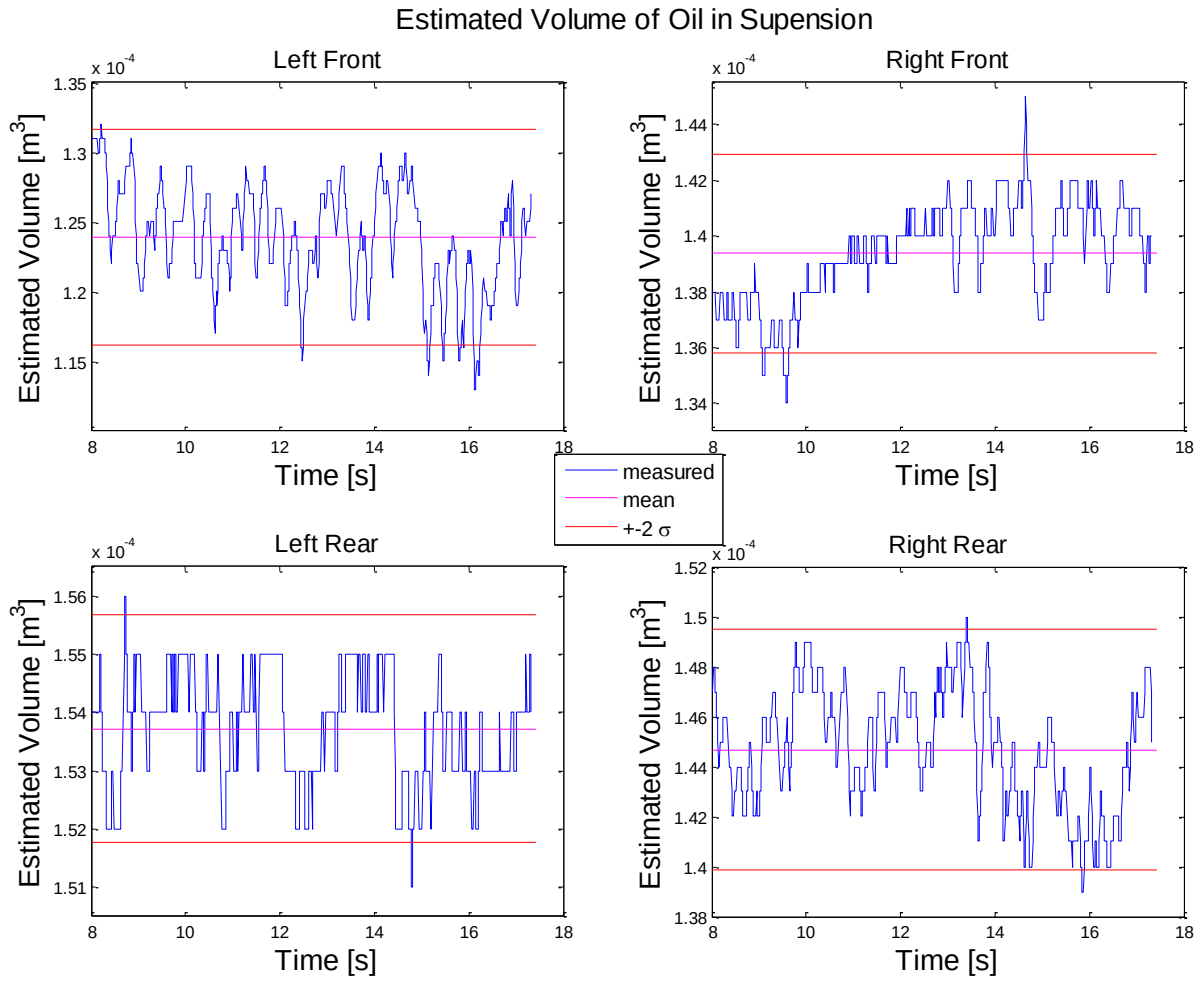

Figure 72 **Estimated volume of oil in suspension**

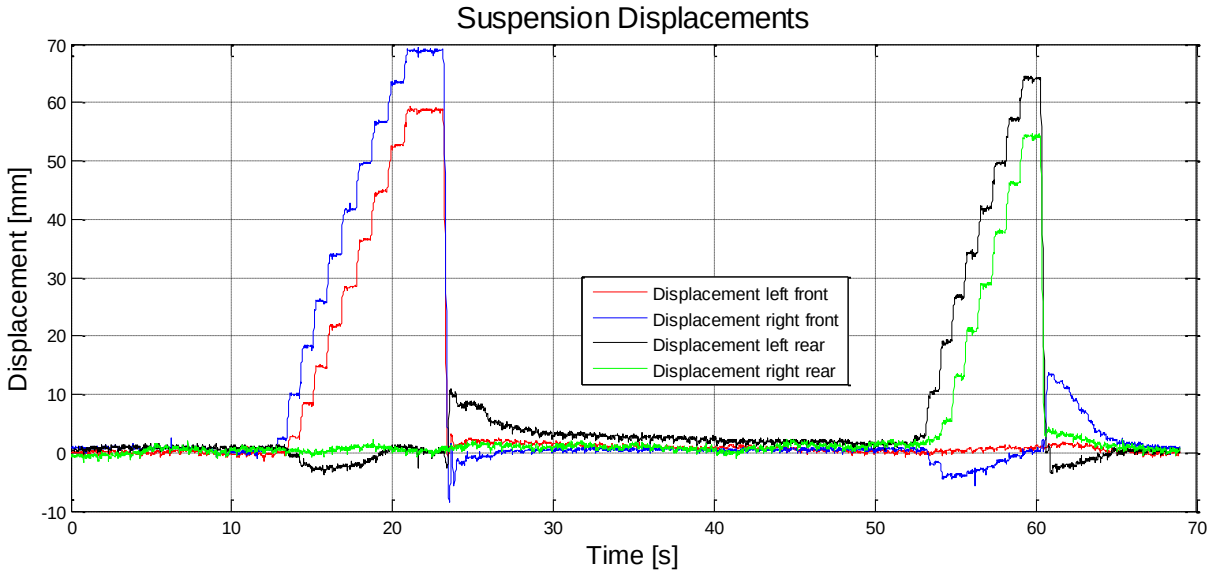

Figure 73 **Suspension displacements during fall test**

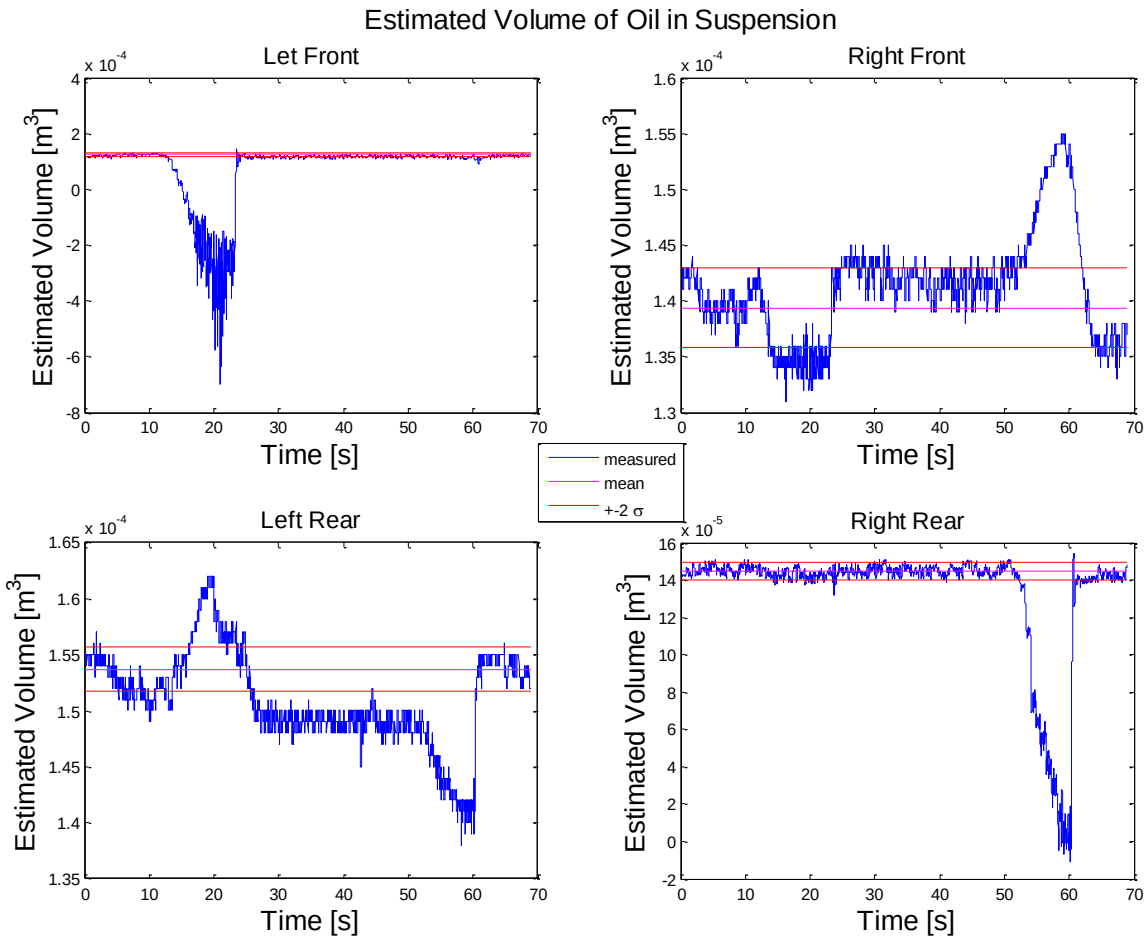

Figure 74 **Estimated volume of oil in suspension during fall test**

4.6 Vehicle Implementation and Experimental Results

4.6.1 Initial problems and modifications

4.6.1.1 Battery Power

The initial test setup used a 2 ℓ accumulator to store the oil and the pump was switched on when the pressure dropped below a certain value. It was however found that the current drawn by the 12V Direct Current (DC) motor, used to pump the oil, drops the voltage of the batteries to such an extent that the directional valves cannot function. Extra batteries were added but this did not solve the problem and the 2 ℓ accumulator was replaced with a larger 10 ℓ accumulator (see Figure 75), to enable a DLC without using the pump. This solution (not using the pump while performing a DLC) however limits the duration that the suspension can be controlled and it also limits the maximum oil flow. From the valve characteristics for the FPPC valve in Figure 30 it can be seen that sufficient flow (more than 14 ℓ/min) is still possible with a ΔP of 2 MPa. During an experimental DLC at 80 km/h a maximum pressure in the suspension of less than 5 MPa was reached and therefore the accumulator was charged to 7 MPa (this means that the gas pressure will be 7 MPa when the gas volume is 10 ℓ), which allows the accumulator to

store about 3 ℓ of oil at 12.5 MPa, which is close to the maximum pressure the pump would deliver with the battery setup.

Figure 75 **10 ℓ bladder type accumulator being charged to 7 MPa**

4.6.1.2 Volume Limit

As mentioned in par. 4.5 the amount of oil in the suspension units are estimated to prevent the control algorithm from draining too much oil from the suspension, as this can result in a negative effect on the suspension response. Although the signals are filtered there is still a substantial amount of noise present, because filtering out lower frequencies will cause an excessively large delay. Due to the change in volume of oil in the suspension being relatively small, the noise on the measured signals has a severe effect on the accuracy of the volume estimation. The volume estimation is shown in Figure 76 where one can see the substantial amount of noise present, also note the small change in volume relative to the noise. Friction affects the estimated volume to some extend as well, but the effect seems relatively small during actual driving as expected due to the constant movement of the strut. During earlier tests an improvement in the results was obtained by reducing the limit by 10% from the limit obtained in par. 4.5. After testing it was found that the new limits were set too low as can be seen in Figure 76, and that it never stopped the algorithm from draining too much oil. The improvement was likely due to the lower limit preventing the

volume algorithm to make any decisions and thus it also prevented it from making erroneous decisions caused by the noise.

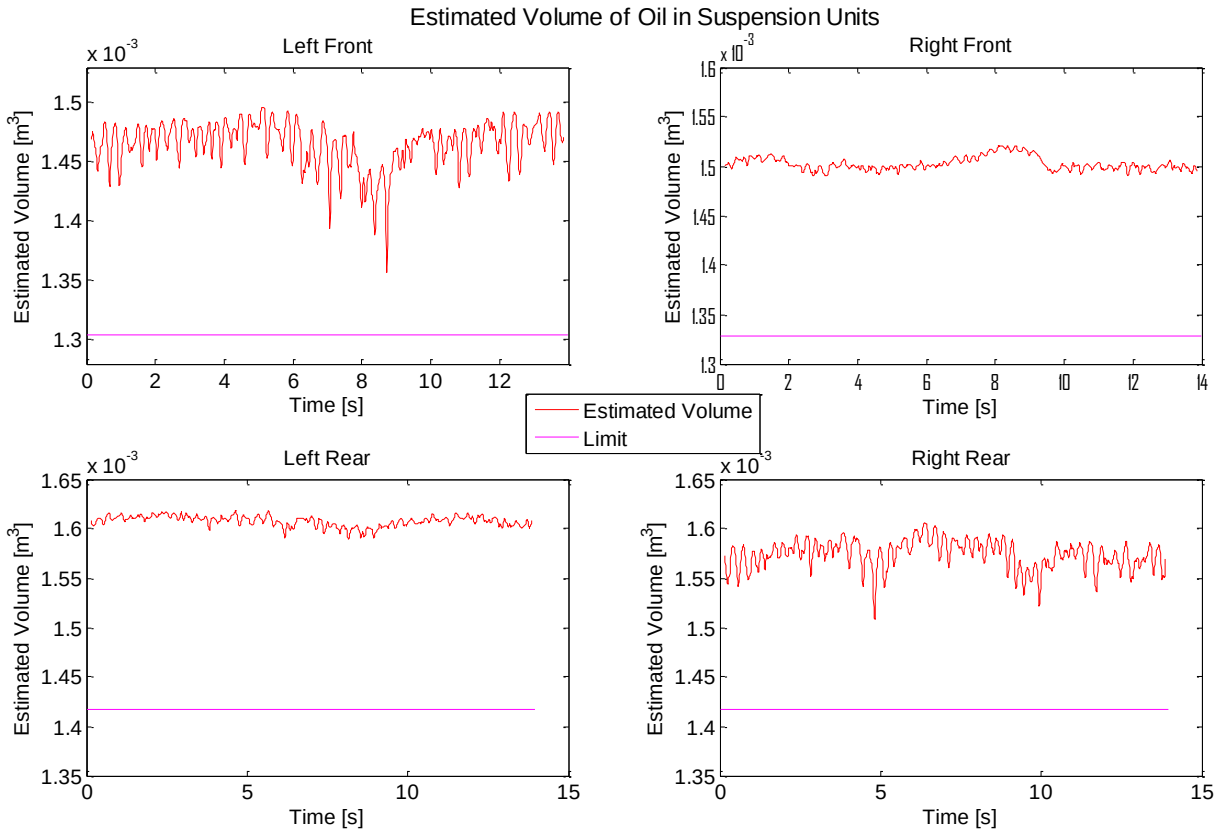

Figure 76 Estimated Volume during a DLC at 60 km/h

4.6.1.3 Valve Response

During the characterisation of the FPCC valve shown Figure 77, a single proportional valve was characterised to determine the flow rate across the valve as a function of the input voltage (See par. 4.3). It was assumed that all valves will share the same characteristics. However it was found during field testing that all the valves do not respond the same, and some adjustments had to be made in the field with limited success due to the limited information available at the time. In Figure 80 (Par. 4.6.2) it can be seen that the flow of the left suspension units were too low, but there is a significant improvement in the displacement of the right suspension units were the flow was somewhat higher.

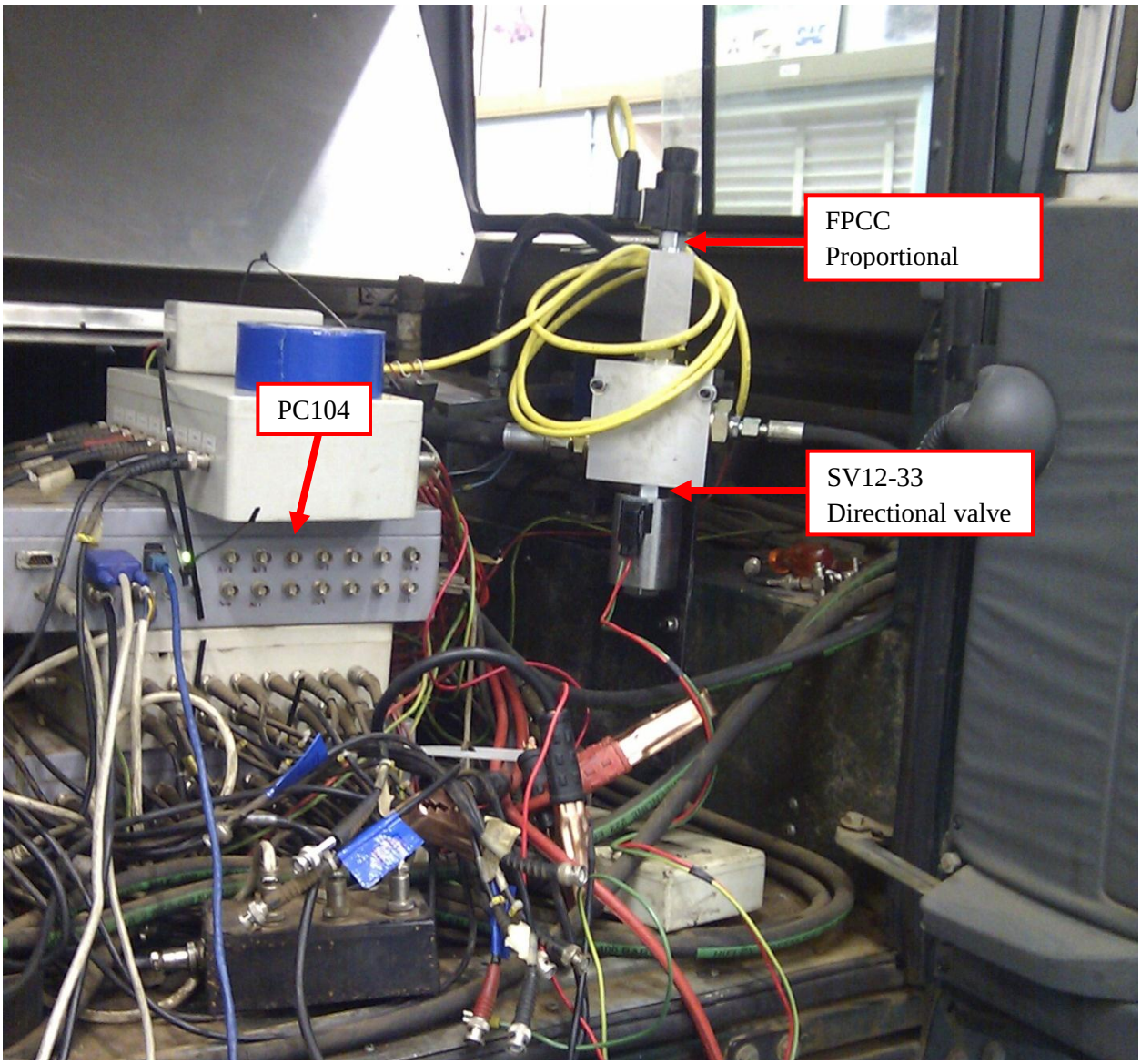

Figure 77 Valves for the rear suspension unit during characterisation

4.6.2 Experimental Results

Experimental testing was done by performing a DLC on a level concrete straight track at Gerotek near Pretoria in South Africa **(Gerotek, 2012)**. A total of 31 DLCs were done at different speeds (50, 60, 70 and 80 km/h) over two testing sessions. After looking at the results of the initial tests it was decided to do the tests at 60 km/h on the stiff suspension setting due to the flow constraints on the system. The Land Rover Defender test vehicle (see Figure 78) was equipped with a VBOX III GPS **(Racelogic, 2012)** to record the path and speed of the vehicle. String displacement sensors were used to measure the suspension displacements, laser displacement sensors were fixed to each side of the vehicle to measure the roll angle as can be seen in Figure 79. Pressure transducers were used to measure the pressure of the accumulator as well as the pressures in the suspension struts. To link the GPS data with the data recorded on the PC104 **(Diamond Systems, 2012)** an optical trigger was fixed to the rear of the vehicle and it was

triggered by a reflective strip placed on the track before the vehicle enters the DLC. An accelerometer was used to measure the lateral acceleration. In total 15 measured channels were used to perform the experimental tests. The control algorithm made use of a PID controller to control the suspension displacement by opening or closing the proportional valves while the magnitude of the valve opening was determined by the amount of lateral acceleration that the vehicle experiences (Table 3). The PID value was calculated digitally using the PC104.

The final setup comprised of the following:

Table 3 Valve opening commands for different lateral accelerations

Lateral Acceleration (a)	$\|a\| \leq 0.1g$	$0.1g < \|a\| \leq 0.2g$	$0.2g < \|a\| \leq 0.3g$	$0.3g < \|a\|$
% Valve Opening Command	43	48	53	58

$$x_{avg} = average(x_{i-4}: x_i)$$

$$PID = k_1 x_{avg} + k_2 \int x_{avg}\, dt + k_3 \frac{dx_{avg}}{dt}$$

if $PID > 0.5$
    Outflow valve is open
end

} Suspension Extended (Outflow Control)

if $PID < -0.5$
    Inflow valve is open
end

} Suspension Compressed (Inflow Control)

if $|PID| < 0.5$
    Both valves are closed
end

It was found during the testing that the results improved when the integral component was excluded and effectively using a Proportional Derivative (PD) controller. This is likely due to the noise present on the signals, which was not present in the simulations. Due to a limit on the size of the variables, the noise on the signals and the fact that simulations showed that the response is not sensitive to changes in the gains above the limit value the gains were chosen as $k_1 = 2$, $k_2 = 0$ and $k_3 = 1$ and the limit was set as 0.5, this will start countering displacement the moment it passes 0.5mm which is sufficiently sensitive relative to the sensitivity of the displacement sensors and the magnitude of the noise. The valve opening command for the left front valve was multiplied with 1.3 and right rear with 1.2 in an attempt to get the same flow at all the suspension units. Afterwards it was however found that these adjustments were not sufficient. The volume limit was also deactivated here due to the reasons explained in section 4.6.1.2.

Figure 78 **Land Rover Defender test vehicle being prepared for testing**

Figure 79 **Laser displacement sensor on the side of the vehicle**

Figure 80 shows the suspension displacement of Run 1 for a DLC at 60km/h and an overall improvement is visible in the displacement of the right suspension units. Improvement in the RMS of the displacement as high as 56% is obtained as can be seen in Table 4. The left front suspension's valve allowed too little flow and therefore it can be seen that the reaction of the control is slower than that of the left rear unit. This added with the volume algorithm not stopping the oil draining resulted in the excessive compression of the suspension around 10s on the x-axis. On the left rear one can see that the system had a faster response due to higher oil flow but here similar to the left front unit too much oil was drained and this resulted in an excessive compression around 10s as well. The body roll angle shown in Figure 81 was improved overall even with the volume estimation and oil flow not optimal. A maximum improvement of 0.9˚ is found just after 5 seconds for run 1, where the roll angle is improved from 1.85˚ to 0.95˚ giving a 49% improvement. In Table 5 it can be seen that the RMS of the roll angle was improved by as much as 30%. Figure 82 shows the vehicle's path and speed during the baseline and controlled runs and the consistency between the two runs is very good.

Table 4 RMS of the displacement for run 1

RMS of the displacement during a DLC at 60km/h for Run 1				
	Baseline [m]	Controlled [m]	Difference [m]	% Improvement
Left Front	3.22	3.16	0.068	2.10
Right Front	4.73	2.09	2.64	55.75
Left Rear	3.61	3.08	0.52	14.50
Right Rear	2.35	1.90	0.45	19.19

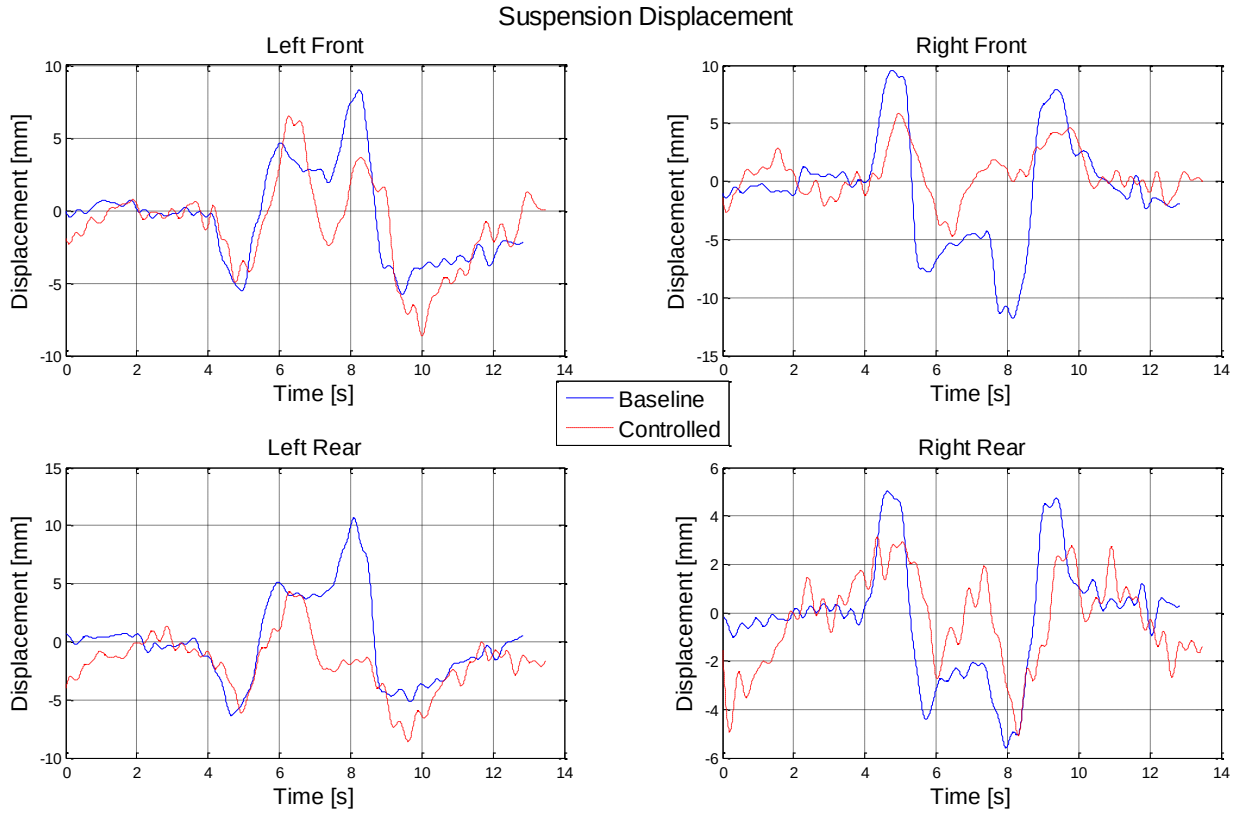

Figure 80 Suspension displacements for Run 1 during a DLC at 60km/h

Table 5 RMS of the roll angle for two different runs

RMS of the roll angle during a DLC at 60km/h				
	Baseline [˚]	Controlled [˚]	Difference [˚]	% Improvement
Run 1	0.81	0.57	0.24	29.6
Run 2	0.81	0.61	0.2	24.7

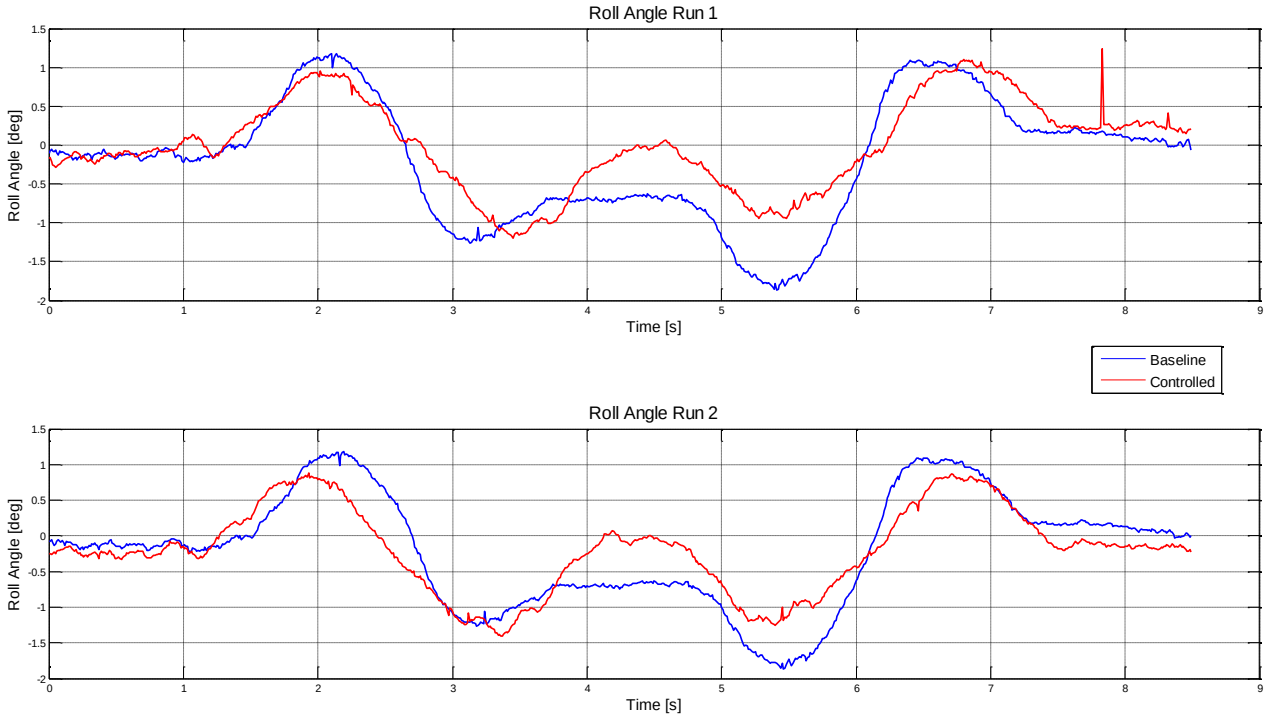

Figure 81 Body roll angle for DLC's at 60km/h

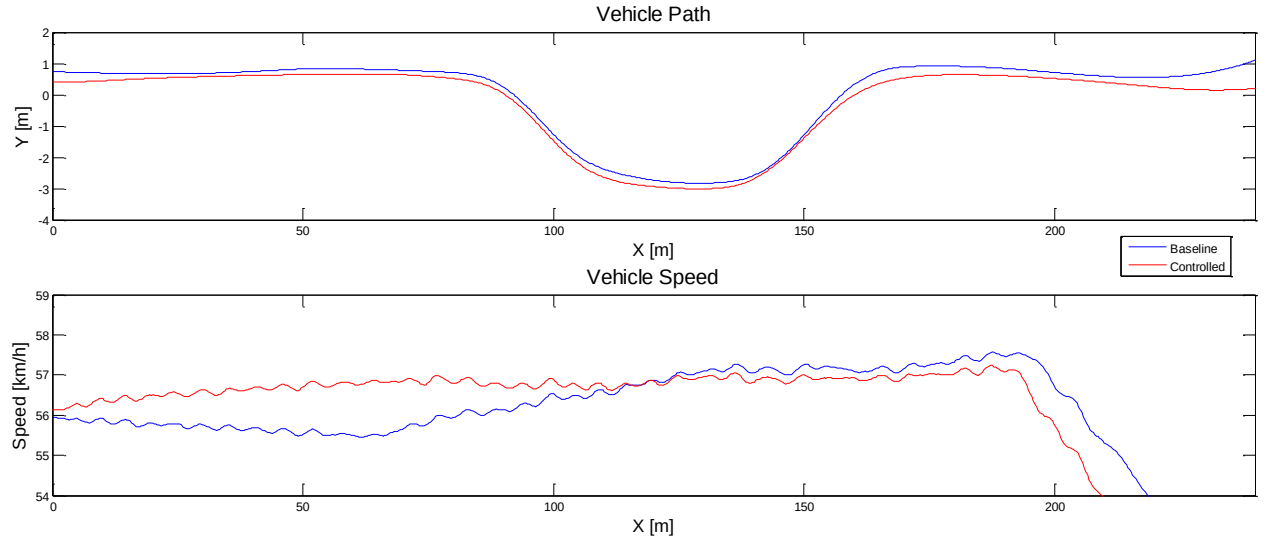

Figure 82 Vehicle path and speed for the baseline run and controlled run1

4.7 Simulation Verification

After experimental data was obtained the simulation model was updated and compared to the experimental data. The results correlated well and using this model the effects of some system changes were investigated.

Although the results correlate well, there are some known shortcomings to the model. The model under estimates the suspension force when it is being drained down into the negative and this can cause quite significant deviations as can be seen in par. 4.1. The suspension does however never compress more than 10mm (due to the control) and therefore the effect of this shortcoming is very small. The valve flow during opening and closing is not modelled. The valves are modelled as if they open fully immediately but this is not the case in reality. The model compensates for this to some extend by using a sample time of 60ms. The effect of this does however seem small and it does make the model less computationally expensive. The road input in reality is not 100% smooth as it is in the simulations. Taking into account that the control system will react differently to different inputs and that these reactions will influence the rest of the decisions still to be made the correlation of the model with the measured is satisfactory. Figure 83 shows the roll angle results of the experimental run and the BWR simulation. These simulations were done by giving the actual speed and path of the experimental run to the model. A major deviation occurs at the right rear unit around 8 s in Figure 84. This might be due to some unknown input that is not modelled into the simulation or due to the mentioned shortcomings of the model.

To see how the system would perform if a larger oil flow was possible and the volume in the suspension could be determined accurately a few different scenarios were simulated. Suspension displacement and roll angle for different flow magnitudes with and without a minimum volume limit is shown in Figure 85 to Figure 89. The flow stated in Figure 85 to Figure 89 is the total average flow for all four suspension units. From these simulation results it becomes visible that the volume limit does not always have a positive effect. But the volume limit does reduce the maximum roll angle in almost all the runs. It also is more advantageous in the case of low oil flow where the flow is not sufficient to counter the quick compression, as was also seen in the experimental data. The left front displacement is not significantly influenced by adjusting the volume limit and this is because of the suspension being compressed initially and a relatively large amount of oil is pumped into the suspension so that the limit of -5 ml is not reached again in some of the cases. These results have also been obtained using the experimental speed and vehicle path and should give an indication what the results would have been if the volume control was successfully implemented during the experimental testing.

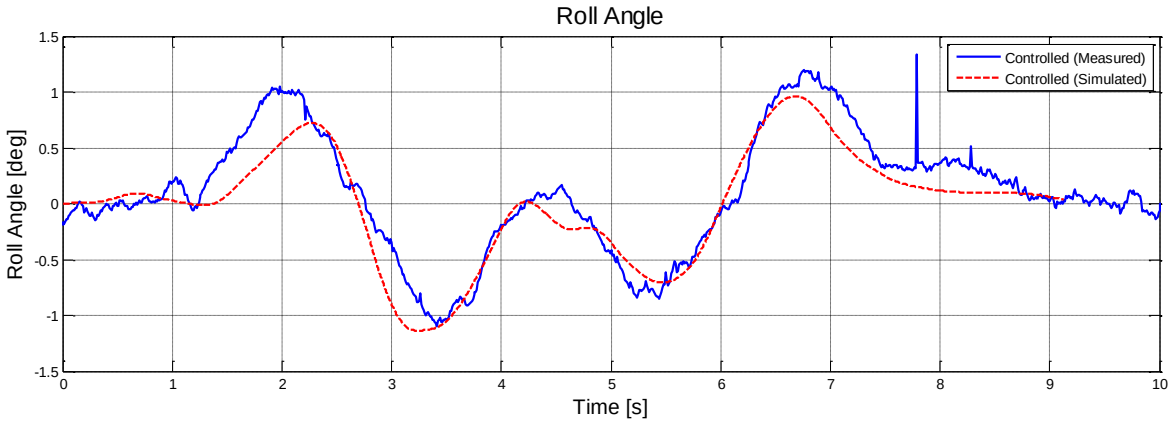

Figure 83 **Simulated and experimental roll angle for a controlled DLC at 60 km/h**

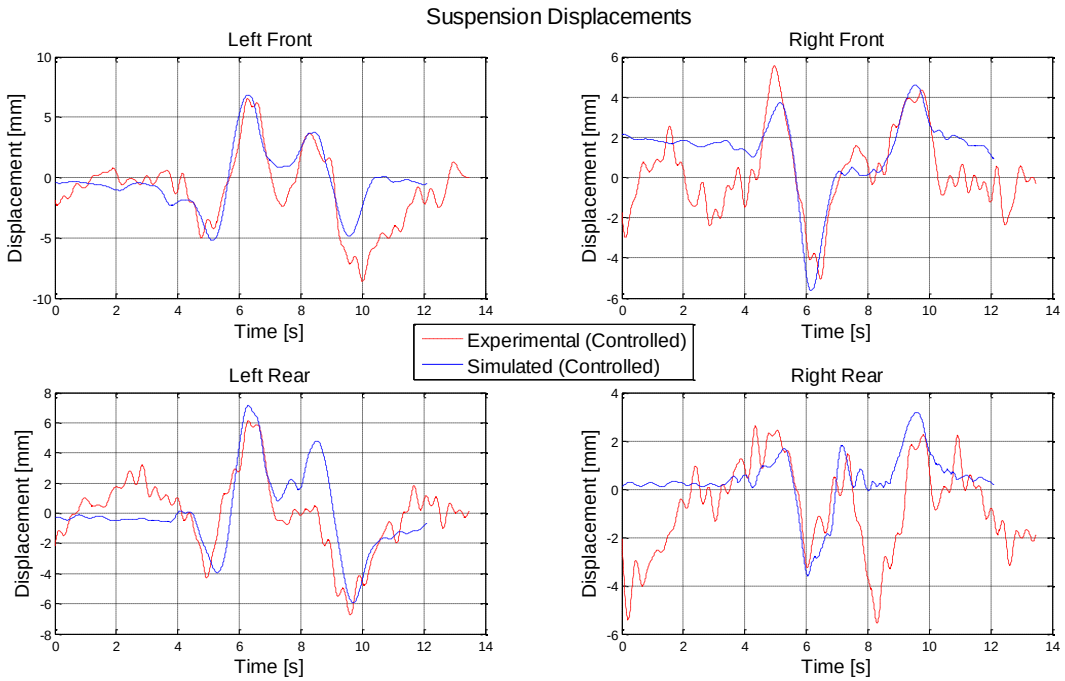

Figure 84 **Simulated and Experimental controlled suspension displacement for a DLC at 60km/h**

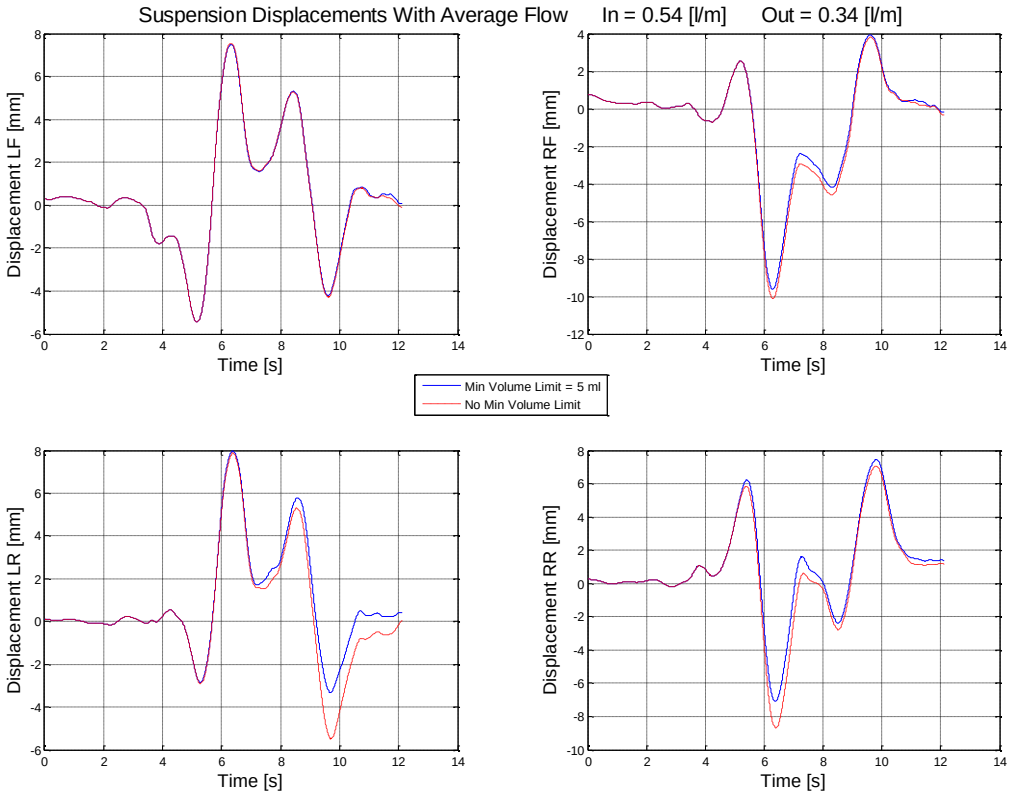

Figure 85 **Suspension displacement for average total inflow of 0.54 l/m during a DLC at 60km/h**

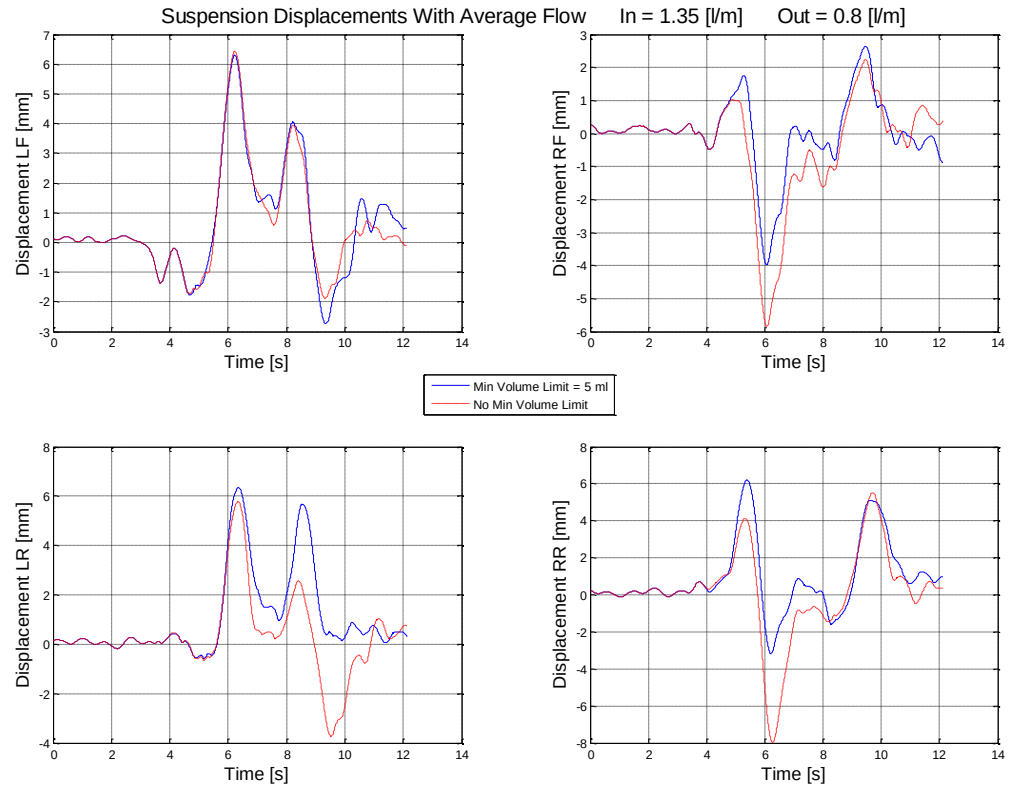

Figure 86 **Suspension displacement for average total inflow of 1.35 l/m during a DLC at 60km/h**

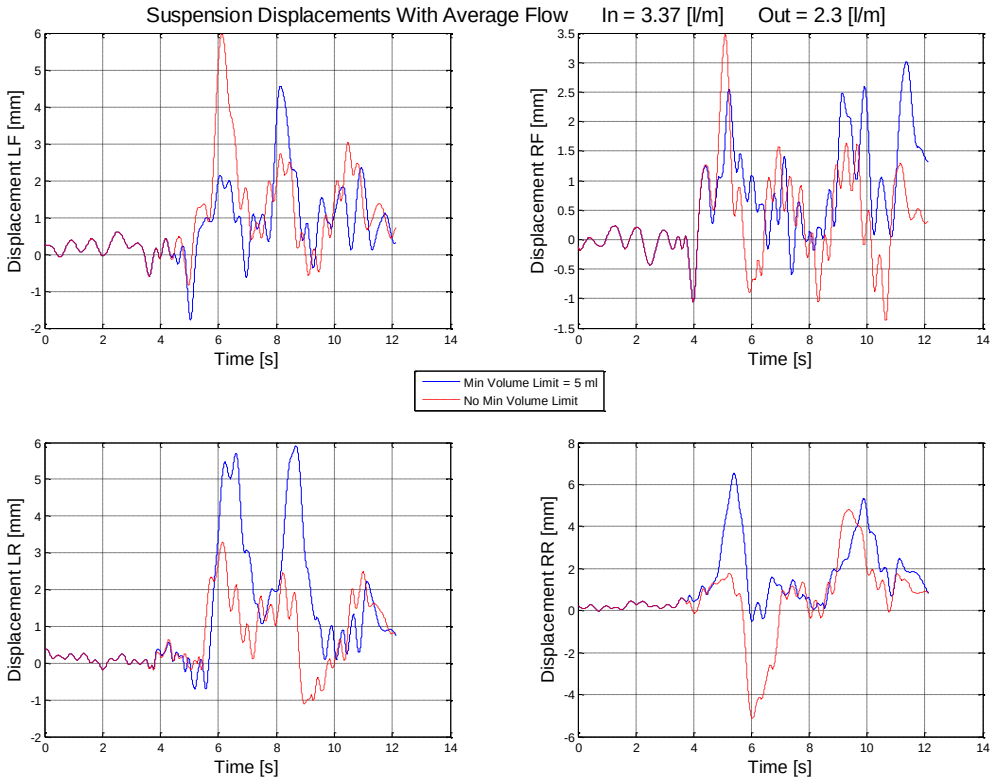

Figure 87 **Suspension displacement for average total inflow of 3.37 l/m during a DLC at 60km/h**

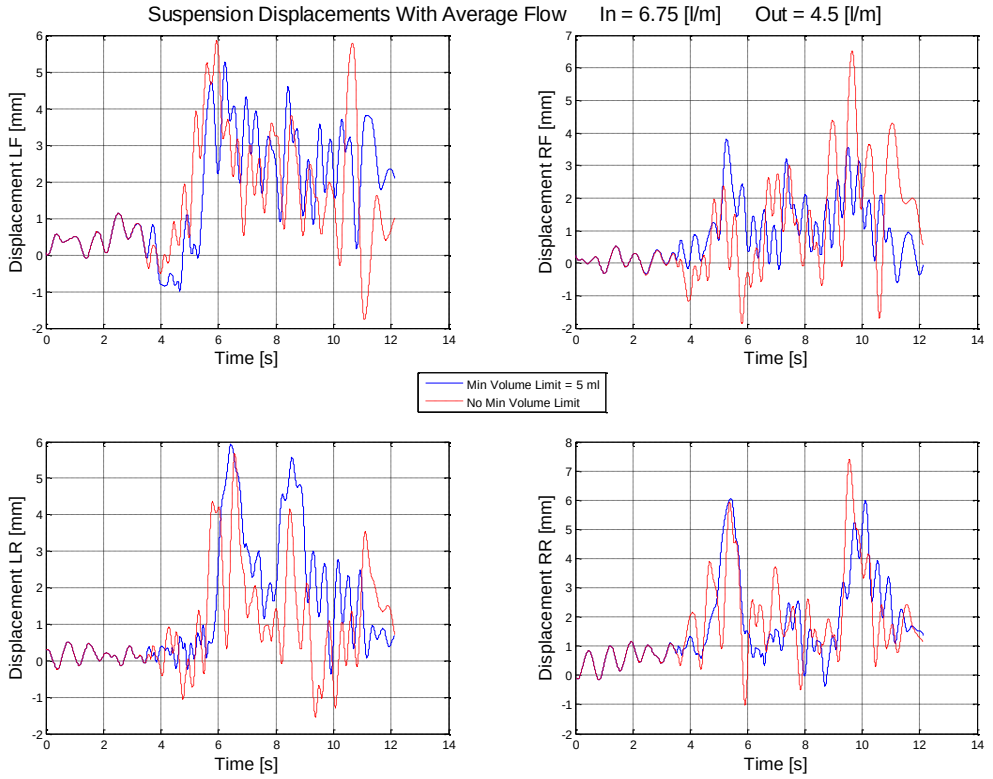

Figure 88 **Suspension displacement for average total inflow of 6.75 l/m during a DLC at 60km/h**

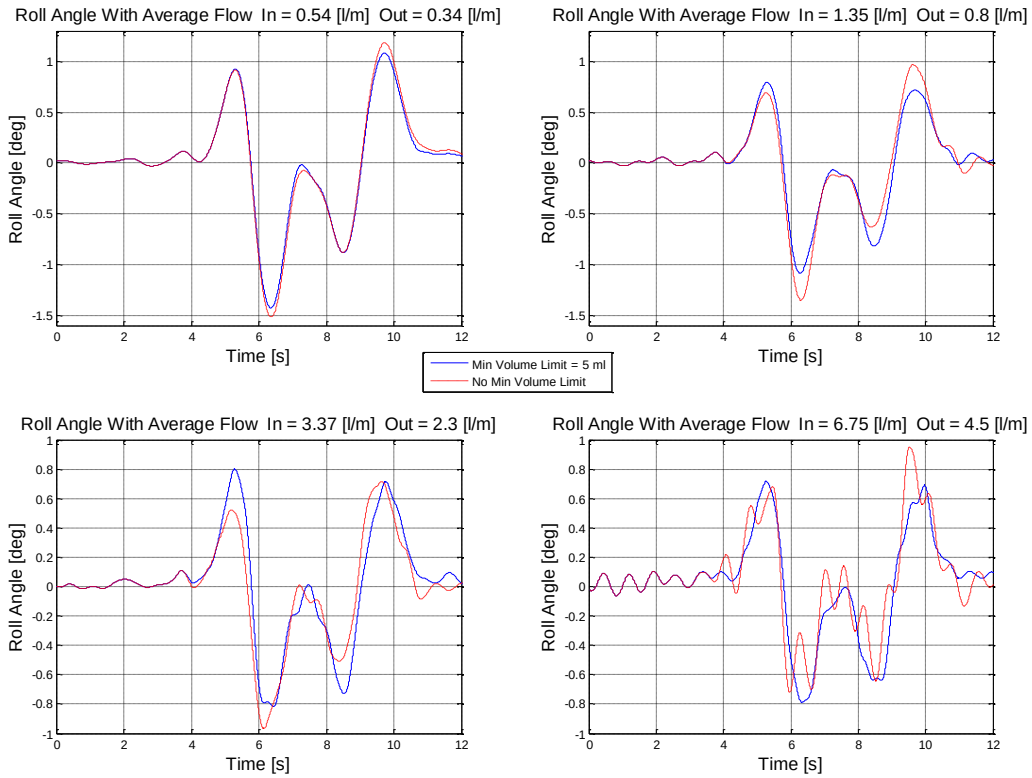

Figure 89 **Roll angle for different total flow magnitudes during a DLC at 60km/h**

4.8 Conclusion

The experimental results show that a significant improvement in the body roll angle is possible with relatively low flow requirements. The average flow for the experimental runs is estimated to be around 3.5 l/min (without losses). The average flow out of the accumulator during the DLC test run shown was 6.1 l/min. The large amount of losses is primarily due to the leakage of the solenoid operated valves and expansion of the rubber pipes. It might be possible to reduce the losses and then the system will be even more effective. An accurate method of determining the volume of oil in the suspension will also improve the results. But even with the mentioned shortcomings a significant improvement was obtained using slow active suspension control. The simulation model also correlates well with the experimental results. The model can be used to predict the effect of changes to the system with good accuracy.

5. Conclusion

Slow active suspension control has been successfully modelled and implemented on a test vehicle. Both the simulation and experimental results show that a significant improvement in body roll angle is possible by actively controlling the amount of oil in each of the hydropneumatic suspension struts. This also provides the possibility to cancel out squat and pitch. This setup will either utilise or enable height adjustment on the vehicle. The average flow out of the accumulator during a DLC test run was 6.1 l/m including the leakage of the valves which can easily be obtained with an engine driven pump.

The suspension displacements on the right were improved in all aspects and similar results should be possible for all the suspension units. A more accurate method of determining the volume of oil in the suspension and a rigid algorithm to adjust the volume limit for the specific situation is also expected to improve the results. The correlation between the experimental data and the simulation data is satisfactory and different setup configurations can be modelled with good certainty. This will allow for faster further development of this system. Better improvement might also be possible on a softer suspension where there are larger displacements but due to oil flow limitations this was not tested.

Using slow active suspension control will enable one to use, with some minor changes, the height control on vehicles to replace the anti-roll bar. Individual suspension control will also give the possibility of changing the handling characteristics while driving to suit the specific situation best. Thus, this method of roll control is feasible with added advantages over that of an active anti-roll bar.

6. Recommendations for future work

During opening and closing phase of a valve a complex flow phenomena takes place. Some work on modelling the flow through a valve in these phases has been done at the University of Pretoria. Including these phases in the model might improve the results. The model also makes many ideal assumptions which make it more effective computationally, but better correlation might be possible if the losses in the system is determined and modelled in.

When the directional valves were chosen the flow was expected to be much higher than it was found to be. The result is that these valves are larger than necessary, this result in slower response times and more leakage than with smaller valves. The solenoid operated valves were chosen for their fast response times and ease of controllability but their leakage does have a detrimental effect on the energy requirements and if a better solution could be found it would increase the effectiveness of the system drastically.

Characterising of each of the proportional valves individually is required. To obtain the flow relative to the other valves will allow one to control the flow of each suspension unit to be the same. This can increase the effectiveness of the control significantly and should be investigated.

Further work can be done on finding a better method to determine the volume of oil in the suspension and an algorithm that will decide what the volume limit should be for certain driving situations. The PID controller and the proportional control can also be optimised some more.

Currently a 12V DC electrical motor drives the pump that supplies the oil. This is an ineffective setup due to the many losses associated with an electrical system. A pump driven directly from the engine of the vehicle can solve the oil flow problems and should be investigated. With an engine driven pump it might also be possible to test the system on a softer suspension.

A theoretical study looking at rollover and not just at the body roll angle can be investigated, to determine the improvement in the rollover threshold.

7. Bibliography / References

A

Abe, M. and Manning, W., 2009, *Vehicle Handling Dynamics*, Elsevier Ltd., Amsterdam, 2009.

B

Bauer, W., 2011, *Hydropneumatic Suspension Systems*, Springer, Heidelberg, 2011

Botha, T. R., 2011, *High Speed Autonomous Off-Road Vehicle Steering*, University of Pretoria, Pretoria, http://upetd.up.ac.za/thesis/available/etd-11212011-125411/unrestricted/dissertation.pdf, Accessed 2 August 2012.

C

Cheney, W. and Kincaid, D., 2004, *Numerical Mathematics and Computing*, Brooks/Cole-Thomas Learning, Belmont, 2004

Choi, S.B., Lee, H.K. and Chang, E.G., 2001, *Field test results of a semi-active ER suspension system associated with skyhook controller*, Mechatronics, Vol. 11, pp. 345-353, 2001

Cimba, D., Wagner, J. and Baviskar, A., 2006, *Investigation of active torsion bar actuator configurations to reduce vehicle body roll*, *Vehicle System Dynamics*, Vol. 44, Nr. 9, pp.719-736, 2006

Cronje, P. H., 2008, *Improving off-road vehicle handling using an active anti-roll bar*, University of Pretoria, Pretoria, http://upetd.up.ac.za/thesis/available/etd-11262009-011206/unrestricted/dissertation.pdf, Accessed 2 August 2012.

D

De Bruyne, S., Van Der Auweraer, H. and Anthonis, J., 2011, *Improving active suspension performance by means of advanced vehicle state and parameter estimation*, International Conference on Mechatronics, Istanbul, Turkey, 13-15 April, 2011

Diamond Systems, 2012, *Diamond-MM-16-AT PC/104 Analog I/O Module*, http://www.diamondsystems.com/products/diamondmm16at, Accesed: 6 January 2012

Dong, X., Yu, M., Liao, C., and Chen, W., 2010, *Comparative research on semi-active control strategy for magneto-rheological suspension*, Nonlinear Dynamics, Vol. 59, pp. 433-453, 2010

Dukkipati, R.V., Pang, J., Qatu, M.S., Sheng, G. and Shuguang, Z., 2008, *Road Vehicle Dynamics*, Society of Automotive Engineers Inc., Warrendale, 2008.

E

Edgar Snyder and Associates, 2010, *Rollover Car Accident Statistics*, http://www.edgarsnyder.com/car-accident/rollover-accidents/statistics.html, Accessed 1 November 2010

Els, P. S., 2006, *The ride comfort vs. handling compromise for off-road vehicles*, University of Pretoria, Pretoria, http://upetd.up.ac.za/thesis/submitted/etd-07152008-102911/unrestricted/00front.pdf, Accessed 2 August 2012.

Els, P. S., 1993, *Die hitteprobleem op hiropneumatiese veer-en-demperstelsels*, Unpublished Masters Thesis, University of Pretoria, Pretoria, 1993.

F

Fischer, D. and Isermann, R., 2004, *Mechatronic semi-active and active vehicle suspensions*, Control Engineering Practice, Vol. 12, pp. 1353-1367, 2004

G

Gerotek, 2012, Gerotek Test Facilities, *http://www.armscordi.com/SubSites/Gerotek/Gerotek01_landing.asp*, Accessed 28 April 2012

Geysen, B.L.J., Paulides, J.J.H., Janssen, J.L.G. and Lomonova, E.A., 2010, *Active Electromagnetic Suspension System for Improved Vehicle Dynamics*, IEEE Transactions on vehicular Technology, Vol. 59, Nr. 3, 2010

Gillespie, T. D., 1992, *Fundamentals of vehicle dynamics*, Society of Automotive Engineers Inc., Warrendale, 1992.

Gohl, J., Rajamani, R., alexander, L. and Starr, P., 2004, *Active roll mode control implementation on a narrow tilting vehicle*, Vehicle Systems Dynamics, Vol. 42, Nr. 5, pp. 347-372, 2004

Governor's Office of Consumer Affairs, 2010, *SUV Rollover Accident and Death Statistics*, http://www.georgia.gov/gta/mcm/content/article_print_front/0,2089,5426814_39039081_38820612,00.html, Accessed 28 July 2010

H

Ha, S.H., Nguyen, Q., Choi, S., Rhee, E. and Kang, P., 2009, *Performance Evaluation of 6WD Military Vehicle Featured by MR Suspension System Considering Lumped Parameter Model of MR Damper*, Second International Conference on Smart Materials and Nanotechnology in Engineering, Weihai, China, Proc. Of SPIE, Vol. 7493, 8-11 July, 2009

Hakima, A. and Ameli, S., 2010, *Improvement of vehicle handling by an integrated control system of four wheel steering and ESP with fuzzy logic approach*, International conference on mechanical and electrical technology, 2010.

Hawley, J.B., 1927, US Patent, 1647518, 1927-11-1

Higuchi, M., Taneda, K., Shibahata, Y. and Minakawa, M., 2001, *A Theoretical Study of Influence of Roll on Vehicle Dynamics*, Proceedings. JSAE Annual Congress, Vol. 107-01, pp. 15-18, 2001.

Holdmann, P. and Holle, M. , 1999, *Possibilities to improve the ride and handling performance of delivery trucks by modern mechatronics systems*, JSAE Review, Vol. 20, 1999.

Hydraforce, 2011, *Solenoid Valves*, http://www.hydraforce.com/Solenoid/Sol-pdf/1-374-1.pdf, Accessed: 5 December 2011.

Hydraforce, 2012, *Solenoid Valves*, http://www.hydraforce.com/Solenoid/Sol-pdf/1-064-1.pdf, Accessed: 10 January 2012.

I

International Organisation for Standardisation, 1975, *International Organisation for Standardisation ISO 3888-1975*: Road vehicles – test procedure for a severe lane – change manoeuvre, ISO/TR 3888-1975.

J

Jo, J.-S., You, S.-H., Joeng, J.Y., Lee, K.I., and Yi, K., 2008, *Vehicle stability control system for enhancing steerability, lateral stability and roll stability*, International Journal of Automotive Technology, Vol. 9, Nr. 5, pp. 571-576, 2008

M

MathWorks, 2012, MATLAB – *The Language of Technical Computing*, http://www.mathworks.com/products/matlab/, Accessed: 05 January 2012.

MathWorks, 2011, *Simulink - Simulation and Model-Based Design*, http://www.mathworks.com/products/simulink/, Accessed: 31 May2011.

Mechanical Simulation, 2012a, *Carsim Mechanical Simulation*, http://www.carsim.com/products/carsim/index.php, Accessed: 5 January 2012.

Mechanical Simulation, 2012b, *Trucksim Mechanical Simulation*, http://www.carsim.com/products/trucksim/index.php, Accessed: 5 January 2012.

MSC.Software, 2011, *ADAMS Multibody Dynamics*, http://www.mscsoftware.com/Products/CAE-Tools/Adams.aspx, Accessed: 30 May 2011.

N

National Highway Traffic Safety Administration, 2002, A Comprehensive Experimental Evaluation of Test Maneuvers That May Induce On-Road, Untripped, Light Vehicle Rollover – Phase IV of NHTSA's Light Vehicle Rollover Research Program, http://www.nhtsa.gov/search?q=+A+Comprehensive+Experimental+Evaluation+of+Test+Maneuvers+That&x=28&y=1, Accessed: 30 May 2012

National Highway Traffic Safety Administration, 2012, Why Choose SSF?, http://www.nhtsa.gov/cars/rules/rulings/rollover/Chapt05.html, Accessed: 27 April 2012

Nell, S.and Steyn, J.L., 2003, *Development and experimental evaluation of translational semi-active dampers on a high mobility off-road vehicle*, Journal of Terramechanics, Vol 40, Page 25-32, 2003

New Zealand Crash Investigators, 2010, *HMV Roll Over*, http://www.nzci.co.nz/img/hmvrollover/roll-over-diagram-b.jpg, Accessed: 1 November 2010

O

Otis. D.R. and Pourmovahed, A., 1985, *An Algorithm for Computing Nonflow Gas Processes in Gas Springs and Hydropneumatic Accumulators*, Transactions of the ASME, Journal of Dynamic Systems, Measurement and Control, Vol. 107, pp.110-118, March 1985

Ozaki, A., 2002, *Basic study of vehicle roll motion and possibility of inward roll: examination by a mechanical model of rigid axle suspension*, JSAE Review, Vol. 23, pp. 465-471, 2002.

P

Pacejka, H.B., 2002, *Tyre and Vehicle Dynamics*, Society of Automotive Engineers, Warrendale, USA 2002.

Ponticel, P., 2003, Dynamic rollover testing on the way, Automotive Engineering International, Vol.111, No. 11, pp.26-28, November 2003.

R

Racelogic, 2012, About Racelogic, *http://www.racelogic.co.uk/?show=VBOX*, Accessed 28 April 2012.

Road Traffic Management Corporation, 2009, *Road Traffic Report for the Calendar Year 2009*, http://www.arrivealive.co.za/documents/Year_2009_-_Road_Traffic_Report_-_V2.pdf, Accessed: 24 January 2011.

Rotpod, 2012, *Hybrid Car/Bike Yields Lower Emissions*, http://www.rotpod.net/rotpod/author/elias-tsang/page/3/, Accessed: 30 April 2012.

S

Sampson, D.J.M. and Cebon, D., 2003, *Active Roll Control of Single Unit Heavy Road Vehicles*, Vehicle System Dynamics: International Journal of Vehicle Mechanics and Mobility, Vol. 40, Nr. 4, pp. 229-270, 2003

Shaout, A., Jarrah, M.A., Al-Araji, H., and Al-Tell, K., 2000, *A nonlinear optimal four wheels steering controller*, Proc 43rd IEEE, Midwest Symposium on circuits and systems, Lansing MI, 8-11 August 2000

Shim, T. and Velusamy, P.C., 2010, *Improvement of vehicle roll stability by varying suspension properties*, *Vehicle System Dynamics*, Vol. 45, pp. 129-152, 2010

Smith, M.C. and Walker, G.W., 2005, *Interconnected vehicle suspension*, Proc IMechE, Part D, Journal of Automobile Engineering, Vol. 219, pp. 295-307, 2005.

Smith, W.A. and Zhang, N., 2009, *Recent developments in passive interconnected vehicle suspension*, Frontiers of Mechanical Engineering China, Vol. 5, Nr. 1, pp. 1-18.

Sontag, R. E. and Van Wylen, G. J., 1991, *Introduction to thermodynamics*, 3rd ed., John Wiley and Sons, New York, 1991.

Stone Hydraulics, 2012, *Pump Kits*, http://www.stonehydraulics.com/catalog/47-2007.pdf, Accessed: 7 August 2012

Sun hydraulics, 2011, *Electro-proportional flow control valve - normally closed*, http://www.sunhydraulics.com/cmsnet/Cartridge.aspx?ModelCode=FPCC&CatModelID=8216&Lang_ID=1, Accessed: 5 December 2011.

T

Takubo, N. and Mizuno, K., 2000, *Accident analysis of sports utility vehicles: human factors from statistical analysis and case studies*, JSAE Review, Vol. 21, 2000.

Theron, N. and Els, P. S., 2007, *Modelling of a semi-active hydropneumatic spring-damper unit*, International journal of vehicle design, Vol.45, pp. 501-521, 2007.

Thoresson, M. J., 2007, Efficient gradient-based optimisation of suspension characteristics for an off-road vehicle, Unpublished PhD thesis, University of Pretoria, Pretoria, South Africa, upetd.up.ac.za/thesis/available/etd-08042008-093103/, Accessed: 5 June 2012

U

Ungoren, A.Y., Peng, H. and Milot, D.R., 2001, *Rollover Propensity Evaluation of an SUV Equipped with a TRW VSC System*, University of Michigan, January 2001.

Uys, P.E., Els, P.S. and Thoresson, M.J., 2006a, Criteria for handling measurement, Journal of Terramechanics, Vol. 43, pp. 43-67, 2006

Uys, P.E., Els, P.S., Thoresson, M.J., Voight, K.G., Combrinck, W.C., 2006b, *Experimental Determination of Moments of Inertia for an Off-Road Vehicle in a Regular Engineering Laboratory*, International Journal of Mechanical Engineering Education 34/4, 2006.

Uys, P.E., Els, P.S. and Thoresson, M.J., 2007, *Suspension settings for optimal ride comfort of offroad vehicles travelling on roads with different roughness and speeds*, Journal of Terramechanics, Vol. 44, pp. 163-175, 2007

W

Wallentowitz, H. and Holdman, P., 2010, *Hardware and Software Demands on Adjustable Shock Absorbers for Trucks and Passenger Cars*, 2001 http://www.ika.rwthaachen.de/forschung/veroeffentlichung/1995/1995-1/index.php, Accessed: 1 November 2010.

Wilde, J.R., Heydinger, G.J., Guenther, D.A., Mallin, T. and Devenish, A.M., 2005, *Experimental evaluation of fishhook manoeuvre performance of a kinetic suspension system*, SAE Technical Paper 2005-01-0392, Society of Automotive Engineers, Warrendale, 2005

Appendix A Derivation of the differential equation used to calculate the gas temperature in the suspension

The first law of thermodynamics (Energy Equation) is:

$$\dot{U} = \dot{Q} - \dot{W} \quad \text{or} \quad m\dot{u} = \dot{Q} - \dot{W} \tag{1}$$

With:

$\dot{U} = Change\ in\ internal\ energy\ of\ the\ gas$

$m = Mass\ of\ the\ gas$

$\dot{u} = Change\ in\ specific\ internal\ energy\ of\ the\ gas$

$\dot{Q} = Heat\ transfer\ rate\ between\ the\ system\ and\ \ the\ environment$

$\dot{W} = Work\ done\ by\ the\ piston\ on\ the\ gas$

In order to apply the method used by **Otis and Pourmovahed (1985)** to a hydropneumatic suspension, **Els (1993)** makes the following assumptions:

- The system is a closed system.
- No Inertia effects are present during the gas compression.
- The process is seen as a homogeneous, quasi-static gas compression process.
- The effect of the thermal capacity of the piston rod and that of the cylinder wall is seen as negligibly small.

The convective heat transfer between the suspension and the environment can be approximated by:

$$\dot{Q} = \frac{mc_v(T_s - T_g)}{\tau} \tag{2}$$

With

$$\tau = \frac{\rho c_v V}{hA}$$

Where

$m = mass\ of\ the\ gas$

$c_v = specific\ heat$

$T_g = Gas\ temperature$

$T_s = Atmospheric\ Temperature$

$\tau = Thermal\ time\ constant$

And the rate of the piston work is given by:

$$\dot{W} = P\dot{V} \tag{3}$$

With

$P = Gas\ Pressure$

$\dot{V} = Change\ of\ volume$ (In terms of the piston movement or the oil flow)

The internal energy per unit mass is given by the thermodynamic relation

$$du = c_v dT_g + \left[T_g \left(\frac{\partial P}{\partial T_g}\right)_v - P\right] dv \tag{4}$$

With $v = specific\ volume$

Replace (2),(3) and (4) into (1)

$$m\left[c_v dT_g + \left[T_g \left(\frac{\partial P}{\partial T_g}\right)_v - P\right] dv\right] = \frac{mc_v(T_s - T_g)}{\tau} - P\dot{V}$$

Simplify:

$$mc_v\dot{T}_g + m\left[T_g \left(\frac{\partial P}{\partial T_g}\right)_v - P\right]\dot{v} = \frac{mc_v(T_s - T_g)}{\tau} - P\dot{V}$$

Divide with mc_v:

$$\dot{T}_g + \frac{T_g \left(\frac{\partial P}{\partial T_g}\right)_v \dot{v}}{c_v} - \frac{P\dot{v}}{c_v} = \frac{(T_s - T_g)}{\tau} - \frac{P\dot{V}}{mc_v}$$

Knowing that $\dot{V} = m\dot{v}$ the differential equation simplifies to:

$$\dot{T}_g = \frac{(T_s - T_g)}{\tau} - \frac{T_g\left(\frac{\partial P}{\partial T_g}\right)_v \dot{v}}{c_v} \tag{5}$$

The BWR Equation is used to represent the $P - v - T$ relationship:

$$P = \frac{RT_g}{v} + \frac{B_o RT_g - A_o - \frac{C_o}{T_g^2}}{v^2} + \frac{bRT_g - a}{v^3} + \frac{a\alpha}{v^6} + \frac{c\left(1 + \frac{\gamma}{v^2}\right)e^{\frac{-\gamma}{v^2}}}{v^3 T_g^2} \tag{6}$$

Differentiate (6) in terms of T:

$$\left(\frac{\partial P}{\partial T_g}\right)_v = \frac{R}{v} + \frac{B_o R}{v^2} + \frac{2C_o}{T_g^3 v^2} + \frac{bR}{v^3} - \frac{2c\left(1 + \frac{\gamma}{v^2}\right)e^{\frac{-\gamma}{v^2}}}{v^3 T_g^3} \tag{7}$$

Replace (7) into (5)

$$\dot{T}_g = \frac{(T_s - T_g)}{\tau} - \frac{\dot{v}}{c_v}\left[\frac{T_g R}{v} + \frac{T_g B_o R}{v^2} + \frac{2C_o}{T_g^2 v^2} + \frac{T_g b R}{v^3} - \frac{2c\left(1 + \frac{\gamma}{v^2}\right)e^{\frac{-\gamma}{v^2}}}{v^3 T_g^2}\right]$$

Regroup:

$$\dot{T}_g = \frac{(T_s - T_g)}{\tau} - \frac{\dot{v}}{c_v}\left[\frac{T_g R}{v}\left(1 + \frac{b}{v^2}\right) + \frac{1}{v^2}\left(T_g B_o R + \frac{2C_o}{T_g^2}\right) - \frac{2c}{v^3 T_g^2}\left(1 + \frac{\gamma}{v^2}\right)e^{\frac{-\gamma}{v^2}}\right]$$

(Otis and Pourmovahed, 1985) and **(Els, 1993)**

This equation can be solved numerically. The ode45 in MATLAB **(MathWorks, 2012),** which is based on the 4th order Runge Kutta method, can be used but this method is computational expensive due to additional features in the code. A basic 4th order Runge Kutta function was written as recommended by **Otis and Pourmovahed (1985)** and it solves in significantly less time.

The 4th order Runge Kutta method formula is as follows:

$$x(t + h) = x(t) + \frac{1}{6}(K_1 + 2K_2 + 2K_3 + K_4)$$

Where:

$$K_1 = hf(t, x)$$

$$K_2 = hf(t + \frac{1}{2}h, x + \frac{1}{2}K_1)$$

$$K_3 = hf(t + \frac{1}{2}h, x + \frac{1}{2}K_2)$$

$$K_4 = hf(t + h, x + K_3)$$

$$t = time$$

$$h = time\ step$$

(Cheney and Kincaid, 2004)

The ideal gas specific heat is given by:

$$c_v^0 = R\left[\frac{N_1}{T_g^3} + \frac{N_2}{T_g^2} + \frac{N_3}{T_g} + (N_4 - 1) + N_5 T_g + N_6 T_g^2 + N_7 T_g^3 + \frac{N_8 y^2 e^y}{(e^y - 1)^2}\right]$$

Where:

$$y = \frac{N_9}{T_g}$$

Knowing c_v^0 the specific heat for the real gas can be calculated:

$$c_v = c_v^0 + \frac{6}{T_g^3}\left(\frac{C_o}{v} - \frac{c}{\gamma}\right) + \frac{3c}{T_g^3}\left(\frac{2}{\gamma} - \frac{1}{v^2}\right)e^{\left(-\frac{\gamma}{v^2}\right)}$$

(Otis and Pourmovahed, 1985)

The constants for the BWR equation and N_1 to N_9 can be found in Appendix B BWR and Nitrogen Constants

Appendix B BWR and Nitrogen Constants

Constants for the BWR equation

$a = 0.115703387$ $\left[\left(\frac{m^3}{kg}\right)^3 \cdot \frac{N}{m^2}\right]$

$A_o = 136.0474619$ $\left[\left(\frac{m^3}{kg}\right)^3 \cdot \frac{N}{m^2}\right]$

$b = 2.96625 \times 10^{-6}$ $\left[\left(\frac{m^3}{kg}\right)^3\right]$

$B_o = 0.001454417$ $\left[\frac{m^3}{kg}\right]$

$c = 7.3806143 \times 10^{-5}$ $\left[\left(\frac{m^3}{kg}\right)^3 \cdot K^2 \cdot \frac{N}{m^2}\right]$

$C_o = 1.0405873 \times 10^{-6}$ $\left[\left(\frac{m^3}{kg}\right)^3 \cdot K^2 \cdot \frac{N}{m^2}\right]$

$\alpha = 5.7863972 \times 10^{-9}$ $\left[\left(\frac{m^3}{kg}\right)^3\right]$

$\gamma = 6.7539311 \times 10^{-6}$ $\left[\left(\frac{m^3}{kg}\right)^2\right]$

$R = 296.797$ $\left[\frac{J}{kg \cdot K}\right]$

Constants for the calculation lf the ideal gas specific heat capacity (Temperature in Kelvin)

$N_1 = -735.210$ $N_2 = 34.224$

$N_3 = -0.557648$ $N_4 = 3.5040$

$N_5 = -1.7339 \times 10^{-5}$ $N_6 = 1.7465 \times 10^{-8}$

$N_7 = -3.5689 \times 10^{-12}$ $N_8 = 1.0054$

$N_9 = 3353.4061$

(Els, 1993)

Appendix C Equation for volume estimation

In order to estimate the volume of oil in the suspension units, the compressibility of the gas and oil is taken into account using the ideal gas law and the bulk modulus of the oil. The pressure of the gas and oil is assumed to be the same.

The Ideal gas law is stated as:

$$V_g = \frac{mRT}{P} \tag{1}$$

Assuming an isentropic relationship the ideal gas law can be written in the following manner:

$$V_{2g} = V_{1g}\left(\frac{P_2}{P_1}\right)^{-1/\gamma_{IG}} \tag{2}$$

The following values are obtained from Els (2006):

$P_1 = 4MPa$ (pressure at which the gas was charged)

$V_1 = 0.1l = 0.0001m^3$ (volume at which the gas was charged)

And the heat capacity ratio for nitrogen is $\gamma_{IG} = 1.404$.

Bulk modulus equations as found on P 4.21 (Els, 2006)

$$\beta = \frac{\Delta P}{\left(\frac{\Delta V_o}{V_o}\right)} \tag{3}$$

(3) can be rearranged to get (4)

$$\beta = \frac{(P_2 - P_1)}{\left(\frac{V_{1o} - V_{2o}}{V_{1o}}\right)}$$

$$\beta = \frac{P_2 - P_1}{1 - \frac{V_{2o}}{V_{1o}}}$$

$$1 - \frac{V_{2o}}{V_{1o}} = \frac{P_2 - P_1}{\beta}$$

$$\frac{V_{2o}}{V_{1o}} = 1 - \frac{P_2 - P_1}{\beta}$$

$$V_{1o} = \frac{V_{2o}}{1 - \frac{P_2 - P_1}{\beta}} \tag{4}$$

In this case the displacement of the suspension and the compression of the nitrogen in the accumulator need to be taken into account. The compression of the nitrogen is taken into account using the ideal gas law and the compression of the oil using the bulk modulus. The change in the height due to oil being

added or removed is taken into account by multiplying the change in the displacement of the suspension unit with the piston area as shown in (5) and (6).

$$\Delta V = A(x - x_o) \tag{5}$$

But $x_o = 0$

$$\therefore\ \Delta V = Ax \tag{6}$$

Thus by placing (2) and (6) into (4) we get the amount of oil in the suspension that can be compared with the original amount of oil in the suspension.

$$V_{1o} = \frac{V_{2o} + (Ax) + \left(V_{1g} - V_{1g}\left(\frac{P_{2g}}{P_{1g}}\right)^{-1/\gamma_{IG}} \right)}{1 - \frac{P_{2o} - P_{1o}}{\beta}}$$

$$V_{1o} = \frac{V_{2o} + (Ax) + V_{1g}\left(1 - \left(\frac{P_{2g}}{P_{1g}}\right)^{-1/\gamma_{IG}} \right)}{1 - \frac{P_{2o} - P_{1o}}{\beta}} \tag{7}$$

Where:

$V_{2o} = 1.6 \times 10^{-3}$ (Rear)

$V_{2o} = 1.5 \times 10^{-3}$ (Front) (50mm less travel)

$P_{1o} = 100 \times 10^{3} Pa$ (Atmospheric Pressure)

$\beta = 1.368 \times 10^{9}$ (Bulk Modulus)